Neurobin/TMPRSS11c, a Novel Type II Transmembrane Serine Protease of the Nervous System which Cleaves Fibroblast Growth Factor-2 *in vitro*

Dissertation

zur
Erlangung der naturwissenschaftlichen Doktorwürde
(Dr. sc. nat.)
vorgelegt der
Mathematisch-naturwissenschaftlichen Fakultät
der
Universität Zürich
von

Robert Stallmach
aus Deutschland

Promotionskomitee
Prof. Dr. Peter Sonderegger
PD Dr. Sergio Gloor

Zürich 2008

in memoriam

Maximilian Leithoff

aka Sky, Leo and Phoenix

29.10.1987 – 1.6.2007

Alles Leben ist Problemlösen.
Lasst Ideen sterben, nicht Menschen!
(Karl Popper)

Publications and Presentations of this Work

Robert Stallmach and Sergio M. Gloor (2008) Neurobin/TMPRSS11C, a novel type II transmembrane serine protease which cleaves fibroblast growth factor-2 in vitro. *Biochem J*. 2008 Jan 21; [Epub ahead of print].

Robert Stallmach and Sergio M. Gloor (2006) Neurobin/tmprss11c, a novel type II transmembrane serine protease cloned from mouse spinal cord is able to process fibroblast growth factor 2. *5th Forum of European Neuroscience, Vienna.* Meeting abstract *A156.16,* July 2006 (poster presentation).

Robert Stallmach, Peter Sonderegger and Sergio M. Gloor (2005) Neurobin, a novel serine protease in developing murine spinal cord. *ZNZ Symposium 2005, Neuroscience Center Zurich*, October 2005 (data blitz talk and poster presentation).

Contents

Abstract

Proteases play important roles in many physiological processes including the development and differentiation of the nervous system. To obtain an inventory of the trypsin-like serine proteases expressed in the spinal cord during the period of the maturation of the neuro-muscular junction, a protease-enriched cDNA library was constructed. The library was generated from postnatal day 10 mouse spinal cord mRNA and allowed the retrieval of 27 different trypsin-like serine protease sequence fragments. One sequence was not yet described to be part of any known protease. Using this fragment and the technique of rapid amplification of cDNA ends, the full-length sequence of a novel protease, designated neurobin, was obtained. Neurobin consists of 431 amino acids. Primary sequence analysis suggested that neurobin is a type II transmembrane serine protease (TTSP). Neurobin has a short N-terminal segment in the cytosol followed by a transmembrane-helix. In the extracellular part, neurobin contains a single SEA domain and the C-terminal serine protease domain. With this domain structure, neurobin belongs to the HAT/DESC subfamily of TTSPs. RT-PCR analysis indicated expression of neurobin in spinal cord and cerebellum. Histochemical analysis of brain sections revealed most distinct staining of Purkinje neurons of the cerebellum. Overexpression of neurobin in the cell-lines COS-7 and HEK293T showed, that neurobin is autocatalytically processed and inserted into the plasma membrane. Autocatalytic activation could be suppressed by mutating Ser381 in the catalytic pocket to Ala. The protease domain of neurobin was produced in *E. coli* and purified from inclusion bodies. After activation, the refolded protease domain cleaved chromogenic peptides with Arg in position P_1. Serine protease inhibitors effectively suppressed the proteolytic activity of recombinant neurobin. Aspartate and cyteine protease inhibitors, as well as EDTA or heparin had no influence on neurobin-activity towards chromogenic peptides. Ca^{2+} or Na^{+} ions did not significantly modulate the catalytic activity of the protease. In *in vitro* assays, fibroblast growth factor-2 was processed by recombinant neurobin at several P_1 Lys and Arg positions to distinct fragments. This fragmentation could be inhibited by heparin in dose-dependent manner. Other proteins like fibroblast growth factor-7, laminin, or fibronectin were not processed in these *in vitro* assays. Taken together, these results indicate that neurobin is an authentic TTSP with trypsin-like activity, possibly high protein-substrate selectivity and restricted tissue distribution.

Zusammenfassung

Proteasen spielen eine wichtige Rolle in vielen physiologischen Abläufen, einschliesslich der Entwicklung und Differenzierung des Nervensystems. Um ein Inventar der trypsinähnlichen Serinproteasen zu erhalten, die während der Reifungsphase der neuromuskulären Endplatte im Rückenmark exprimiert werden, wurde eine Proteasedomänen-angereicherte cDNA-Bibliothek erstellt. Bei der Herstellung der Bibliothek wurde mRNA aus dem Rückenmark von zehntägigen Mäusen verwendet. In der Bibliothek wurden cDNA-Klone gefunden, die Sequenzabschnitte von 27 verschiedenen Serinproteasen codieren. Einer der Sequenzabschnitte liess sich keiner bekannten Protease zuordnen. Mit Hilfe einer Technik zur schnellen Vervielfältigung von cDNA-Enden wurde die vollständige cDNA Sequenz einer neuen Protease entdeckt, die den Namen Neurobin erhielt. Neurobin besteht aus 431 Aminosäuren. Die Analyse der Aminosäuresequenz ergab, dass Neurobin eine Typ II Transmembran-Serinprotease (TTSP) ist. Neurobin besteht aus einem kurzen zytosolischen Segment am N-Terminus, dem eine transmembranale Helix folgt. Im extrazellulären Teil des Moleküls befinden sich eine SEA- und dann die C-terminale Proteasedomäne. Wegen seiner Domänenkomposition gehört Neurobin in die HAT/DESC-Unterfamilie der TTSPs. RT-PCR Experimente zeigten, dass Neurobin vor allem im Rückenmark und im Kleinhirn exprimiert wird. In histochemischen Färbungen wurde die deutlichste Neurobin-Immunoreaktivität in Purkinje-Zellen gefunden. Bei der Überexpression von Neurobin in den Zelllinien COS-7 und HEK293T wurde Selbstaktivierung des Proteins und Insertion in die Zellmembran festgestellt. Diese Selbstaktivierung konnte durch die Mutation von Ser381 im katalytischen Zentrum zu Ala unterdrückt werden. Die Proteasedomäne wurde in *E.coli* hergestellt, aus Einschlusskörperchen aufgereinigt und rückgefaltet. Nach enzymatischer Aktivierung war die rückgefaltete Proteasedomäne in der Lage, chromogene Peptide nach Arg-Resten zu schneiden. Serinprotease-Inhibitoren hemmte diese proteolytische Aktivität. Aspartat- und Cysteinprotease-Inhibitoren sowie EDTA oder Heparin zeigten keinen Einfluss auf die Neurobin-Aktivität gegen chromogene Peptide. Der Einfluss von Calcium- und Natriumionen auf die katalytische Aktivität war gering. In *in vitro* Versuchen wurde der Wachstumsfaktor FGF-2 von Neurobin nach mehreren Lys- und Arg-Resten geschnitten. Diese Prozessierung konnte mit ansteigender Heparin-Konzentration vollständig unterdrückt werden. Andere Proteine, wie der Wachstumsfaktor FGF-7, Laminin oder Fibronektin wurden in keinem *in vitro* Versuch

prozessiert. Zusammengefasst zeigen die Resultate der Experimente, dass Neurobin eine TTSP mit trypsinähnlicher Aktivität und möglicherweise hoher Proteinsubstrat-Selektivität ist und eine klar beschränkte Gewebeverteilung aufweist.

Abbreviations

aa	Amino acid(s)
ATP	Adenosine triphosphate
bp	Base pair(s)
BSA	Bovine serum albumin
Ca-P	Calcium-phosphate
cDNA	Complementary deoxyribonucleic acid
CIP	Calf intestinal alkaline phosphatase
CMV	Cytomegalovirus
(C)NS	(central) nervous system
COS-7	Monkey African green kidney, SV40 transformed
CS	Cover slip(s)
CTP	Cytidine triphosphate
d	Deoxy
dd	Dideoxy
DESC	Differentially expressed in squamous cell carcinoma
DIG	Digoxigenin
DMEM	Dulbecco’s modified Eagle’s medium
DNA	Deoxyribonucleic acid
(E)GFP	(enhanced) green fluorescent protein
ER	Endoplasmic reticulum
FCS	Fetal calf serum
FGF-2	Fibroblast growth factor 2

GTP	Guanosine triphosphate
H/MAT	Human/mouse airway trypsin-like
HEK	Human embryonic kidney
IF	Immunofluorescence
kDa	Kilodaltons
LTD	Long-term depression
LTP	Long-term potentiation
(m)NT	(murine) Neurotrypsin (full-length)
(m)RNA	(messenger) Ribonucleic acid
NS	Nervous system
nt	Nucleotide(s)
OD	Optical density
ORF	Open reading frame
PA	Plasminogen activator
PBS	Phosphate-buffered saline
PCR	Polymerase chain reaction
PFA	Paraformaldehyde
PLL	Poly-L-lysine
POD	Peroxidase
PRB	Proline-rich basic
RACE	Rapid amplification of cDNA ends
RCF	Relative centrifugal field
rpm	rotations per minute
RT-PCR	Reverse transcription - polymerase chain reaction
SDS-PAGE	Sodium dodecylsulfate-polyacrylamide gelelectrophoresis
SEA	Sea-urchin/enteropeptidase/agrin
SV40	Simian virus 40
TBS	Tris buffered saline
TMPRSS	Transmembrane serine protease
tPA	Tissue-type plasminogen activator
Tris	Tris-(hydroxymethyl)-methane
TTP	Thymidine triphosphate
TTSP	Type II transmembrane serine protease
uPA	Urokinase-type plasminogen activator (urokinase)
UTR	Untranslated region
WB	Western blotting

1 Introduction

1.1 Proteases

Enzymes are proteins that serve as bio-catalysts. Thus, they enable living organisms to conduct most of the chemical reactions of their requirements in a narrow temperature- and pH-range in aqueous solution. Proteases, also known as peptidases, proteinases or proteolytic enzymes, catalyze the hydrolysis of peptide bonds. The analysis of deciphered genomes from a large variety of organisms revealed that about 2 % of all genes encode proteases making them the largest group of enzymes (Rawlings et al., 2006).

Proteases cleave amid bonds between amino acids. By catalyzing this hydrolysis step, proteases are involved in a wide variety of biological functions ranging from unspecific protein degradation like in food digestion to sophisticated cascades like in blood coagulation where cleavage modulates the activity and function of proteins ((Mann, 2003); and references therein). Similarly, proteases exert their function in wound healing, angiogenesis, clot dissolution, tissue development, antigen presentation, complement activation, memory formation/learning and apoptosis ((Puente et al., 2003a); and references therein). Thus, alterations in protease activity and/or expression pattern result in a large variety of pathological conditions. This makes activity modulation of certain members of this enzyme group a recognized concept for the treatment of conditions as different as thrombosis, Alzheimer and cancer.

Proteases are often subdivided according to their catalytic types. Five types are classified depending on the amino acid in their catalytic center being aspartate, cysteine, glutamate, serine or threonine. Additionally, there is one type in which metal ions such as Zn^{2+} or Cu^{2+} form the catalytic center. A seventh division of proteases summarizes those enzymes, of which the catalytic type is unknown till date (*MEROPS*, the peptidase database, Release 7.90, http://merops.sanger.ac.uk). Besides, proteases are divided into (a) exopeptidases, which cleave either amino acids from the N-terminus (aminopeptidases) or from the C-terminus (carboxypeptidases) of a peptide chain, and (b) endopeptidases, which cut within a peptide chain. The largest family of endopeptidases consists of serine proteases of the chymotrypsin-type, the peptidase family S1 or chymotrypsin family (Rawlings et al., 2007).

Another useful classification into clans is based on structural fold similarities which suggest common evolutionary origins (Rawlings and Barrett, 1999). Family S1 members belong to the clan PA and, being serine proteases, to subclan PA(S). This introduction will focus mainly on proteases of family S1 and repeatedly refer to subfamily S1(A) which contains three quarters of all family S1 members (*MEROPS*, the peptidase database, Release 7.90, http://merops.sanger.ac.uk).

1.2 Peptidase subfamily S1(A)

The serine proteases of subfamily S1(A) can be further subdivided according to the substrate amino acids preceding the cleaved peptide bond into (I) chymotrypsin-like (hydrolysis after hydrophobic amino acids), (II) elastase (after alanine), (III) granzyme B (after acidic amino acids) and (IV) trypsin-like (after the basic amino acids arginine and lysine) enzymes ((Hedstrom, 2002); and references therein). Numbering of the amino acids of the catalytic domain is often adjusted to the chymotrypsin numbering proposed by W. Bode (Bode et al., 1989) to facilitate comparisons and generalizations while analyzing different family S1(A) members. Using chymotrypsin numbering, e.g. the most conserved amino acids of subfamily S1(A) members will always be found in sequence position 57, 102 and 195, respectively. Chymotrypsin numbering will be used throughout the whole introduction section when referring to catalytic domains.

In subfamily S1(A) proteases, the catalytic domain is often preceded by one to several non-catalytic domains of various types that mediate substrate- and other protein-interactions ((Bowen et al., 2000; Chang et al., 1997; Stahl et al., 1996; Xue et al., 2001); and others). An obvious difference between subfamily A and B is that in subfamily B non-catalytic domains occur also C-terminally of the protease domain. Interestingly, while most non-catalytic domains are modules also found in other proteins, the apple and kringle domains almost exclusively occur in proteases of family S1 (*MEROPS*, the peptidase database, Release 7.90, http://merops.sanger.ac.uk).

Subfamily S1(A) proteases are secreted or membrane-bound proteins with the catalytic domain facing the extracytosolic lumen.

1.3 The catalytic mechanism of peptide hydrolysis by family S1 proteases

The structure of the catalytic domains of family S1 proteases is molded by two six-stranded beta barrels. The fold allows the primary substrate recognition region and the catalytic center to arrange in the cleft between the barrels (Figure 1.1).

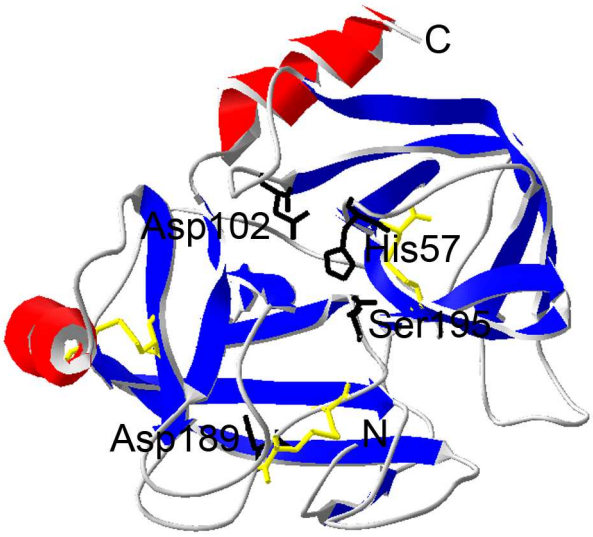

Figure 1.1: To represent the fold of subfamily S1(A) peptidases a ribbon model of trypsin is shown with the two six-stranded beta barrels (blue) at right angle to one another. Backbone and side chain atoms of the catalytic triad and Asp189 at the bottom of the primary specificity pocket are depicted in black sticks, six cysteine residues forming three highly conserved disulfide bridges are shown in yellow and the termini are labeled. The model was generated using the x-ray structure 1YP9 in the Swiss PDB Viewer (Guex and Peitsch, 1997).

The catalytic center is composed of the catalytic triad consisting of His57, Asp102 and Ser195 and the oxianion hole, formed by the backbone NH-groups of Gly193 and Ser195. The catalytic triad is part of a long ranging hydrogen bonding network. This hydrogen bonding system allows the activation of Ser195 for the nucleophilic attack on the carbonyl group of the scissile peptide bond (the bond which is hydrolyzed). The positively charged oxianion hole in turn prepares the attacked carbonyl group by increasing its electrophilicity and it stabilizes the resulting oxyanion of the first tetrahedral intermediate. The intermediate collapses expulsing the C-terminal peptide of the cleaved substrate carrying the proton originating from Ser195. The resulting acylenzyme intermediate is nucleophilically attacked by water activated by the hydrogen bonding network around His57. After collapse of the resulting second tetrahedral

intermediate, the second peptide is released and the enzyme is obtained in the original state after propagation of the proton captured by His57 to Ser195 (Figure 1.2).
The catalytic mechanism was nicely reviewed in more detail by L. Hedstrom (Hedstrom, 2002) but is also comprehensively explained in textbooks like “Biochemistry” by D. Voet & J.Voet.

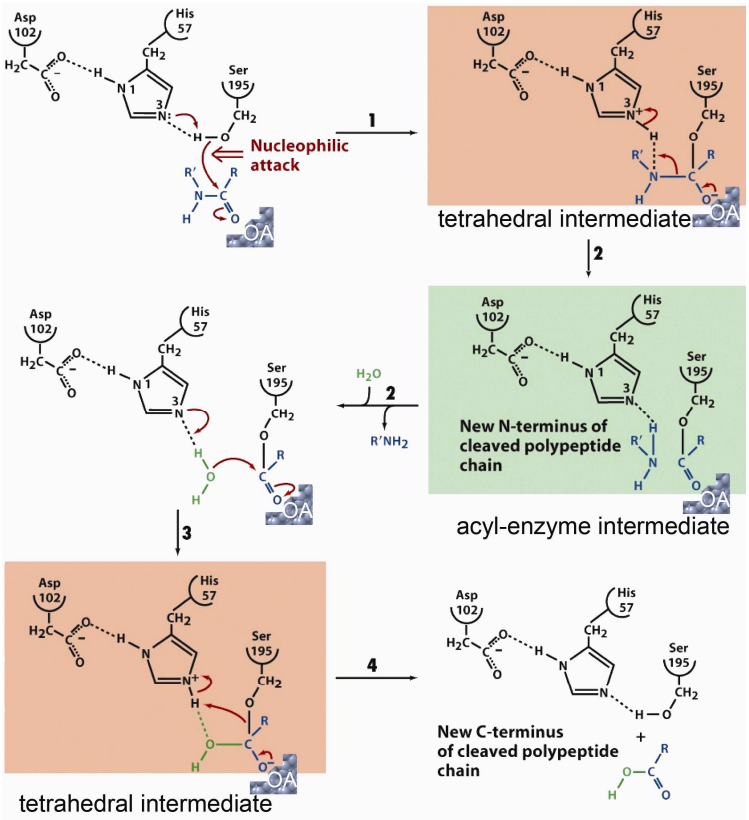

Figure 1.2: The generally accepted catalytic mechanism of serine proteases is shown. The oxyanion hole (OA) prepares the substrate’s carbonyl group for the nucleophilic attack by Ser195, which leads to the first tetrahedral intermediate (1). Upon collapse, the acyl-enzyme intermediate is obtained, which is attacked by water while the N-terminal cleavage product is released (2). This leads to the second tetrahedral intermediate (3). Upon collapse, the active enzyme is retained as soon as the C-terminal substrate peptide diffuses away (4). Figure was modified from Voet&Voet, 1996.

Interestingly, a catalytic mechanism similar to that applied by S1 proteases appears to have evolved independently in subtilisin (clan SB) in which another sequence order of the catalytic triad (Asp-His-Ser) and a different form of oxianion hole (side chains of two amino acids plus one backbone NH-group) was found (Matthews et al., 1975). Moreover, the catalytic triad is found in proteases of the clans SC (Ser-Asp-His) and SK (Ser-His-Asp) but also in e.g. lipases (Asp-His-Ser) (Dodson and Wlodawer, 1998). These various manifestations of the catalytic triad are considered as examples for convergent molecular evolution to obtain an efficient charge relay system. However, the charge relay system

generating the nucleophilic potential of the Ser195 side chain oxygen in S1 family members can also be obtained by a different composition of the triad as observed for proteases of the clan SH in which the Asp is substituted by His (His-Ser-His; Figure 1.3). In this chase the rest of the catalytic machinery is conserved, suggesting another variant of convergent evolution (Chen et al., 1996).

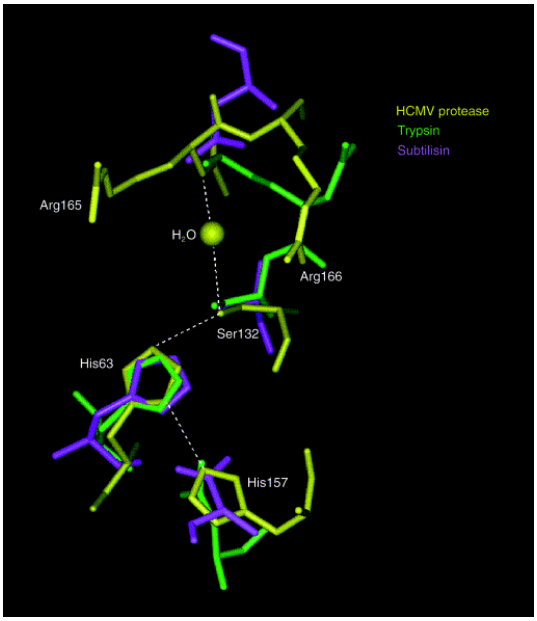

Figure 1.3: Superposition of the catalytic triads of clan PA(S) (trypsin), clan SB (subtilisin) and clan SH (human cytomegalovirus assemblin) reveals striking similarities of the overall architecture of the catalytic center. Picture taken from (Dodson and Wlodawer, 1998).

1.4 Control of catalytic activity and introduction to additional characteristics of family S1 proteases

Cells and organisms make use of a variety of techniques to prevent destructive effects of proteolytic activity: Often proteases are produced in a catalytically inactive proform, the zymogen. Further, proteases activity is modulated by inhibitors and degradation of the protease (Bode and Huber, 2000). Controlled secretion, high specificity for substrate cleavage motifs, strict spatio-temporal expression patterns of proteases, and allosteric regulation and exosite interactions are further ways to minimize unwanted harmful effects of proteolysis.

Activation in family S1 proteases occurs by proteolytic cleavage of the zymogen after an Arg or Lys residue in position 15. Upon cleavage, the newly generated protonated N-

terminus forms a salt bridge with the side chain carboylate group of Asp194. The resulting structural rearrangements open the substrate binding cleft and adjust the residues of the oxianion hole (Khan and James, 1998). This activation mechanism is conserved in mammalian S1 family members and generally leads to an enzyme that is six to seven orders of magnitude more active than the zymogen. A famous exception is the zymogen of tissue-type plasminogen activator (tPA) which is only one order of magnitude less active than the activated enzyme. In this special case, the Lys156 side chain forms an ion pair with the side chain carboylate group of Asp194 which has a similar effect as the salt bridge formed by this residue to the N-terminus generated upon activation cleavage (Renatus et al., 1997).

Once activated, several S1 family members like trypsin and human kallikrein 6 are capable of self-activation by autocatalytic cleavage of zymogens (Magklara et al., 2003).

In general, the noncatalytic part of family S1 proteases stays covalently linked to the protease domain after activation cleavage. This is possible due to a disulfide bridge formed by a cysteine residue preceding the activation cleavage site and a cysteine in position 122 on the surface of the protease domain.

In living organisms, inhibition of serine proteases is frequently realized by proteins that bind in a substrate like manner, with a fixed distance to the catalytic center too far to induce catalysis. As an example the complex of the trypsin-like serine protease thrombin and rhodniin (an inhibitor that prevents blood coagulation in the prey of the assassin bug *Rhodnius prolixus*), in which the scissile peptide bond is fixed at a van der Waals distance of 2.7 Å from the Oγ atom of the Ser195 residue of thrombin, was reviewed recently (Bode and Huber, 2000).

Other important physiological inhibitors are from the serpin family (serine protease inhibitor, MEROPS family I4). For inhibition, serpins become first cleaved in their reactive-center loop like normal substrates. However, immediately upon cleavage the reactive-center loop, ester-linked to Ser195, flips over and becomes inserted into a beta sheet of the serpin structure. The process is very fast and the energy gained from the loop insertion is large enough to tear Ser195 away from its catalytic partners and deform the oxianion hole (Huntington et al., 2000). Thus, formation of the second tetrahedral intermediate is prevented and the enzyme is blocked (Figure 1.4).

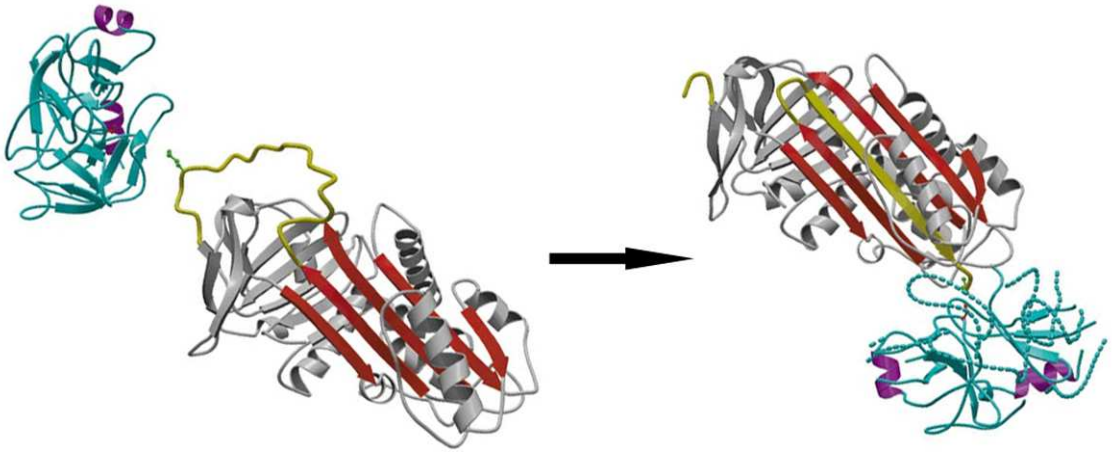

Figure 1.4: Ribbon depictions to visualize the inactivation mechanism of serpins on serine proteases. Left: Trypsin (cyan, with helices in magenta for orientation) attacks the reactive-center loop (yellow,; green ball-and-stick, P1 Met) of the serpin α_1-antitrypsin (gray, with its β-sheet A colored in red). Upon cleavage, the cleaved reactive-centre loop is fully inserted into the A-sheet (right). This rapidly flips the complexed trypsin to the other side of the serpin molecule leading to disordered regions in the protease domain. Picture modified from (Huntington et al., 2000).

Specificity of family S1 proteases is strongly influenced by the polypeptide binding site and the substrate (side chain) binding pockets. The enzyme's polypeptide binding site is generated by the main chain atoms of residues 214-216 forming an antiparallel beta sheet with the backbone of the substrate residues preceding the scissile peptide bond. The extended conformation of the substrate in the antiparallel beta sheet is referred to as the "canonical conformation". Because of the canonical conformation, the substrate's side chains point in alternating directions (Hedstrom, 2002). In the nomenclature proposed by Schechter and Berger (Schechter and Berger, 1967), P1 denotes the peptide residue on the acylgroup side of the scissile bond and the adjacent residues are numbered outward P2-Pn, respectively. The corresponding substrate binding pockets on the enzyme are termed S1-Sn, respectively. Similarly, the residues on the substrate's leaving group side are termed P1'-Pn' and their binding pockets on the enzyme S1'-Sn', respectively.

As mentioned in paragraph 1.2, the preferred amino acids binding to the S1 pocket allows further subdivision of subfamily S1(A) proteases. Specificity of the S1 binding pocket lying adjacent to Ser195 is mainly determined by the residues at positions 189, 216 and 226 (Czapinska and Otlewski, 1999). Interestingly, exchanging the S1 binding pocket residues does not efficiently convert the specificity of one subfamily member to that of another one. Thus, to obtain for example a significant chymotrypsin-like activity of the trypsin framework additional mutations in surface loops are required (Hedstrom et al.,

1994). However, since crystal structure analysis revealed that mutations in the S1 pocket had unanticipated effects on the arrangement of the catalytic center, it is likely that the additional loop mutations were necessary to simply counterbalance these effects (Szabo et al., 2003a).
Substrate specificity as a real measure of protection from unwanted proteolysis is of cause only realized when additional binding pockets display clear side chain selectivity as observed for enteropeptidase in which ideally four aspartate residues bind to pockets S2-S5 (Lu et al., 1999). Another possibility to generate protection via specificity is realized in induced fit proteases like complement factor D, which only upon binding of its natural substrate, the complement complex C3bB, recovers from the self-inhibited state (Jing et al., 1999).
Restrictions in the expression pattern as a measure of protection might be realized by matriptase-2 and hepsin, both mainly expressed in liver and kidney in adult mice and with varying peaks also in other organs during embryonic development (Hooper et al., 2003).

Often nature makes use of a combination of the activity control mechanisms mentioned above. Virtually all mechanisms are involved in the activity control of the digestive enzyme trypsin. Trypsin is produced by the pancreas - as a zymogen as a first safety measure to prevent digestion of this organ. Trypsinogen, accidentally activated in this organ is inhibited by kunitz-type inhibitors like bovine pancreatic trypsin inhibitor. A further safety measure is the storage in zymogen granules thought to be resistant to enzymatic degradation. Besides, the four aspartate residues preceding the Lys15 in the zymogen activation region are thought to reduce self-activation or activation by other proteases produced by the pancreas (Voet&Voet, 1995). Upon secretion into the duodenum trypsinogen is activated by enteropeptidase. Enteropeptidase with its very restricted expression in the duodenum activates by cleaving trypsinogen's DDDK15 motif with high specificity. Trypsin activates further zymogens ranging from in turn enteropeptidase and trypsin, to chymotrypsins, elastase, kallikreins and carboxipeptidases that in concert digest peptides from food uptake. After nutrition-substrate depletion, trypsin and the other proteases inactivate themselves by self-cleavage (Szmola and Sahin-Toth, 2007) - the final control and recycling step.

1.4.1 Possible ways of initial enteropeptidase activation

There is a theoretical “egg-hen” problem in the trypsin activation model. How does the first trypsinogen become activated if mainly trypsin activates its activator enteropeptidase (Lu et al., 1997). Actived enteropeptidase might reside in the sober duodenum starting very early in development without causing harm due to the high cleavage motif specificity, its low concentration and also because of being membrane-bound to the mucous-coated duodenum wall. However, initial enteropetidase activation might well occur via trypsin since once in the duodenum trypsinogen is not longer strictly controlled by high inhibitor concentration. Single trypsin molecules, capable of starting a snowball-like amplification of active proteases, will be generated by one way or the other. Interestingly, not only proteases surviving their gastric journey are candidate initial activators of trypsin or enteropeptidase. Even peptides might do the job since it was shown that the free dipeptide Ile-Val, by binding in the Ile16-cleft, can form a salt bridge to Asp194 that leads to catalytically active trypsinogen form (Khan and James, 1998). Besides, duodenase was proposed to be the initial activator of enteropeptidase (Zamolodchikova et al., 2000). However, if this was true, is would only shift the problem to another zymogen. Nonetheless, “shifting” up the activation cascade might be adequate; eventually proteases with a zymogen activity similar to that of tPA might be encountered. Alternatively somewhere up the activation cascade another type protease might be found, that is not activated as a zymogen.
A surprising observation was that for human enteropeptidase the DDDK15 motif is not needed for trypsin activation (Nemoda and Sahin-Toth, 2005). It was argued that exosite interactions ensure efficient trypsin activation in this case. At least partially, these exosite interactions reside on the one or several of the seven noncatalytic domains of enteropeptidase (Lu et al., 1997). Exosite interactions, as further elements of substrate specificity are extensively used by coagulation proteases (Page et al., 2005).

1.4.2 Allosteric Regulation and Exosite Interactions in Thrombin

Thrombin is famous for its dual role in blood coagulation (Griffin, 1995). The varying activities of thrombin are strongly dependent on exosite interactions, interactions of substrate molecules with the protease via regions other than the catalytic cleft. In thrombin exosite interactions are thought to reside mainly if not completely on the protease domain. There are two exosite interaction regions found in thrombin that are conserved in family S1 proteases. Exosite I overlaps with a potentially calcium binding loop (Page et al., 2005), a site of allosteric regulation (see below). On the opposing side

of the catalytic cleft locates exosite II. Exosite II bears a high number of positively charged residues and is the main interaction site for polyanionic ligands like glucosaminoglycans and heparin (Carter et al., 2005).

Varying exosite interactions of the thrombin protease domain with different substrates are crucial for the procoagulant and anticoagulant functions. Na^+-binding allosterically regulates specificity and promotes these opposing effects of thrombin (Di Cera, 2007). In general, family S1 proteases are known to be allosterically regulated by Na^+ if tyrosine is present in position 225 (like in thrombin) and sodium-insensitive if this position is occupied by proline (Dang and Di Cera, 1996). Binding of the sodium ion orients Asp189 in the S1 pocket and, via a network of buried water molecules, positions Ser195 for catalysis (Pineda et al., 2004). Additional allosteric effects in several family S1 proteases are mediated by Ca^{2+} complexation via acidic side chains of peptide residues in the 70-80 loop. However, thrombin is Ca^{2+}-insensitive because its Lys70 side chain occupies the position of the calcium ion.

In the concrete case of thrombin, Na^+-binding determines whether several interactions of the protease domain lead to blood clot formation or to the activation of protein C .

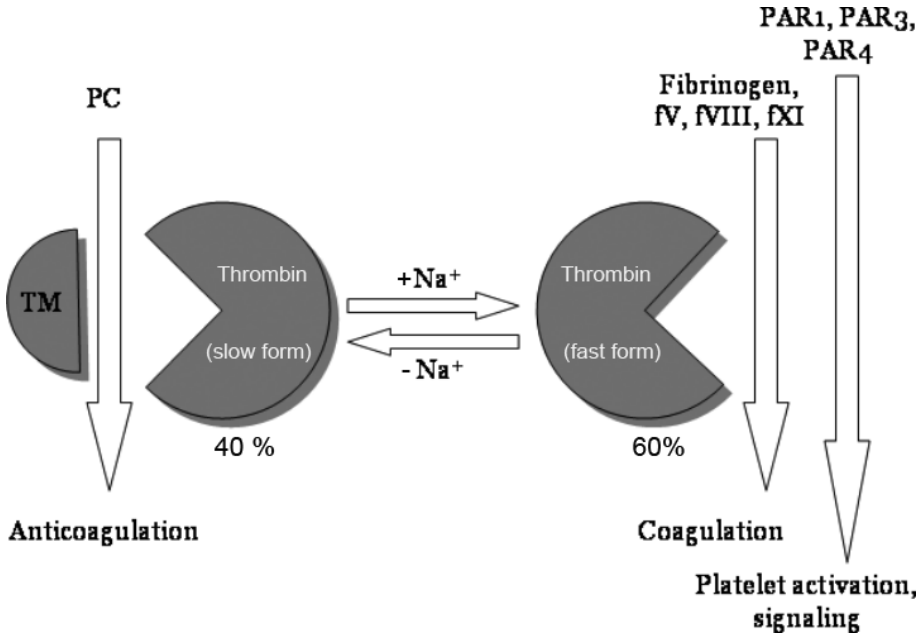

Figure 1.5: Schematic representation of the sodium-dependent multiple roles of thrombin. Under physiological conditions 60 % of all thrombin molecules in the blood are in the sodium-bound form. This allows efficient activation of factors V, VIII and XI leading to coagulation. This thrombin form also efficiently induces signaling by cleaving protease activated receptors (PARs) 1, 3, and 4. All effects that abolish sodium-ion complexation favor association of thrombin with its cofactor thrombomodulin (TM) leading to protein C (PC) activation and the resulting anticoagulating effects. Modified from (Di Cera, 2007).

Under physiological sodium concentrations 60 % of thrombin is in the sodium-bound form (Di Cera, 2007) which allows fibrinogen cleavage (leading to fibrin polymers), transglutaminase activation (crosslinks the polymers thereby stabilizing the fibrin clot) and activation of molecules upstream of its own zymogen (factors V, VIII and XI), further accelerating and strengthening the coagulation cascade (Voet and Voet, 1995). Besides, the sodium-bound form of thrombin efficiently activates protein coupled receptors (PAR1, PAR3 and PAR4) by cleavage, leading to cell signaling and, in the case of blood coagulation, to platelet activation and aggregation (Coughlin, 2000). The other 40 % of thrombin are sodium-free and incapable of promoting physiologically relevant fibrin or PAR1 activation (Page et al., 2005). However, upon binding to the cofactor thrombomodulin this thrombin form efficiently activates protein C, which cleaves and inactivates factors V and VIII leading to a shut down of the coagulation cascade (Esmon, 2003). Interestingly, by mutating only two surface residue, the protein C activating effect of thrombin becomes so dominant that the coagulation protease thrombin gains interest as antithrombotic agent (Gruber et al., 2007).

1.5 The Extracellular Matrix (ECM)

Extracellular matrix proteins are a prerequisite for the existence of multi-cellular organisms (Patthy, 2003). In cartilage and bone the ECM is dominant for the function of these tissues, whereas in many organs the ECM functions as glue between cells. A lot of signaling in this glue ensures proper functioning and adaptations to changing needs of the organism. The ECM has three main components. The (I) collagens, differentially combined from a large variety of alpha subunits, render stability and flexibility to the ECM. The (II) linking proteins like fibronectin and laminin mediate interactions between the various parts of the ECM and build the connections between ECM and cells via the integrin family of cell surface receptors. The (III) proteoglycans fill most of the space in the ECM by generating a hydrated gel via their attached glycosaminoglycans (GAGs). GAGs consist of large unbranched polymers composed of 20-200 repeating disaccharide units. Depending on the disaccharide units one differentiates between chondroitin/dermatan sulfate, heparin/heparan sulfate, and keratan sulfate and hyaluronan GAGs (Bandtlow and Zimmermann, 2000; Kjellen and Lindahl, 1991). Proteoglycans bind many growth factors, proteases, and protease inhibitors, mainly via their GAGs. In part this provides the basis for the signaling function of the ECM (Flaumenhaft and

Rifkin, 1991). In addition, proteoglycans have signaling function by themselves. As observed for example in agrin (Bezakova and Ruegg, 2003) in which the physiological effects are at least partially dependent on proteolytic processing by the S1 family protease neurotrypsin (Reif et al., 2007). The same is true for the other components of the ECM. For example in fibronectin, cleaved by the S1 family protease human kallikrein 8 or in type IV collagen, cleaved by the matrix metallo protease 9, proteolytic processing is necessary to liberate the signaling function of certain protein fragments (Hamano et al., 2003; Sher et al., 2006). The fragments are thought to possess antiangiogenic properties mediating favorable outcomes in cancer. This is evidence for the emerging roles of proteases in tumor suppression (Lopez-Otin and Matrisian, 2007) in addition to the long known effects of proteases in tumor progression by e.g. increased tumor cell motility upon matrix degradation.

1.6 FGF-2

FGF-2, also known as basic fibroblast growth factor, is a heparin binding molecule (Gleizes et al., 1995). This prototypic member of a family of 22 proteins is an ubiquitous growth factor conserved throughout the eukaryotic world (Yu et al., 2007a). FGF-2 signaling contributes to proliferation, angiogenesis, cell survival, migration and differentiation (Mason, 1994).

FGF-2 is peculiar in many ways. For example, it can be found in the cytosol, the nucleus and in the extracellular space. While most extracellular proteins in eukaryotes are secreted via the endoplasmic reticulum (ER)/Golgi dependent main export route (Lee et al., 2004), FGF-2 belongs to the small group of unconventionally secreted molecules (Cleves, 1997; Nickel, 2005). Consistently, FGF-2 lacks post-translational modifications of the type added in the ER/Golgi complex and, for example, does not contain disulfide bridges involving any of its four cycteines (Arakawa et al., 1989).

Recently, it was shown that heparan sulfate proteoglycans are essential for the unconventional FGF-2 secretion - probably ensuring directionality of the transport by serving as molecular traps (Zehe et al., 2006). Upon secretion, FGF-2 is stored bound to proteoglycans and mediates short-range signaling in the ECM but also mediates long range signaling by traveling attached to proteolytically processed proteoglycans (Hou et al., 2007). Interestingly, FGF-2 signaling is not always depend on FGF-receptor mediated phosphorylation cascades. To induce proliferation, FGF-2 is translocated to the nucleus

upon import from endosomes. This import was recently shown to require the cytosolic chaperon Hsp90 (Wesche et al., 2006). Another noteworthiness of FGF-2 is the existence of high molecular weight (HMW) isoforms (four in human with molecular masses of 22, 22.5, 24 and 34 kDa, respectively) that are generated upon translation from unconventional CUG start codons (Arnaud et al., 1999). Translation of only the low molecular weight (LMW) form of FGF-2 (most often referred to as “18 kDa form”, although the full-length protein containing 155 amino acids has a molecular mass of 17.2 kDa) starts from a conventional AUG codon (Figure 1.6).

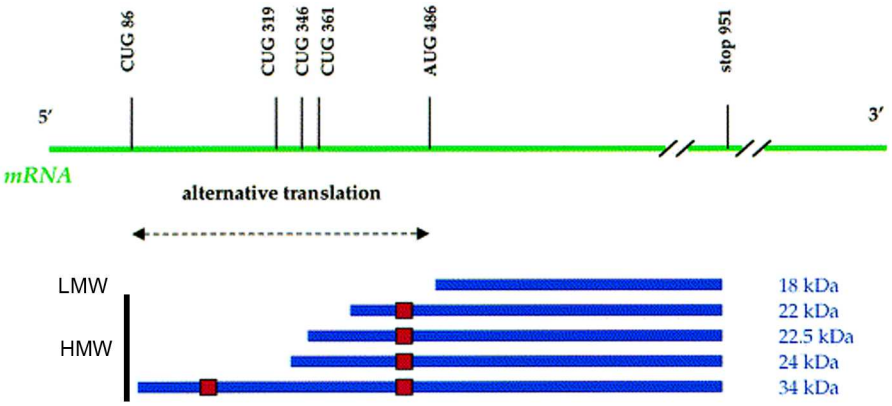

Figure 1.6: Schematic representation of FGF-2 isoforms resulting from alternative translation. In the upper part, the human FGF-2 mRNA is shown in green with the relative positions of translation starts and stop indicated. Below, the low-molecular weight (LMW) form and the four different high-molecular weight (HMW) isoforms of FGF-2 are shown with nuclear localization signals depicted in red. Figure adapted from (Okada-Ban et al., 2000).

Post-translational methylation of arginines in the RG-rich N-termini of HMW FGF-2 isoforms leads to nuclear accumulation (Klein et al., 2000). Oxidative stress induces increased secretion of all variants (Yu et al., 2007b). Such effects likely influence the various biological roles of FGF-2. More complexity in the mode of action is introduced by FGF-2 proteolysis. Thrombin converts the HMW forms of FGF-2 to a LMW-like form. These cleavages convert cell transforming and cell migration arrest effects of HMW FGF-2 to the proliferative and pro-migratory effects of the short form (Yu et al., 2007b).

1.7 Introduction of Selected Family S1 Proteases in the Nervous System

Also in the central nervous system (CNS) proteases of family S1 play important roles. Like in other organs, they exert their function by inducing signaling via cleavage of PARs, release of signaling molecules or the processing of growth factors. And like in blood coagulation family S1 members in the CNS participate in peptidase cascades or degrade ECM components like in other tissues. In the CNS, however, some of the proteolytic processes lead to effects exclusively associated with the function of this organ. These effects include axonal outgrowth, synapse elimination (Figure 1.7) and structural plasticity associated with learning and memory ((Molinari et al., 2003); and references therein).

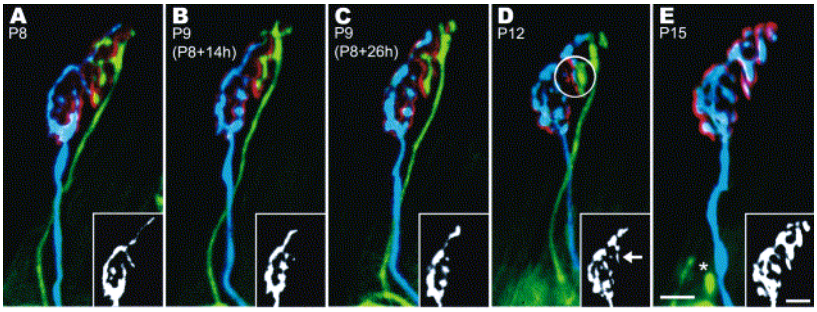

Figure 1.7: Impressive *in vivo* fluorescence microscopy follow-up pictures illustrating the process called synapse elimination: At post natal day 8 (P8), two axons, two axons (labeled with different fluorescent proteins) innervate the same neuromuscular endplate. In the following days the axons compete for the control of the entire muscle nerve interaction interface. On P15, the blue axon won the battle while the green labeled axon retracted completely. Scale bars equal 10 µm, pictures taken from (Walsh and Lichtman, 2003).

The family S1 proteases with a specialized function in the CNS are often known already to play important roles in other processes. Thrombin for example, encountered already in the blood coagulation, potentiates the NMDA (*N*-methyl-*D*-aspartate) receptor activity in the hippocampus via PAR-activation. This leads to long-term potentiation (LTP) of synaptic strength (Gingrich et al., 2000). LTP and long-tern depression (LTD), the reduction of electric efficacy of synapses are associated with the only morphological changes observed in processes of memory formation and learning (Kandel, 2001). PARs are widely expressed in the brain (Striggow et al., 2001). However, it is likely that thrombin might not promote all of its effects on neuronal survival and migration by activating these receptors but as well by using other signaling pathways e.g. involving FGF-2 processing (Yu et al., 2007b).

Another example of a famous protease with a specialized function in the brain is tissue-type plasminogen activator (tPA). In the blood, tPA activates plasmin resulting in fibrin degradation and clot dissolution. In the brain increased levels of tPA were detected upon

motor learning sessions and LTP induction (Qian et al., 1993). Mice in which the tPA gene was knocked out showed impaired motor learning (Seeds et al., 2003). Probably, in this process tPA cleaves plasminogen like in the blood. In the CNS, plasmin cleaves the proform of brain-derived neurotrophic factor (proBDNF) and it was shown that tPA/plasmin-dependent release of BDNF is essential for LTP in the hippocampus (Pang et al., 2004).

On the other hand, there are family S1 proteases that appear to exert their function predominantly in the CNS. For example mouse neuropsin (human tissue kallikrein 8, mentioned already for its reducing effect on tumor cell invasiveness (Sher et al., 2006)) is predominantly expressed in pyramidal neurons of the hippocampus and influences synapse formation by cleaving the presynaptic adhesion molecule L1 (Matsumoto-Miyai et al., 2003). Another example is neurotrypsin. mRNA expression of neurotrypsin is upregulated in many brain regions of mice in the developmental stage around birth (Wolfer et al., 2001). As mentioned, neurotrypsin cleaves agrin (Reif et al., 2007), thereby exerting a crucial role during the establishment of the neuromuscular junction (Bolliger, in prep.) in mice. The absence of neurotrypsin activity in the brain leads to severe mental retardation in humans (Molinari et al., 2002).

1.8 Type II Transmembrane Serine Proteases

More than 20 % of all human proteases are membrane-bound, which emphasizes the relevance of proteolytic activity at this cellular interface (Puente et al., 2003a). Recently performed extensive database analyses and experimental screens revealed the existence of a novel family S1 protease subgroup named type II transmembrane serine proteases (TTSPs) ((Hooper et al., 2001; Netzel-Arnett et al., 2003; Szabo et al., 2003b; Wu, 2003); and others) with more than 30 mammalian members to date (Kyrieleis et al., 2007). Enzymes of this subgroup are composed of a usually short cytosolic N-terminus, a single transmembrane helix, a stem region containing a variable set of six different noncatalytic domains (low-density lipoprotein receptor class A (LDLA), SEA, Frizzled, MAM, CUB, and Group A scavenger receptor domain), and the C-terminal trypsin-like protease domain. TTSPs are divided into four subfamilies (Figure 1.8) based on the phylogenetic analysis of their protease domain, the composition of their stem region, and the chromosomal location of their genes (Szabo et al., 2003b). Their genes, as is the case for other proteases, are often organized in clusters, suggesting evolution via gene duplication (Puente et al., 2003a). The N-terminal segments of TTSPs might interact with cytosolic

components like the cytoskeleton and often contain phosphorylation sites. However, no study addressed the function of these segments till date.

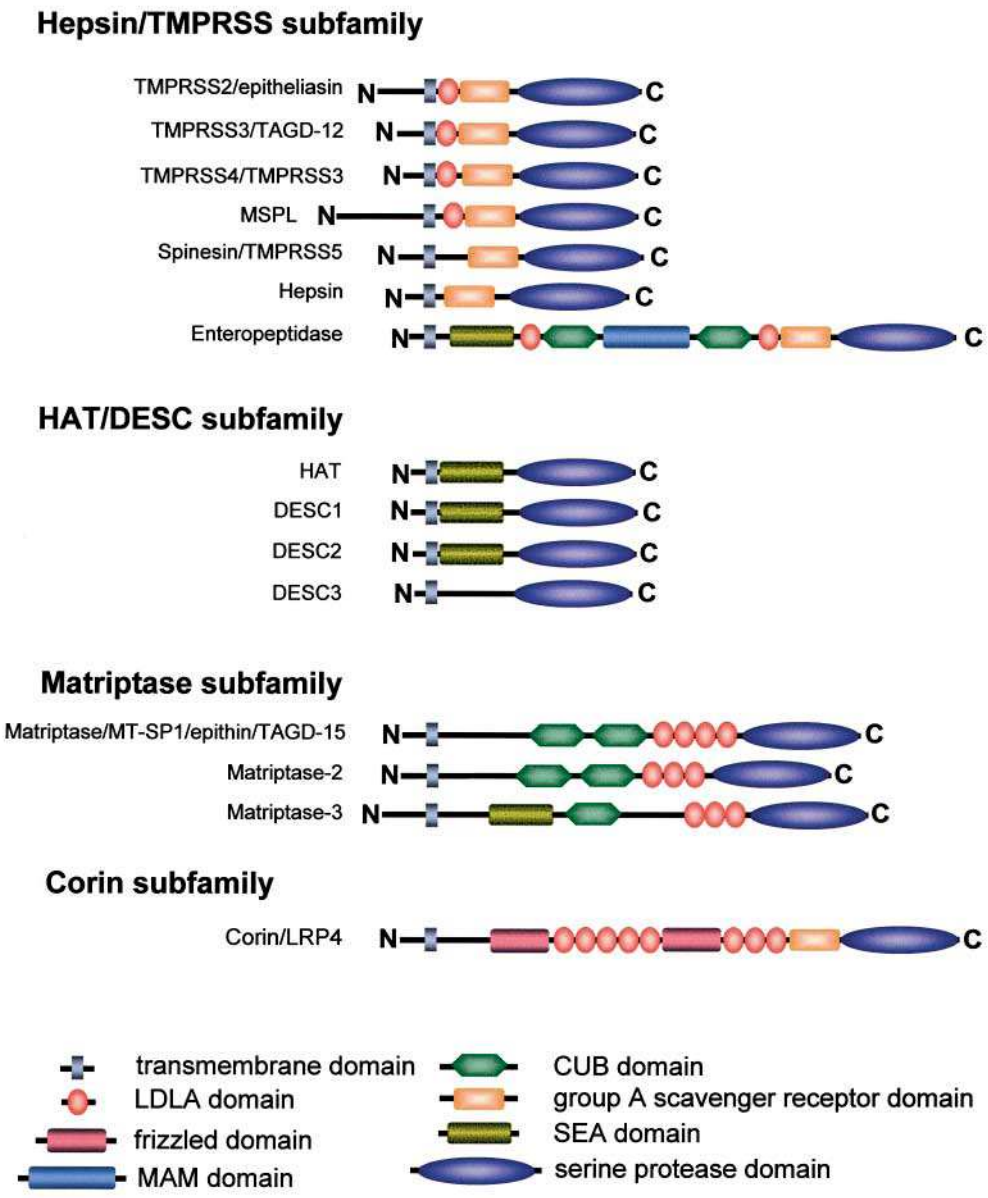

Figure 1.8: Schematic representations of the fifteen best-known human TTSPs grouped into the four subfamilies. Taken from (Szabo et al., 2003b).

The non-catalytic domains in the stem region might be important for substrate interaction as already mentioned for the human form of the TTSP enteropeptidase (Lu et al., 1997). Additionally, these domains are involved in targeting the molecule to secondary

interaction partners on the cell surface or in the ECM and contribute to the orientation of the catalytic domain (Kyrieleis et al., 2007). The non-catalytic domains of TTSPs also contribute to the activation of the enzyme. Interestingly, in such processes even non-enzymatic hydrolysis of peptide bonds might play a role. For example in the sophisticated activation process of matriptase, which involves transient interactions with its cognate inhibitor HAI-1 via LDLA domains(List et al., 2006), hydrolysis after Gly149 in the conserved G-SVIA motif in the SEA domain always occurs during activation under physiological conditions (Oberst et al., 2003). Recently, SEA domain autohydrolysis was discussed as a general way to enable dissociation as a result of mechanical rather than chemical stress on apical cell membranes (Macao et al., 2006).

Physiological functions of TTSPs were increasingly uncovered in recent years. The identification of mutations in the gene coding for TMPRSS3, in patients with congenital autosomal recessive deafness, suggested a role of this TTSP in hearing (Scott et al., 2001). Ablation of the matriptase gene in mice demonstrated a critical role of this TTSP in the development of the epidermis, hair follicles, and cellular immunity (List et al., 2002). Transgenic overexpression of matriptase caused spontaneous squamous cell carcinoma and potentiated carcinogen-induced tumor formation (List et al., 2005). Mice with a null mutation in the gene encoding the TTSP corin developed hypertension (Chan et al., 2005). Deletion of the hepsin gene in mice demonstrated a significant role of this protease in auditory function (Guipponi et al., 2007). Experimental overexpression of hepsin promoted prostate cancer progression and metastasis (Klezovitch et al., 2004). Such findings underscore the involvement of TTSPs in a variety of vital functions.

Molecular analysis of TTSP proteolytic activity allowed the identification of a broad spectrum of possible substrates. Matriptase-2 multiply cleaved type I collagen and fibronectin (Velasco et al., 2002). TMPRSS3 activated epithelial sodium channels (Guipponi et al., 2002). TMPRSS2 activated protease-activated receptor-2 in prostate cancer cells (Wilson et al., 2005), and hepsin cleaved and activated pro-hepatocyte growth factor and pro-urokinase (Kirchhofer et al., 2005; Moran et al., 2006).

Many TTSPs show a restricted expression pattern, suggesting tissue-specific functions. Enteropeptidase, e.g., is confined to the proximal part of the small intestine and acts as an activator of trypsinogen (Yuan et al., 1998). Corin is mainly present in heart myocytes (Hooper et al., 2000) and mediated pro-atrial natriuretic peptide activation (Yan et al., 2000). Interestingly however, corin was recently reported to be also expressed in the dermal papilla of all pelage hair follicle types (but nowhere else in skin) and to be responsible for the coat color development in agouti mice (Enshell-Seijffers et al., 2008).

HAT (human airway trypsin-like) is predominantly expressed in the trachea (Yamaoka et al., 1998) and DESC1 (differentially expressed in squamus cell carcinoma) is expressed in skin, additionally in the salivary gland and epididymis (Hobson et al., 2004). Together these two TTSPs give name to the yet scarcely investigated HAT/DESC subfamily with five members in humans and seven members in mice (Hobson et al., 2004), located in clusters on chromosome 4q13.3 and 5E1, respectively (Figure 1.9).

DESC1 was initially found being downregulated or absent in squamus cell carcinoma of the head and neck and thus, was suggested as a tumor marker (Lang and Schuller, 2001). Recently however, exogenous DESC1 expression was shown to confer tumorigenic properties to Madin-Darby canine kidney cells and DESC1 was found upregulated in tumors originating from tissues of different origin than the head and neck (Viloria et al., 2007). DESC1 might have a physiological role in normal keratinocyte differentiation (Sedghizadeh et al., 2006).

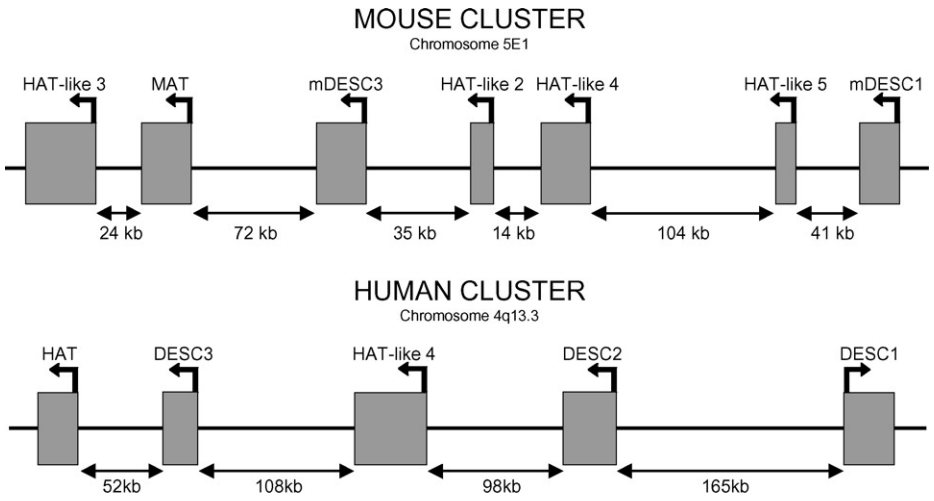

Figure 1.9: Schematic representation of the gene clusters of the HAT/DESC TTSP-subfamily in mice and man, with seven and 5 members, respectively. Taken from (Hobson et al., 2004).

In the nervous system, only spinesin was so far identified as a TTSP expressed by neuronal cells (Yamaguchi et al., 2002). The function of spinesin is not known till date.

2 Aim of the project

In view of the complex differentiation processes of the nervous system, it is evident to assume that many proteases of family S1, including known and possibly novel TTSPs, are involved. This assumption is supported by results of extensive mouse genome analyses that predict the existence of more than 220 serine protease genes or pseudogenes (Puente et al., 2003b). Therefore, the first aim of the project was to obtain an inventory of trypsin-like serine proteases expressed during CNS development and during such fascinating differentiation processes as synapse elimination.

Therefore, we established a PCR-based screening approach using postnatal day 10 (P10) mouse spinal cord. We detected expression of at least 21 non-TTSP serine proteases and five known TTSPs. Additionally, we discovered a novel TTSP which became subject of our characterization attempts.

3 Results

3.1 Generation of a protease domain enriched cDNA library and library screening by colony hybridization

To estimate the number of serine proteases expressed in differentiating mouse spinal cord, we generated and screened a serine protease domain-enriched cDNA library. The library contained the 400 – 600 bp products of a PCR in which cDNA from P10 mouse spinal cord mRNA had been used as template with degenerated primers. The primers were designed to anneal to the regions of His57 and Ser195 (chymotrypsin numbering as proposed by (Bode et al., 1989)), the most conserved motifs in the catalytic triade of trypsin-like serine proteases. To design the primers we used the alignment of 177 sequences of known and postulated serine proteases (http://supfam.org/SUPERFAMILY/index.html, version 1.61). After the elimination of 48 false positive entries among the postulated proteases, e.g. hepatocyte growth factor like sequences, the most prevalent sequences in the alignment were *WVLTAAH57C* and *GDS195GGP* (Figure 3.1). Four degenerated primers allowing codons of these and a few other amino acids and introducing a 5' endonuclease restriction site (EcoRI) were ordered (Figure 3.2).

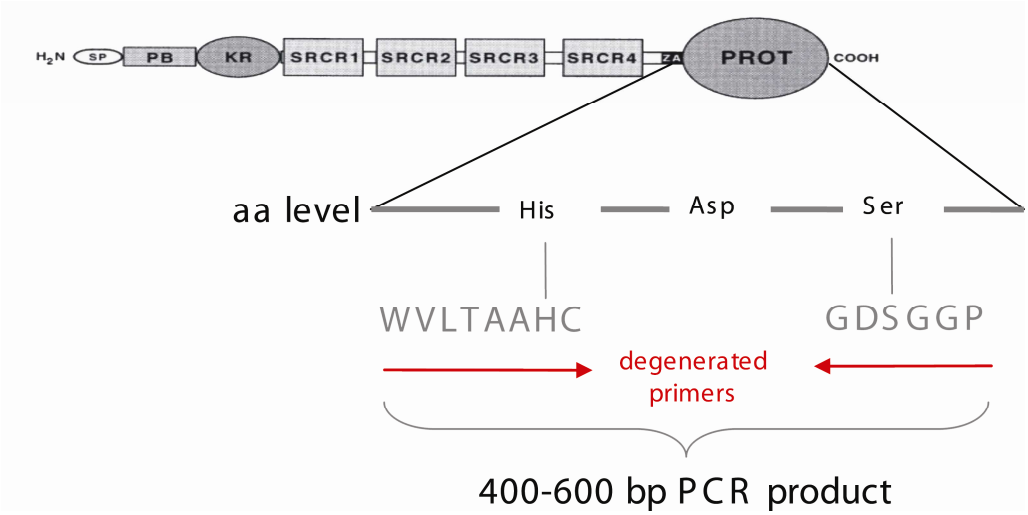

Figure 3.1: Human Neurotrypsin with its noncatalytic N-terminal domains is depicted as a typical example of a trypsin-like serine protease. The sequence of the protease domain (PROT) is relatively well conserved amongst trypsin-like serine proteases. The order of its catalytic triad in the amino acid (aa) sequence is shown. Especially in the region around His57 and Ser195 the sequence is highly conserved (the most prevalent sequence is shown). Degenerated primers annealing in this region result in PCR products of the indicated length for most members of this protein family.

First, combinations of the four primers were tested on a mixture of 10 pg plasmid containing the mouse neurotrypsin sequence. The primer-combination +PrimerH long and –PrimerS short gave a very clear single PCR product band with our pretest conditions. For this degenerated primer pair, DMSO and Mg^{2+}- ion concentrations as well as annealing temperature and cycle number were subsequently optimized in PCR with single-stranded cDNA as template. The PCR products of 400 to 600 bp in length were purified and ligated into pBlueskriptSK+ vector via the EcoRI sites. We realized a strong bias towards small inserts of around 200 bp. The problem was solved by introducing a second gel purification step of the PCR products prior to ligation (it also became obvious that the planned use of X-Gal based blue/white colony selection was not necessary since even the small population of blue *E.coli* colonies contained inserts). With annealing temperatures of 42, 45 and 47 °C, three differently composed subsets of the library were generated. Sequence analysis of 50 clones demonstrated that about 50, 85 and 90%, respectively, of the clones in the library indeed contained plasmids with protease domain inserts.

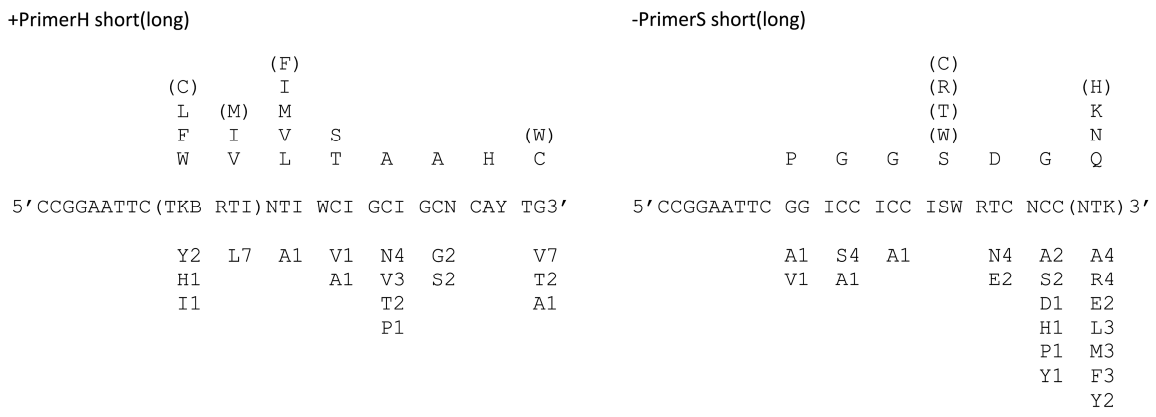

Figure 3.2: The four tested primers are shown. Above the primer sequence, the amino acids encoded by the degenerated codons are given (amino acids encoded but not observed in our protease domain alignment, are given in brackets). Below the amino acids not encoded by the degenerated primers are given followed by a number. The numbers (in percent) indicate that less sequences of the alignment harbored this amino acid in the particular position.

The library screening was performed in an iterative two-step manner. First, clones were randomly selected and submitted to DNA sequencing. Secondly, sequences occurring frequently in this selection were used to generate digoxigenin-labeled DNA probes to deselect identical clones by colony hybridization. Probes were first tested for crossreactivity on dot-blotted plasmids (Figure 3.3). After two rounds of screening six probes were in use (tissue-type plasminogen activator, neurotrypsin, hepsin, neurosin, neuropsin and myeloid associated differention marker - a non protease sequence encoding the amino acid stretches DYTGAAH and GGGGGP separated by 450 bp) that turned out to be applicable in

combination, to label all clones containing sequences of the above molecules (Figure 3.3). False positive labeling of other sequences was never observed sequencing labeled clones. Figure 3.4 gives a flowchart of the library construction and screening process. Our screening assessed about 5'000 colonies of which 420 were not labeled and therefore sequenced. We found 27 different serine proteases. Interestingly, only eight of these proteases were so far described to be expressed in the nervous system, whereas another 18 serine proteases were not associated with CNS tissue before. Since the multiple use of the same serine protease in different processes was already learned from enzymes such as thrombin, plasmin or tPA, (first known for their specific function in blood clot formation/dissolution and meanwhile recognized as players in tissue remodeling), it was not unexpected that a sensitive analysis would identify more than the previously reported eight serine proteases. Besides the 26 trypsin-like serine proteases listed below (Table 3.1) we could identify a clone coding for a formally unknown serine protease. We designated this trypsin-like serine protease neurobin (neuronal and Ca-independent like thrombin) later on.

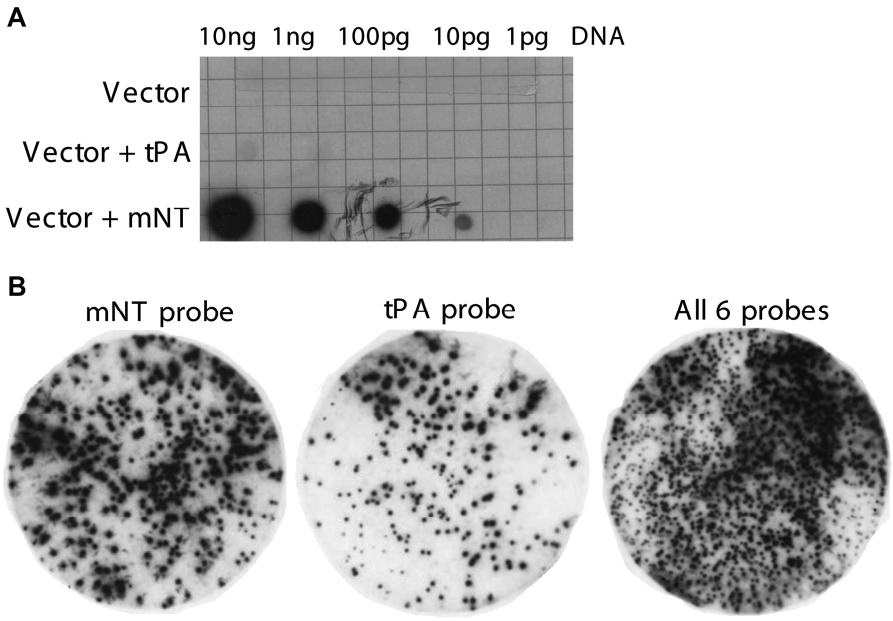

Figure 3.3: Crossreactivity testing of the digoxigenin- labeled probes. A, DNA, as indicated at the left margin was blotted onto a nylon membrane and UV-linked. The membrane was incubated with the digoxigenin-labeled neurotrypsin probe. Crossreactivity was so low that all probes could be used in combination in colony-hybridations (round nylon membranes). As revealed by DNA sequence analysis, colonies from black or gray signals only contained sequences corresponding to the probes.

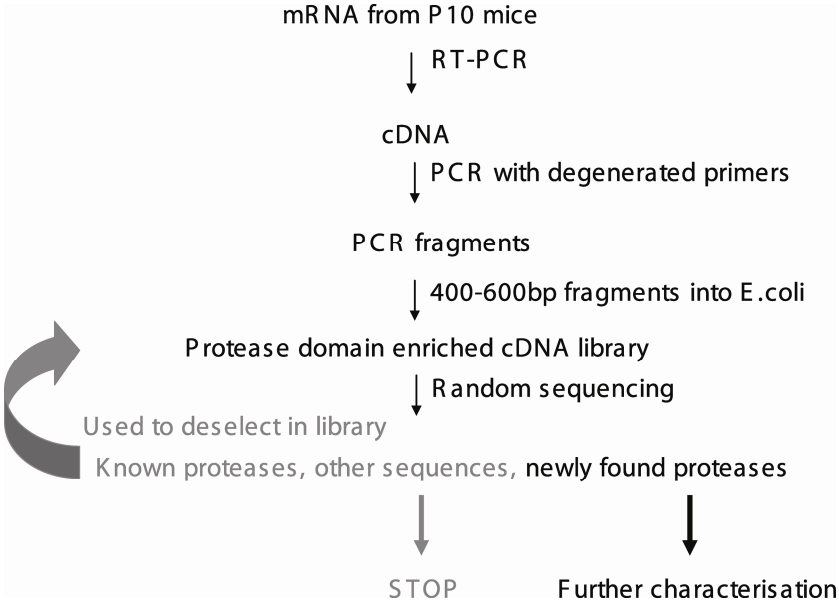

Figure 3.4: Flowchart describing the generation and screening of our trypsin-like-protease-domain-enriched cDNA library.

hepsin	elastase 2
airway trypsin-like serine protease	kallikreinB
myonase/mast cell protease 4	kallikrein 5
mast cell protease 5	Kallikrein 1-related peptidase b8
mast cell protease 8	kallikrein 24
elastase I	**tissue-type plasminogen activator**
trypsin 15	**neurotrypsin**
acrosin	**thrombin**
matriptase/epithin	**plasmin**
complement component factor I	**neuropsin**
intestinal serine (8) protease	**neurosin**
neutrophil elastase	**transmembrane serine protease 3**
chymopasin	**spinesin**

Table 3.1: Of the 26 known proteases (from which sequences were found in the library) only the 8 printed in bold are reported to have a function in neuronal tissue.

3.2 Neurobin full length cDNA cloning and primary sequence analysis

Having discovered a cDNA clone encoding the region between His57 and Ser195 of a new serine protease we stopped screening the library and focused on molecular cloning of

the full length cDNA of neurobin. First we combined the results of several gene prediction programs. As confirmed later on, not a single one of the programs available online at that time correctly predicted the open reading frame of neurobin over the complete sequence length. Since at least the prediction in a segment 5' to the sequence found in the clone from our library was identical with several programs, primers were designed that resulted in a PCR product encoding an N-terminally elongated fragment of neurobin. The information of the subsequent DNA sequencing allowed designing further gene specific primers that were suitable for 5' RACE. 3' RACE was performed using primers annealing to the neurobin segment initially found in the library. We retrieved several 5' and 3' RACE-sequences. Finally, using gene specific primers, a clone containing an open reading frame of 1293 bp was produced. The corresponding mRNA is of at least 1.7kb (Figure 3.5). The encoding gene maps to mouse chromosome 5E3.1. It is spread over 10 exons in a 60 kb sequence stretch. The corresponding human gene lies on chromosome 4, near q13.

The open reading frame of the isolated cDNA codes for a protein of 431 amino acids (Figure 3.5). It is very likely that neurobin indeed starts with the predicted Met residue, since two in frame stop codons, 45 and 30 bp in front of the initiation codon, respectively, are present in the 5'-nontranslated part. Thus, neurobin has a cytosolic domain of about 35 amino acids.

Hydropathy analysis indicated the presence of a single hydrophobic segment between residues 34 and 56 of the amino acid sequence from the longest ORF of the found cDNA. This segment was followed by a predicted SEA domain (sea-urchin/enteropeptidase /agrin, residues 58 to 183), a short zymogen activation segment (residues 184 to 199), and a serine protease domain (residues 200 to 431). Within the protease domain the three residues His, Asp, Ser, forming the catalytic triad of serine proteases, were found at position 240, 285, and 381, respectively, flanked by amino acids highly conserved in trypsin-like serine proteases. Apparently, looking at the motifs around H240 and S381, respectively (Figure 3.6, boxed), during PCR with degenerated primers for library construction, a single-base misspriming was allowed. Three consensus motifs for N-linked glycosylation were identified in the putative extracellular part, one in the SEA domain and two in the protease domain. These structural characteristics, together with the absence of a hydrophobic signal peptide segment at the N-terminus, provided strong evidence that neurobin is a type II transmembrane serine protease.

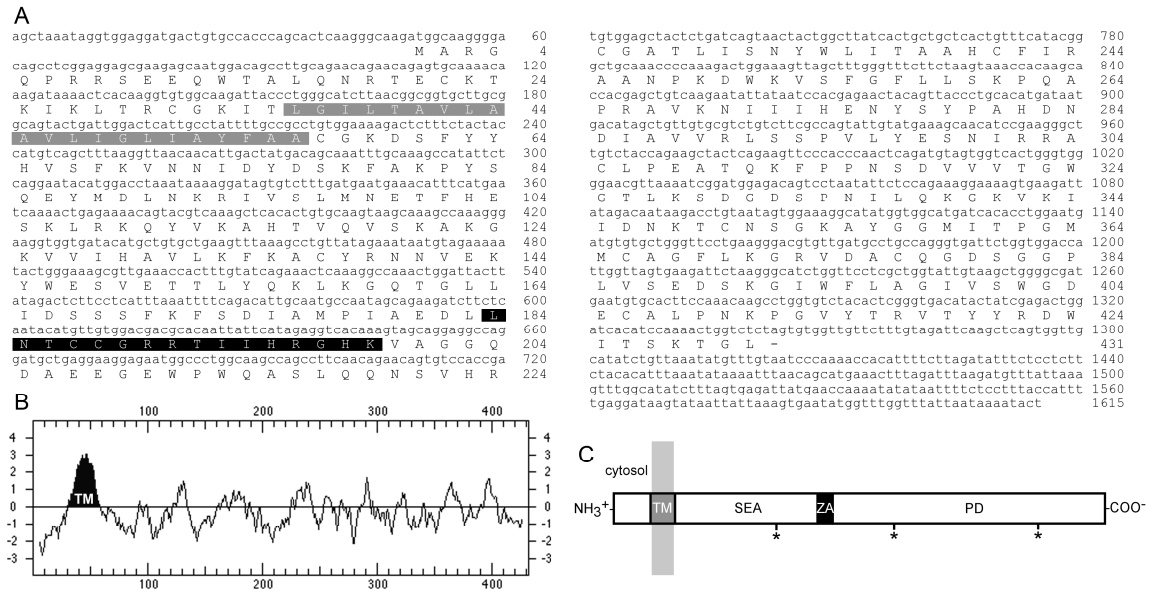

Figure 3.5: Neurobin cDNA and protein sequence and neurobin domain composition. A, The amino acid sequence of neurobin deduced from the cDNA sequence is given in single letter code. The 1615 bp cDNA from 10 (nine coding and one 3' non-coding) exons on a 60kB genomic segment on mouse 5E1 contains a 1293bp open reading frame, encoding a protein with 431 amino acids and a calculated mass of 48,07 kDa. The predicted transmembrane segment is shaded gray and the zymogen activation domain is shaded black. B, Hydropathy analysis of the neurobin protein sequence identifies a single hydrophobic segment (gray) close to the N terminus. C, Protein sequence analysis by SMART predicts a type two transmembrane protein with a 33 amino acid cytosolic N terminus, a transmembrane helix (TM, residues 34-56), an extracellular SEA domain (SEA, residues 58-183), a zymogen activation region (ZA, residues 184-199)) and a trypsin-like protease domain (PD, residues 200-431). Asterisks mark positions of glycosylation motifs.

All members of this family have a short cytosolic N-terminus followed by the transmembrane domain. Then come one to several non-catalytic domains and always localized at the C-terminus follows the protease domain. In humans this family currently consists of 14 members and can be subdivided in 4 subfamilies (Szabo et al., 2003b). The best known member of the family is enteropeptidase, which is involved in the initiation of the cascade of digestive enzymes. Neurobin belongs to the HAT (human airway trypsin-like protease)/DESC subfamily of type II transmembrane trypsin-like serine protease family (in both human and mouse the neurobin gene lies about 10kb downstream of HAT/MAT, suggesting that these two genes might have evolved by gene duplication).

3.3 Sequence analysis of the protease domain of neurobin

Six highly conserved Cys residues were identified in the protease domain (Figure 3.6). These Cys residues usually form three disulfide bonds in serine protease domains (C42-C58, C168-C182, C191-C220, chymotrypsin numbering (Bode et al., 1989)). A seventh Cys (C122) could theoretically form a disulfide bond to one of the two Cys residues present in the zymogen activation domain, thereby linking stem region and protease domain after activation cleavage. A homology search with the protease domain of neurobin uncovered highest sequence identities to the protease domains of other TTSPs such as DESC1 (58%), HAT (53%), and enteropeptidase (41%). Sequence identity to secreted serine protease like tissue-type plasminogen activator, thrombin and factorXa was 34-36% (Figure 3.6).

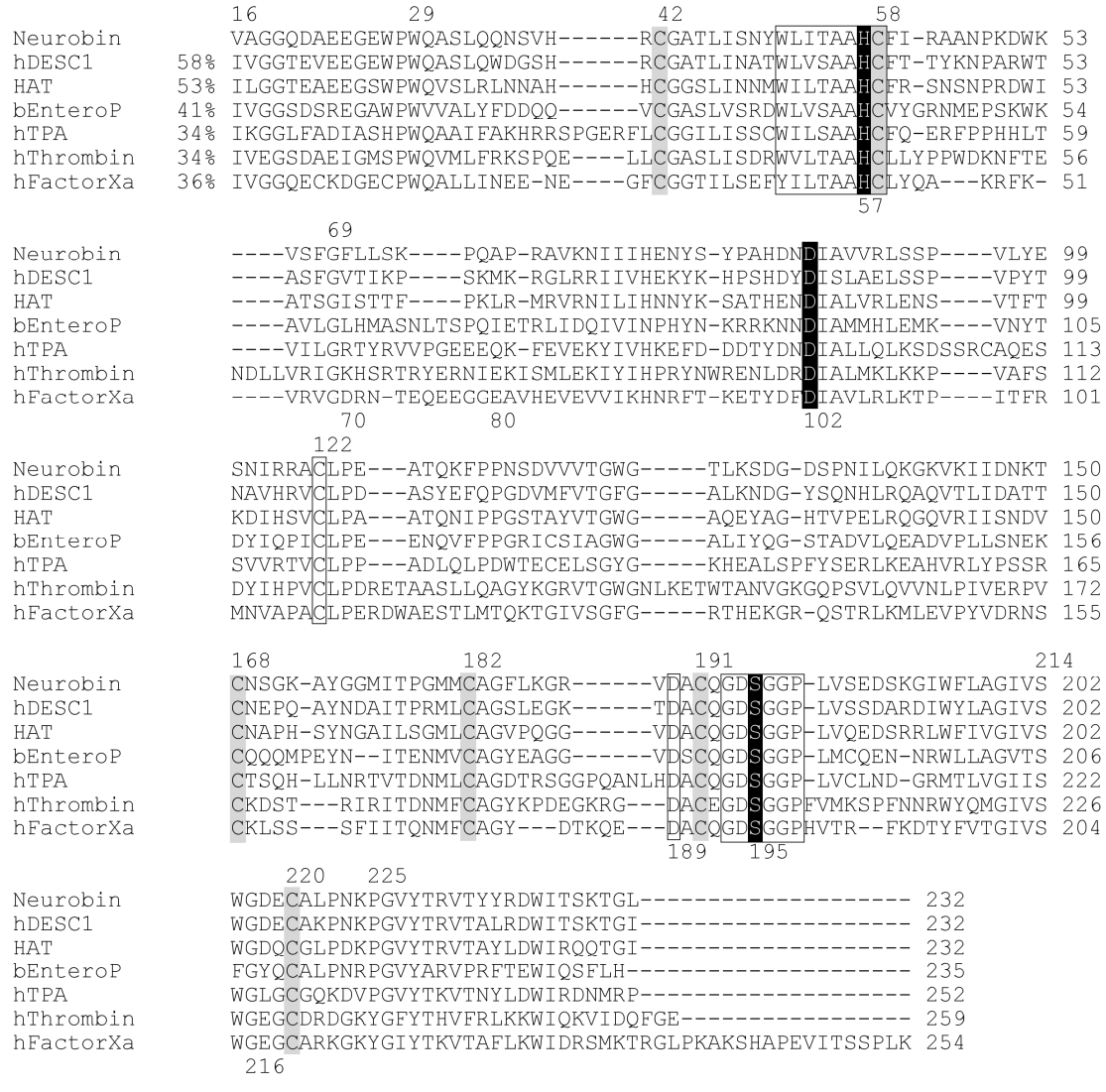

Figure 3.6: Amino acid sequence alignment of the protease domain of neurobin with selected trypsin like serine protease domains. The amino acid sequences of the protease domains of human DESC1, HAT, bovine enteropeptidase and the human variants of tissue-type plasminogen activator, thrombin

and factorXa are aligned to the protease domain of neurobin. All sequences begin with the residue following the predicted activation cleavage site. Sequence identities to neurobin are given in percent. The numbers above and below the alignment indicate amino acid positions using chymotrypsin numbering (Bode et al., 1989)). Numbers at the right margin indicate amino acid numbering of each individual protease domain sequence. Boxed in black with white letters are the residues His, Asp, Ser, forming the catalytic triad. The six Cys residues giving rise to the disulfide bridges 42-58, 168-182 and 191-220 are boxed in gray. C122 (boxed) is the residue usually forming a disulfide bridge to a Cys residue in the zymogen activation region. D189 (boxed) forms the bottom of the S1 pocket of serine proteases and determines the preference of Arg or Lys at position P1. Also boxed are the highly conserved sequence regions around His and Ser which were used to derive degenerate oligonucleotides for library construction. The alignment was generated using ClustalW (http://www.ebi.ac.uk/Tools/clustalw/index.html)

3.4 Expression of neurobin in mouse tissues

Several lines of evidence suggest that neurobin is expressed at a very low level. First, there is no EST database entry till date. Secondly, in the library only three of the analyzed clones contained the sequence (in contrast, about every third clone contained cDNA of tPA). Thirdly, in PCR with two different specific primer pairs high cycle numbers (>37) were necessary to obtain detectable product bands. Fourthly, in all our trails we failed to detect neurobin by Northern blot or *in situ* hybridization analysis, though controls worked. Hence, to investigate the tissue expression of neurobin in P10 mice we performed RT-PCR analysis. As shown in figure 3.7, neurobin was expressed in spinal cord and cerebellum. No signal was detected in cortex, heart, kidney, spleen, lung and liver, suggesting that neurobin has a rather restricted tissue distribution at this stage. Spinal cord of adult mice indicated clear expression of neurobin as well.

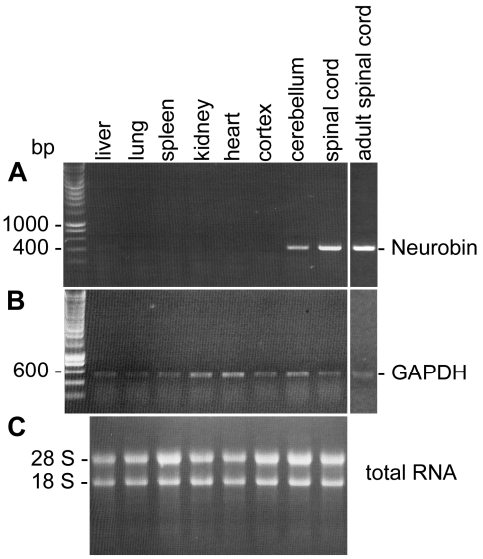

Figure 3.7: Tissue expression of neurobin in P10 mice. A, cDNA was produced from total RNA from P10 mouse tissue using oligo(dT) priming. Only spinal cord was used from P90 animals. The region encoding Neurobin C241 to V374 of the protease domain was used for amplification. The PCR products were verified by DNA sequencing. B, cDNA quality and amount were controlled in an exponential phase PCR reaction using primers for GAPDH. C, Quality of the total RNA preparations from P10 tissues is shown on an agarose/formamid gel. DNA molecular mass markers are given at the left side in (A) and (B).

3.5 Expression and activation of neurobin in transfected HEK293T cells

To study neurobin protein production and zymogen activation, we transiently transfected HEK293T cells with neurobin-encoding cDNA vectors. Protein production was tested by western blot analysis. Using neurobin-mycHis cDNA for transfection and the anti His antibody to detect the C-terminal His tag, we found a doublet signal at 53 kDa, reflecting tagged full-length neurobin with a calculated mass of 51 kDa without glycosylation (Figure 3.8a). Overexposure of the blot showed a second signal around 30 kDa, presumably the tagged protease domain after activation cleavage (not shown, but see figure 3.9). With Neurobin-mycHis S381A, a catalytically inactive mutant, only the 53 kDa product was present (Figure 3.8a). An affinity-purified antibody raised against the recombinant SEA domain of neurobin detected the 53 kDa signal as well (Figure 3.8a). We next overexpressed untagged neurobin. With neurobin Ser381Ala a doublet product at 50 kDa was found, representing full-length untagged neurobin. With overexpression of wild-type neurobin, we predominantly detected a product at 23 kDa, but virtually no 50

kDa product. None of these signals was found in control samples using empty vector for transfection (Figure 3.8a). The 23 kDa product likely represents N-terminal chain neurobin without protease domain and, thus, is evidence for efficient (auto-) activation of untagged wild-type neurobin in HEK293T cells, whereas activation of tagged neurobin is only poorly efficient.

To test glycosylation of overexpressed neurobin, HEK293T detergent extracts were treated with N-glycosidaseF and endoglycosidaseH, respectively. Neurobin was detected with the anti SEA domain antibody. The enzymatic treatment resulted in a mass shift of about 2-3 kDa of both non-activation-cleaved and of activation-cleaved neurobin (Figure 3.8b), indicating that neurobin is subject to N-linked glycosylation in HEK293T cells.

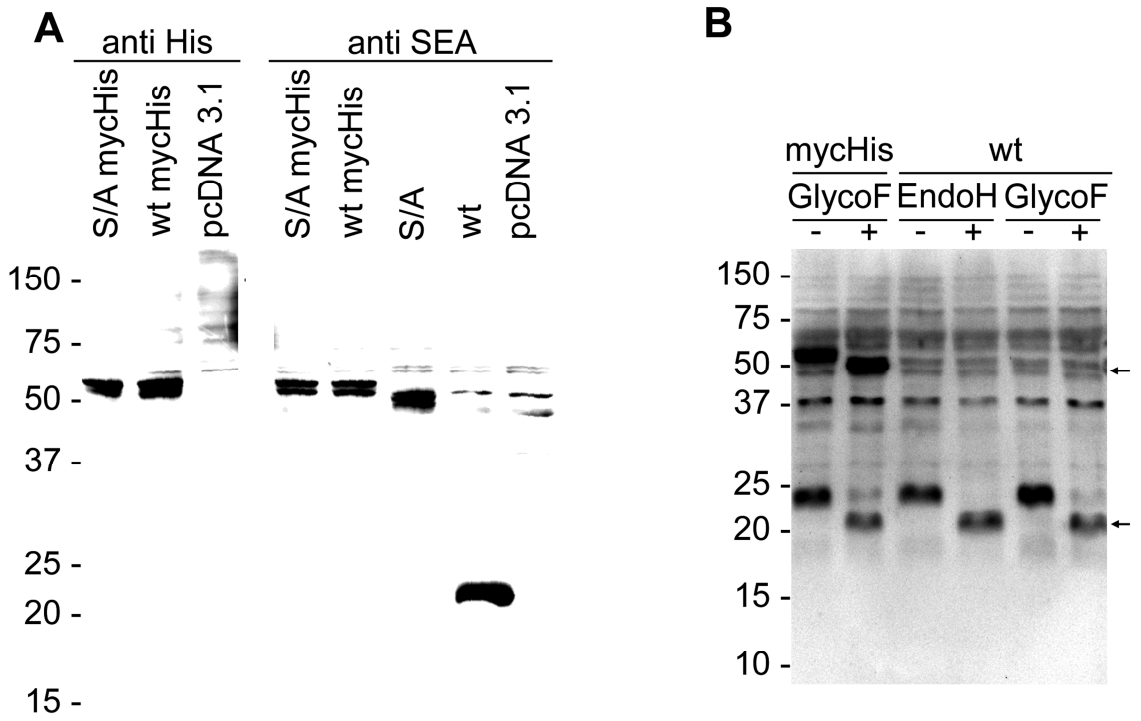

Figure 3.8: Overexpression of neurobin in HEK293T cells. Western blot analysis of neurobin wild-type and mutant forms in transiently transfected HEK293T cells. A, Detection of neurobin proteins with a mycHis tag (wt mycHis, S/A mycHis) reveals a doublet band around 53 kDa. Processing of tagged neurobin is only seen after blot overexposure (see B). The affinity purified antibody raised against the SEA domain of neurobin gives the same signal. This antibody also reacts with untagged neurobin proteins. Wild-type (wt) and neurobin S381A (S/A) are detected as processed 23 kDa and unprocessed 50 kDa band, respectively. pcDNA3.1 indicates control transfections with empty vector. Molecular mass markers in kDa are given at the left margin. B, Deglycosylation of neurobin. Cell extracts used in (A) were treated with N-glycosidaseF and endoglycosidaseH, respectively, before electrophoresis and analyzed with the anti SEA domain antibody. The arrows at the right indicate the position of the degylcosylated neurobin forms. Molecular mass markers are as in (A).

By homology to other serine proteases, activation cleavage of neurobin was expected to take place after K199 (Figure 3.5). To test whether neurobin is cabable of self-activation, we generated a K199A variant, termed m2, of neurobin-mycHis S381A (designated m1 in Figure 3.9a). The catalytically inactive mutants m1 and m2 were overexpressed in HEK293T cells without or with wild-type neurobin for activation. No protease domain was detected upon cotransfection with the empty pcDNA3.1 vector (0Figure 3.9b, lanes p). Coexpression with wild-type neurobin (Figure 3.9, lanes w) resulted in zymogen activation, indicated by the appearance of the mycHis-tagged protease domain (Figure 3.9b, PD) in neurobin-mycHis S381A (m1). With K199A (m2), cleavage was reduced, but a faint PD signal was still present. However, the full-length signal was strongly reduced. This observation led to the hypothesis that neurobin was a protease with self-shedding, rather than self-activation properties. A supporting hint for the self-shedding hypothesis was that for wild-type neurobin in Western blotting with SDS-PAGE under non reducing conditions we only detected the 23 kDa product (Figure 3.10c). This was surprising since primary sequence analysis had shown that suitable cysteines for a disulfide bridge between protease domain and the non-catalytic part of neurobin were present. Self-shedding N-terminally of C187 or C188, both candidates for participating in link formation, would have been the simplest explanation for our observations. Cleavages after K156, K158 and/or K171 were therefore postulated to result in the observed “23 kDa” signal. To test this postulate, four variants of m1 were generated with alanines substituting either one of basic amino acids or all of them. Processing of all these variants was not reduced in co-transfections with wild-type neurobin. Therefore we decided to analyze the zymogen activation region in more detail. We generated the three additional mutants (m3 to m5). In the mutant m3 (R196A, K199A), processing was almost completely suppressed and clearly no protease domain signal was detected in the mutant m4 which contained no basic residues in the zymogen activation region. Also the weakening of the full-length signal intensity was smallest compared to all other mutants. Mutant m5, a form carrying the activation site, but containing all other mutations, was still cleaved, indicating that the mutations per se did not prevent neurobin from activating its zymogen form. The presence of auto-catalytically activated wild-type neurobin was confirmed with the anti SEA domain antibody (Fig. 11b, lower panel). These results indicate that K199 is likely the sequence-predicted zymogen activation cleavage site. The observation that mutant m3 was needed to efficiently suppress the release of the protease domain is an indication that possibly *in vitro* in the mutant forms neurobin can use alternative motifs for cleavage.

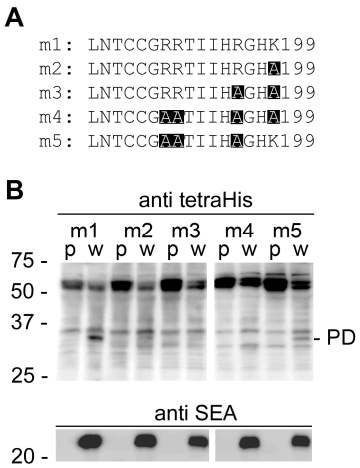

Figure 3.9: A, Mutants m1 to m5 used to identify the zymogen activation site. C, HEK293T cells were cotransfected with one of the mutants in the presence of either pcDNA3.1 (lanes p) or wild-type neurobin (lanes w). Protein extracts were probed with the anti His antibody. The position of the processed protease is indicated by PD. The protease domain is clearly detected in m1 (second lane) and in mutant m5 (last lane), but not mutants m2-m4. Presence of wild-type neurobin is shown in the lower panel of B. Molecular mass markers in kDa are given at the left margin.

Whether these cleavages can occur *in vivo* is unknown. However it is not very likely that, for instance, cleavage after R196 alone would result in an active protease domain, given the observation that predominantly the hydrophobic residues Ile or Val contribute to further protease domain stabilization (Song et al., 2002) after activation cleavage. It is more likely that alternative sites are used when normal activation is not possible. This hypothesis is strengthened by the observation that in co-transfections using mutant m4, where no cleavage motifs are present close by, additional signals appear (Figure 3.10a). The appearance of these bands in case of only mutant m4 is dependent on the activity of neurobin, since they are absent in co-transfections with the S381A mutant of wild-type neurobin and weaker in transfections with only half the amount of wild-type neurobin (Figure 3.10b). Running behavior and the fact that the signal remains visible under non-reducing conditions (Figure 3.10c) indicate that in mutant m4, alternative cleavage might take place after R224 (preceding the first conserved Cys involved in disulfide bonding within the protease domain). R224 is part of the motif VHR which is similar to the activation motif GHK199 and the most prevalent substitution motif IHR196.

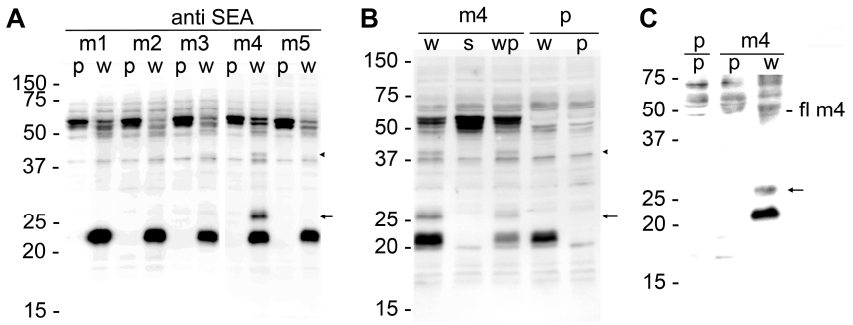

Figure 3.10: Detailed analysis of co-transfections using mutant m4 (transfections as before, additionally one co-transfection with the untagged S/A mutant, lane s in B). A, Western blotting using the anti SEA domain antibody allowed the detection of m4-specific additional bands (arrow in A-C, arrow head in A and B). B, The fragment production is dependent on neurobin activity, since absence in co-transfection with the S/A mutant (lane s) and weaker in co-transfections with reduced amount of neurobin (lane wp, 1:1 mix of wt-neurobin and empty vector). C, Under non-reducing conditions the stronger one of the additional signals remains detectable, indicating alternative cleavage N-terminally of C225. Molecular mass markers in kDa are given at the left margin.

All mutants show the same pattern of additional processing within the protease domain upon co-expression with wild-type neurobin (Figure 3.11). Fragmentation of the protease domain was also observed for the refolded recombinant protease domain of neurobin after refolding (chapter 3.8). Intra-domain-cleavages do not necessarily abolish catalytic activity as known from chymotrypsin.

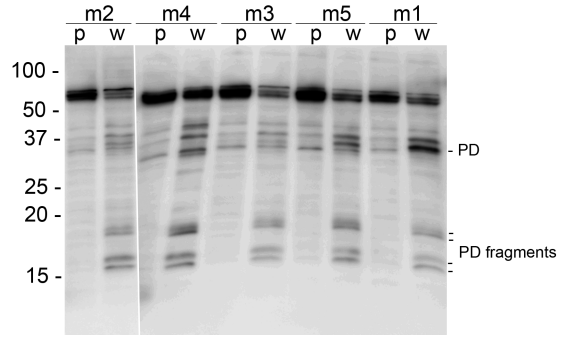

Figure 3.11: Additional processing of the protease domain. Western blotting using the anti tetra His antibody revealed additional fragments (PD fragments) running between 15 and 20 kDa in co-transfections of the mutants with wild-type neurobin (lanes w, co-transfected as before); 15 % polyacrylamid gel. Molecular mass markers in kDa are given at the left margin.

3.6 Localization of neurobin in transfected HEK293T and COS7 cells

Neurobin, with its domain composition predicted to be a type II transmembrane serine protease was expected to reside in the ER, Golgi-compartment and/or at the plasma membrane. To investigate the subcellular distribution of neurobin, transiently transfected HEK293T cells were studied by indirect immunofluorescence analysis. Using neurobin-mycHis as well as neurobin-mycHis S381A and the anti His antibody, we detected immunoreactivity at the plasma membrane of non-permeabilized HEK293T cells (Figure 3.12a,d). Immunostaining with the anti SEA domain antibody revealed a very similar distribution (Figure 3.12b,e). Untagged wild-type neurobin and neurobin S381A were also detected at the cell surface (Figure 3.12g,I less than half the exposure time resulted in similar signal intensity as for the tagged variants). Together with the western blot analysis these results demonstrate the ability of the anti SEA-domain antibody to detect neurobin and support the sequence-predicted topology of neurobin with SEA and protease domain on the extracellular side. Because COS-7 cells grow much more adherently and flatly than HEK293T cells do, their cell morphology is more apprehensive. Therefore, we further studied the subcellular distribution of neurobin by indirect immunofluorescence analysis in transiently transfected COS-7 cells. Using mycHis-tagged neurobin, double-staining of permeabilized cells with the anti SEA domain (Figure 3.13a) and the anti His antibody (Figure 3.13b) revealed ER-like intracellular imunoreactivity, respectively. With untagged neurobin the intracellular pattern was more Golgi-like (Figure 3.13d) and immunoreactivity on the surface of non-permeabilized cells was much stronger (Figure 3.13f).

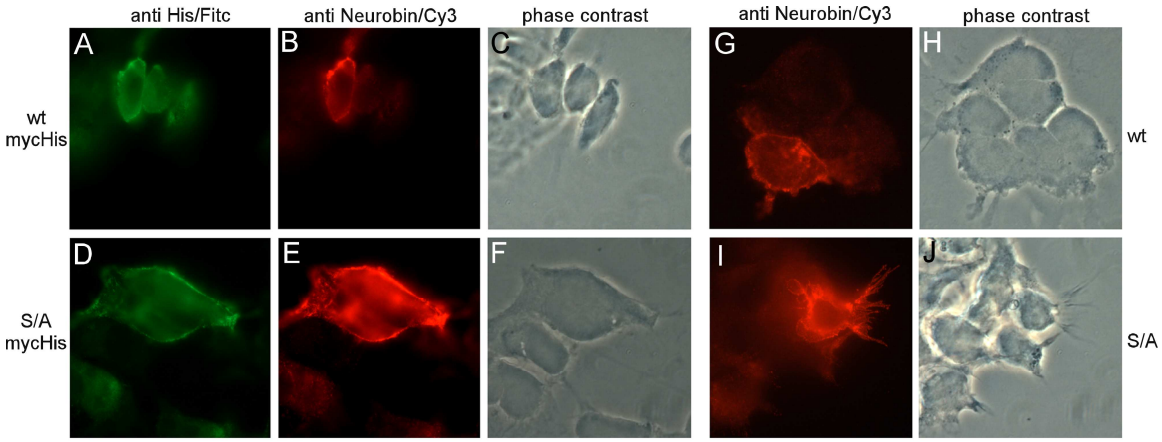

Figure 3.12: Cytochemical detection of neurobin in HEK293T cells. Cells were fixed 48hrs after transfection. MycHis-tagged (wt mycHis, S/A mycHis) as well as untagged forms of neurobin (wt, S/A) are found at the cell surface (A,D,G,I). Tagged neurobin is detected by the anti SEA domain antibody as well (B,E).For the anti His antibody, FITC-labeled anti mouse IgGs were used. To visualize the affinity-purified anti SEA domain antibody, Cy3-conjugated anti rabbit IgGs were used. Phase contrast images are shown in C,F,H,J. Pictures A-J were taken by a LeicaDC300F camera using a 100x objective.

Taken together, especially the untagged neurobin is efficiently propagated to the cell membrane of transfected HEK293T and COS-7 cells. However, most intense fluorescence in cells transfected with untagged neurobin was observed in the Golgi-compartment. This might be explained by the fact, that all neurobin must pass this small compartment before it can become distributed all over the plasma membrane.

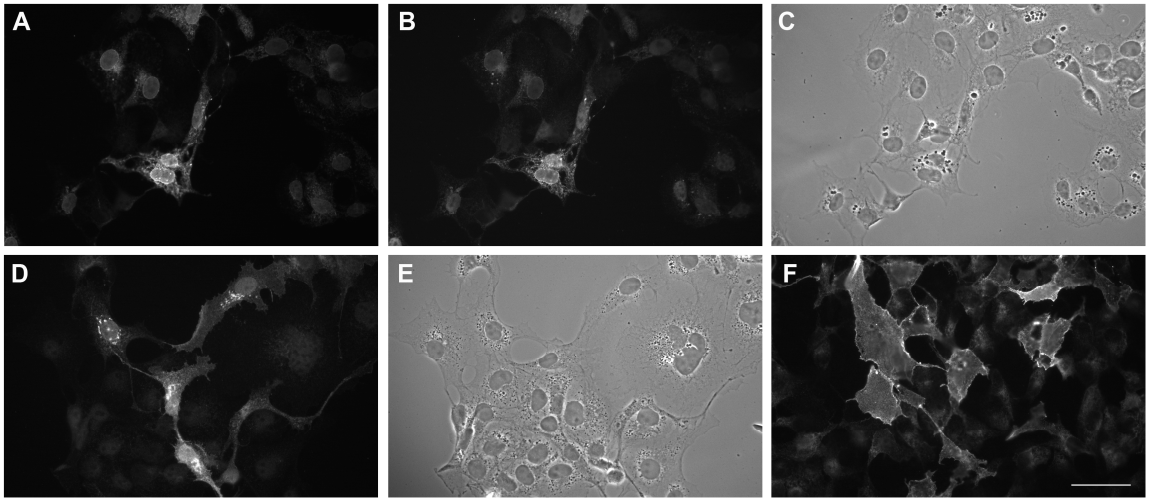

Figure 3.13: Cytochemical detection of neurobin in COS-7 cells. Cells were fixed 24 hrs after transfection. For intracellular detection of neurobin, cells transfected with the mycHis-tagged variant of neurobin were permeabilized and probed with the anti SEA domain antibody (A) and the anti His

antibody (B). Cells display perinuclear, ER-like labelling. Cells transfected with untagged wild-type neurobin showed a more Golgi-like labelling pattern (D) and clear surface labelling when probed without permeabilization (F). C shows the phase contrast image of A and B, E that of D. Scale bar in I: 50 μm (for A to F).

3.7 Histochemical detection of neurobin in mouse CNS

To identify neurobin *in vivo* we used the affinity-purified anti SEA domain antibody. Histochemical analysis of P10 mouse brain sections revealed immunoreactivity in the cerebellum (Figure 3.14a), consistent with the RT-PCR analysis. Higher magnification indicated that this reactivity was confined to Purkinje neurons, in particular to the cell body and to the dendritic tree of Purkinje neurons (Figure 3.14). Preimmun serum showed no reactivity (Figure 3.14c). The restricted localization of neurobin is consistent with our inability to unambiguously detect neurobin in spinal cord and cerebellar protein extracts with our available antibodies, again suggesting that the overall amount of neurobin *in vivo* is fairly low.

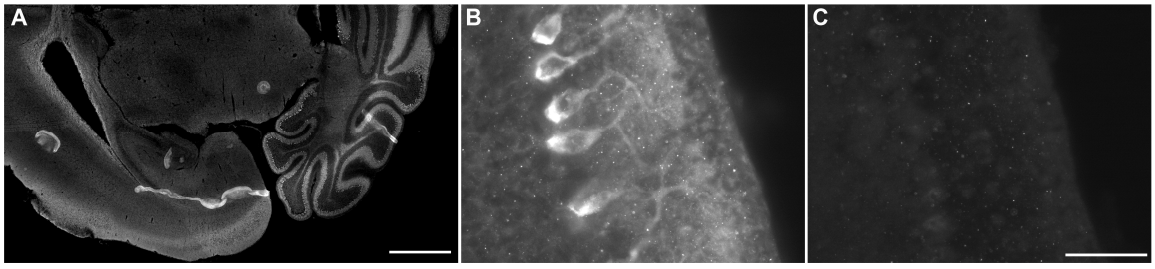

Figure 3.14: Histochemical detection of neurobin in mouse brain. A, Detection of neurobin in horizontal brain sections of adult mice with the affinity-purified anti SEA domain antibody, used at a concentration of 3 μg/ml. For visualization Cy3-conjugated anti rabbit IgGs were used. Compared to preimmune serum diluted 1:1000, immunoreactivity was confined to the Purkinje cell layer in the cerebellum. B, Magnification of the Purkinje cell layer. Only Purkinje cell bodies and their dendritic processes are strongly labelled. C, Corresponding region of a brain section incubated with preimmune serum. Scale bars in A: 1 mm, C: 50 μm (for B and C).

3.8 Production of recombinant neurobin and enzymatic activity

To investigate the catalytic potential of neurobin we used a construct encoding an N-terminal His tag, an enteropeptidase cleavage motif, and the entire protease domain of neurobin beginning with V200 and ending with L431. The protein was expressed in *E. coli*, solubilized from inclusion bodies, and purified via Ni-NTA affinity chromatography.

Refolding was tried by either dialyzing against or slow dilution into a wide variety of refolding buffers. Conditions under which a significant fraction of the refolded protein was present in a soluble monomeric form were detected by centrifugation of the refolding sample followed by silver staining after separation on non-reducing SDS-PAGE gels. Samples with soluble monomeric protein were concentrated and cleaved by incubation with enteropeptidase (EKMax from Invitrogen, overnight at room temperature turned out to be the most suitable activation condition). Whenever there was still soluble protein present after enteropeptidase incubation, samples were tested for activity using different chromogenic peptides. As a positive control the peptides were incubated with trypsin. As negative control buffer alone or supplemented with enteropeptidase was used. Using this procedure we finally discovered conditions under which active neurobin was generated. Careful choice of pH, arginine concentration and the redox system turned out to be most critical. Besides, refolding was much more efficient when using slow dilution instead of dialysis. Interestingly refolding of the protease domain solubilized in guanidinium hydrochloride instead of urea never resulted in active enzyme though we encountered conditions under which a significant fraction of protein was soluble after cleavage by enteropeptidase. Under optimized conditions the yield was 1.2 % of the protein initially purified from inclusion bodies (~ 200 ug active protease domain per liter *E.Coli* culture).

Silver gel analysis of the purified protease domain revealed a predominant band of 30 kDa, the non-activated protease domain (Figure 3.15a) after optimized refolding conditions. Activation of purified neurobin with enteropeptidase resulted in a new band of 27 kDa. Two additional faint bands were detected at the bottom of the gel (Figure 3.15a). Under non-reducing conditions the apparent mass of activated neurobin was reduced to 24 kDa and the low molecular bands were absent, suggesting that these bands are disulfide bridge-linked fragments of recombinant activated neurobin (Figure 3.11). To remove enteropeptidase after neurobin activation, MonoS cation-exchange chromatography was applied, resulting in homogeneously pure neurobin (Figure 3.15b). Size exclusion chromatography indicated that activated neurobin is a monomeric protein,

since the protein eluted from a Superdex200 column (23.6 ml volume) at 16.1 ml, very similar to chymotrypsinogen (25 kDa, elution at 16.5 ml).

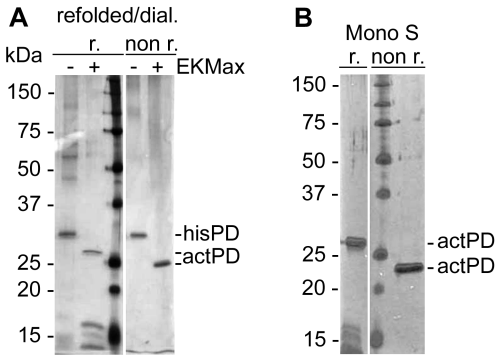

Figure 3.15: Production of recombinant neurobin. Recombinant neurobin was solubilized from inclusion bodies, purified via nickel affinity chromatography and refolded. A, The protease domain (hisPD) of neurobin after incubation for 16 h at 37 °C with (+) or without (-) enteropeptidase (EKMax) was submitted to SDS-PAGE either under reducing (r.) or non-reducing (non r.) conditions and visualized by silver staining. EKMax removed the 4.6 kDa N-terminal fragment containing the His-tag and the enteropeptidase cleavage motif leaving the activated protease domain (actPD). B, Further purification of actPD and removal of EKMax by MonoS cation-exchange chromatography. 400 ng of actPD were resolved by SDS-PAGE and visualized by silver staining. Molecular mass markers in kDa are indicated at the left of panels A and B, respectively.

3.9 Enzymatic activity of recombinant neurobin towards chromogenic peptide substrates

Because Asp is present in the neurobin sequence in position 375 (position 189 in chymotrypsin numbering), forming the bottom of the S_1 subsite (Hedstrom, 2002), acceptance of Arg and Lys in the P1 site was expected. Activated neurobin was used to cleave chromogenic peptide substrates in which upon cleavage a paranitroanilde group is released, resulting in yellow color accumulating in the buffer. Therefore, cleavage efficiency could be measured via the absorption at 405 nm. Neurobin cleaved peptides with Arg in position P_1 and uncharged residues in positions P_2 and P_3 (Figure 3.16a). In contrast to trypsin, which hydrolyzed all peptide substrates used, neurobin did not accept a single Arg residue for cleavage and poor cleavage was measured with Pro in position P_2. Hardly any cleavage was observed with acidic amino acids in positions P_2 and P_3. We

obtained best cleavage with the peptide Val-Gly-Arg-pNA. The peptide Gly-His-Arg-pNA, resembling the sequence of the zymogen activation cleavage site (Gly-His-Lys, see Figure 3.5), was used for the experiments shown in figures 17b-d. Neurobin had a pH optimum around pH 8 (Figure 3.16b), and it was insensitive to a broad range of NaCl concentrations (Figure 3.16c), the latter being in accordance with the presence of Pro in position 225 (chymotrypsin numbering, (Dang and Di Cera, 1996)). Peptide cleavage by neurobin was inhibited by a variety of serine protease inhibitors, but not by E-64, a cysteine protease inhibitor, and pepstatin, an aspartate protease inhibitor. Heparin, added at two concentrations, did not suppress neurobin activity against peptide substrates (Figure 3.16d) and neither the removal of Ca^{2+} and other divalent cations by EDTA nor the extra addition of Ca^{2+} ions modulated neurobin activity (Figure 3.16d). Ca^{2+} ion-independence is consistent with the absence of characteristic acidic amino acids in the 70 to 80 loop (chymotrypsin numbering) responsible for Ca^{2+} ion-complexation in other serine proteases (Page et al., 2005).

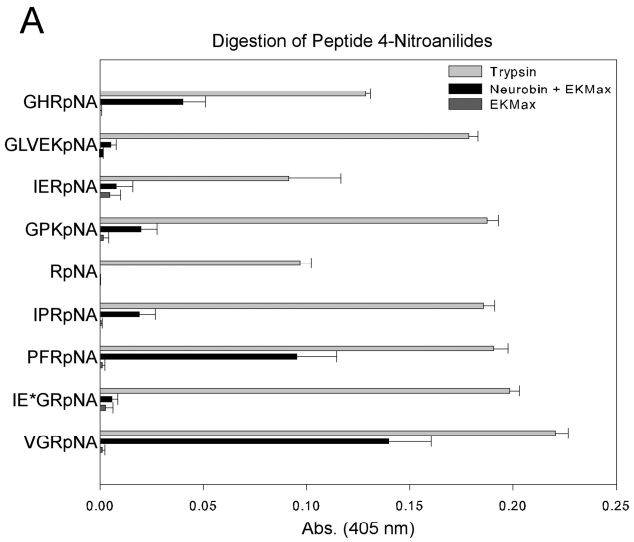
A
Digestion of Peptide 4-Nitroanilides
Trypsin
Neurobin + EKMax
EKMax
GHRpNA
GLVEKpNA
IERpNA
GPKpNA
RpNA
IPRpNA
PFRpNA
IE*GRpNA
VGRpNA
0.00
0.05
0.10
0.15
0.20
0.25
Abs. (405 nm)

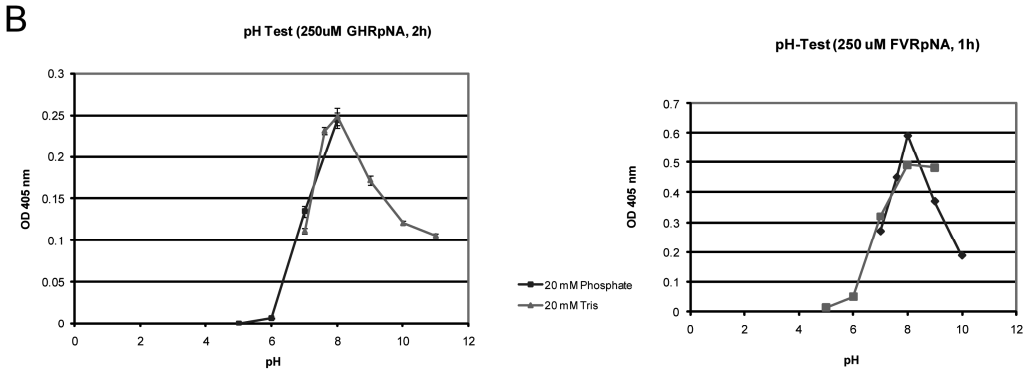
B
pH Test (250uM GHRpNA, 2h)
OD 405 nm
pH
pH-Test (250 uM FVRpNA, 1h)
20 mM Phosphate
20 mM Tris

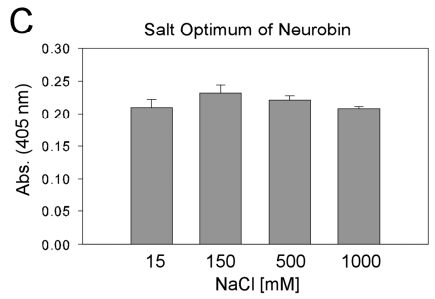
C
Salt Optimum of Neurobin
Abs. (405 nm)
15
150
500
1000
NaCl [mM]

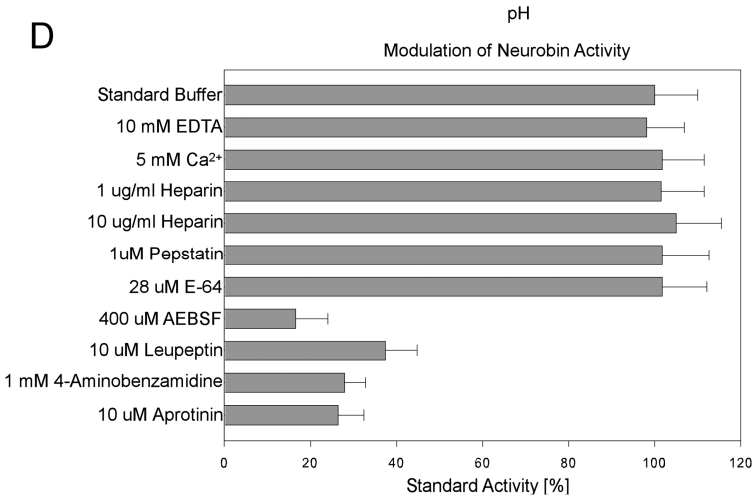
pH
D
Modulation of Neurobin Activity
Standard Buffer
10 mM EDTA
5 mM Ca2+
1 ug/ml Heparin
10 ug/ml Heparin
1uM Pepstatin
28 uM E-64
400 uM AEBSF
10 uM Leupeptin
1 mM 4-Aminobenzamidine
10 uM Aprotinin
0
20
40
60
80
100
120
Standard Activity [%]

Figure 3.16: Specificity of recombinant neurobin against peptide substrates. A. 100 mM of each pNA peptide was incubated for 2.3 h at room temperature with either trypsin, neurobin activated by EKMax, or EKMax alone. Absorbance was measured at 405nm. Data are derived from two independent experiments done in duplicates and expressed as mean±S.D. Values of non-activated neurobin and buffer alone, respectively, were identical and below 0.05 absorption units and were subtracted before calculating. B, pH optimum of recombinant neurobin. 250 mM GHR-pNA was incubated for 2 h at 30°C with purified activated protease domain in 20 mM phosphate buffer (dashed line) and 20 mM Tris-HCl buffer (solid line) at the pH values indicated. Measurements were done in triplicate and are represented as mean±S.D. The pH-test was repeated once with the well cleavable peptide Phe-Val-Arg-pNA to confirm that His in P2 was not responsible for low neurobin activity at low pH. C, Activity of neurobin in the presence of increasing concentrations of NaCl. Experimental conditions were as in (B) with 20 mM Tris-HCl buffer pH 8.0. D, Suppression of neurobin proteolytic activity. Measurements were done in triplicate and are represented as mean±S.D.

Since we did not determine the percentage of catalytically active molecules in the purified preparations of refolded neurobin, we did not attempt to determine kinetic parameters but simply checked that the reactions never reached a plateau during activity assays.

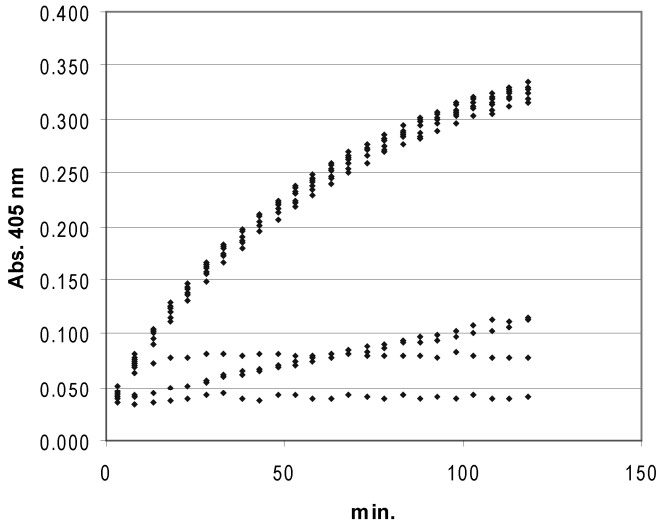

Figure 3.17: Example for reaction control-monitoring. Shown here is one of the datasets used for figure 17d.

3.10 Catalytic activity of recombinant neurobin towards protein substrates

Several previously identified TTSPs substrates were recruited among extracellular matrix components, cell surface molecules and growth factors. Therefore, to identify potential protein substrates of neurobin we incubated fibronectin, laminin, FGF-7, and FGF-2 with trypsin and recombinant neurobin, respectively. All substrate proteins were degraded by trypsin, whereas neurobin did not cleave the large extracellular matrix proteins fibronectin and laminin, or the growth factor FGF-7 (Figure 3.18a). Neurobin, however, selectively processed FGF-2. This cleavage resulted in the formation of a 13 kDa and further fragments (Figure 3.18a and b). Since FGF-2 has strong heparin binding properties (Moscatelli et al., 1987), we wondered whether the presence of heparin in concentrations used during the peptide cleavage assays modulated FGF-2 processing by neurobin. In the presence of heparin FGF-2 cleavage by neurobin was suppressed in a dose-dependent manner (Figure 3.18a). A more detailed analysis of the FGF-2 cleavage showed that neurobin processed FGF-2 to at least three major fragments. Cleavage occurred after Lys or Arg residues, as deduced from sequence analysis of the cleavage products (Figure 3.18b). Fragments 1a, b and 4a begin with the N- terminus of recombinant human FGF-2. All other fragments start after a basic amino acid preceding the cleavage site. Cleaved FGF-2 was also analyzed by MALDI-TOF-MS. Average masses of 12794.0, 8581.8 and 4348.8 were detected. These masses reflect the theoretical masses of A2-R116 (12792, Figure 3.18b, fragment 1a), I43-R116 (8517.6, Figure 3.18b, fragment 2) and S117-S154 (4349.1, Figure 3.18b, fragment 5a). Together with the peptide substrate assays, these enzyme activity experiments demonstrate that neurobin is an authentic serine protease with amino acid preference for Arg or Lys in the P_1 position and, possibly, very selective protein substrate specificity.

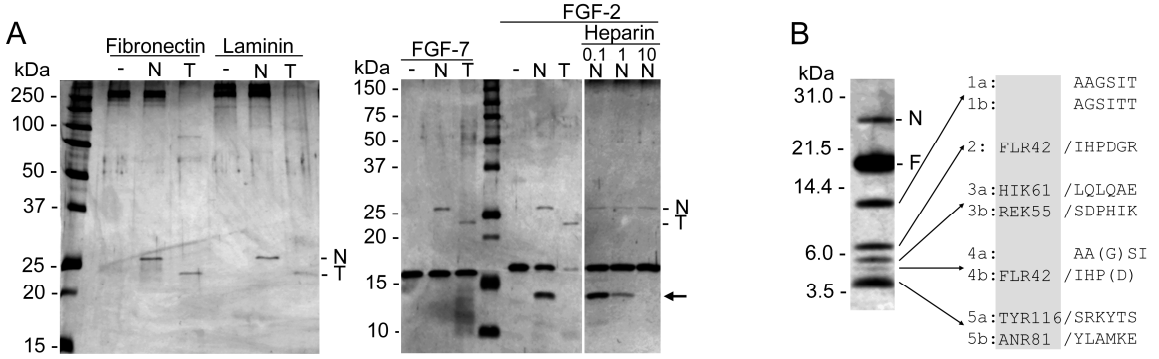

Figure 3.18: Activity of recombinant neurobin towards protein substrates. A, 200 ng of fibronectin, laminin, FGF-7, and FGF-2, respectively, were incubated for 4 h at 37°C with either buffer (-), 2 ng neurobin (N) or 2 ng trypsin (T). The reaction was stopped by the addition of loading buffer. Samples were resolved by SDS-PAGE and proteins visualized by silver staining. With the exception of FGF-7, all proteins were almost completely degraded by trypsin. N and T at the right margin indicate the protease in the reaction mixture. The arrow indicates the position of the 13 kDa fragment of FGF-2. Molecular mass markers are given in kDa at the left margins. B, FGF-2 was digested as in A. 10% of the reaction were used for silver gel analysis on a 4-12 % NuPAGE gel. N and F at the right margin indicate recombinant neurobin and full-length FGF-2, respectively. The rest of the reaction was identically resolved and the proteins transferred onto a PVDF membrane. Bands 1 to 5 were analyzed by Edman degradation. Whenever the sequence did not begin with the N-terminus of recombinant human FGF-2 the last three amino acids preceding the cleaved peptide bond are given in the grey box with position number of the P1 residue.

3.11 Trials to investigate FGF-2 cleavage by neurobin in cell culture experiments.

Interestingly, histochemical localization of FGF-2 in the cerebellum revealed strong expression in Purkinje cells with a distribution very similar to the distribution of neurobin (Reynolds et al., 2005), indicating that FGF-2 could indeed be an *in vivo* substrate of neurobin. To obtain further evidence for this hypothesis we tried to observe FGF-2 cleavage by neurobin in cell culture experiments. Thus, we first cloned FGF-2 from spinal cord cDNA from P10 mice. Since FGF-2 is secreted via an alternative ER-/Golgi-independent secretion pathway we cotransfected cells with neurobin and FGF-2 containing expression vectors and analyzed the cell extracts and the culture media by SDS-PAGE/Western blotting. In our first attempts we expressed FGF-2 with a C-terminal ONEstrep tag variant. C-terminal tags are reported not to interfere with efficient secretion by the alternative pathway (Florkiewicz et al., 1995). However, in HEK293T and COS-7 cells our construct, though well expressed, could hardly be detected in the cell media (Figure 3.19a).

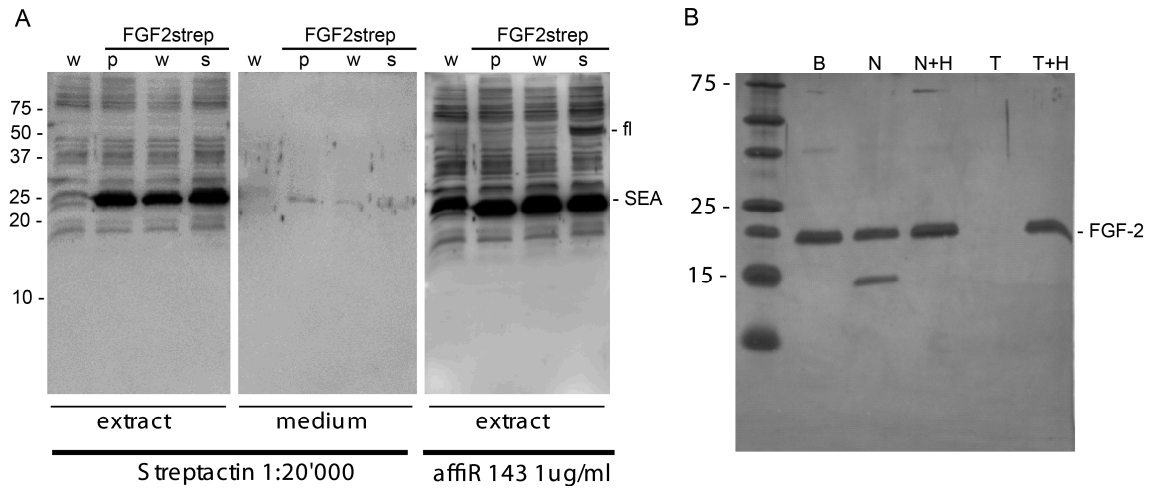

Figure 3.19: A, Western blot analysis of extracts and media of HEK293T cells, co-transfected with mouse FGF-2 fused to a C-terminal ONEstrep tag (FGF2strep) and either pcDNA-vector (p), wild-type neurobin (w) or the S/A mutant thereof (s). Streptactin linked to horseradish peroxidase allowed detection of FGF-2 wherever expected (though very little could be detected in the medium). The most right blot in A is the same as shown on the left, reprobed without stripping using the anti SEA domain antibody. The SEA domain stump resulted in a band running a little higher than the ONEstrep-tagged FGF-2. A weak band could be detected resulting from the full-length S/A mutant of neurobin (fl). B, Silvergel of recombinant human FGF-2 was incubated with only buffer (B), neurobin (N), neurobin plus 10 µg/ml heparin (N+H) or trypsin (T) as before. Additionally this time FGF-2 was incubated with trypsin plus 10 µg/ml heparin (T+H). Heparin strongly protects FGF-2 also from digestion with trypsin. Molecular mass markers in kDa are indicated at the left of panel A and B.

Purifying the strep-tagged FGF-2 from the medium of co-transfected HEK293T cells via Magstrep magnetic beads, we could not find any processed FGF-2. From a control experiment we learned that the cleavage of FGF-2 by trypsin can be inhibited by the addition of heparin too (Figure 3.19b).

With a commercially available anti FGF-2 antibody which recognized FGF-2 fragments from an *in vitro* digest with neurobin (Figure 3.20a), we repeated the experiments with untagged FGF-2. Secretion efficiency was still low and no cleavage could ever be detected in the medium (Figure 3.20a). Therefore we introduced FGF-2 into the normal secretory pathway by fusing the secretion signal of human calsyntenin 1, a type I transmembrane protein, to the N-terminus. The protein was expressed but also not secreted and no cleavage of FGF-2 could be detected in the cell extracts (Figure 3.20c).

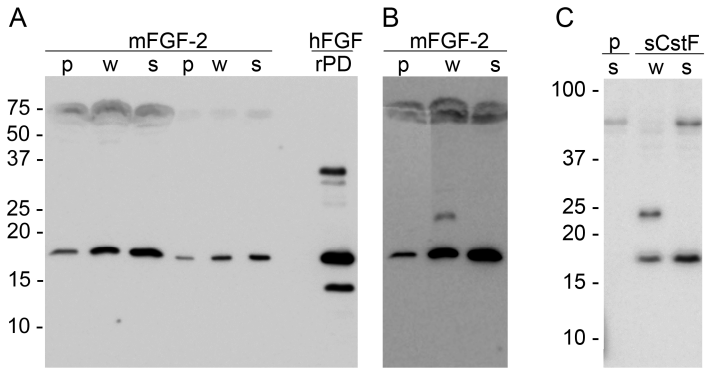

Figure 3.20: Westernblot analysis of (C-terminally) untagged FGF-2 variants in cotransfections. A, The proteins from media of HEK293T cells, co-transfected with mouse FGF-2 and either pcDNA-vector (p), wild-type neurobin (w) or the S/A mutant thereof (s) were precipitated with the Wessel-Flücke method and analysed by western blotting using the affinity-purified anti FGF-2 antibody purchased from Prepotech. In the first three lanes the equivalent of 300 µl medium and in the second three lanes the equivalent of 50 µl medium were loaded. In the last lane the partial digest of 50 µg human FGF-2 (hFGF-2, from Invitrogen) was loaded as a control for blotting and antibody quality. Clearly the dimer, monomer and the 13 kDa fragment were detected as strongest bands. B, Reprobing the first three lanes of the blot shown in A (without stripping) with the anti SEA domain antibody resulted in the detection of the transmembrane stump containing the SEA domain. This suggested that cell disruption was at least partially responsible for the FGF-2 signal. C, Western blotting using the extracts of HEK293T cells co-transfected with mouse FGF-2 fused to an N-terminal calsyntenin secretion signal (sCstF) was performed with a mixture of the affinity-purified anti FGF-2 and the anti SEA domain antibodies. Full-length neurobin and activated neurobin as well as uncleaved FGF-2 could be detected. Molecular mass markers in kDa are indicated at the left of panel A and C.

In a control experiment we were surprised to realize that DMEM without FCS, used as cell culture medium, reduced cleavage efficiency of neurobin towards the peptide substrates. To rule out the detrimental effect of the medium, we switched back to the co-transfection experiments in COS-7 cells using the untagged FGF-2, and, one day post transfection removed the medium, washed the cells with PBS and kept them in the incubator in PBS for 6 hrs. In the subsequent analysis of the PBS supernatant we detected small amounts of FGF-2. However, also after incubation in PBS no processing could be detected. The finding that irrespective of the used secretion pathway well detectable amounts of FGF-2 were found intracellularly, but only minimal amounts were secreted, suggested that FGF-2 might adsorb to the plasma membrane. To test this idea, immunofluorescence was performed. Indeed, using transiently transfected COS-7 cells, FGF-2 immunoreactivity was detected at the plasma membrane (Figure 3.21). From the outcome of our experiments and given the heparin binding properties of FGF-2 we

assume that FGF-2 binding to proteoglycans from the cells is responsible for both, difficulties to detect FGF-2 in the medium and our failure to observe its cleavage by neurobin in the cell-culture system.

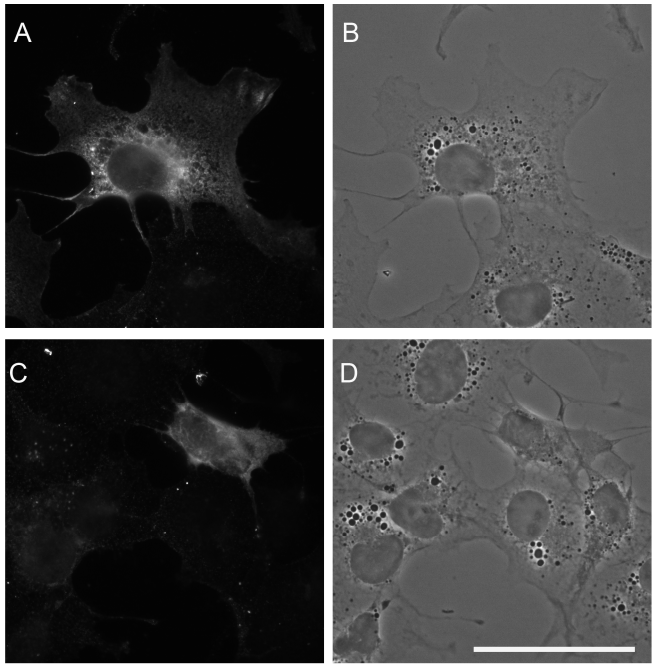

Figure 3.21: Imunnofluorescence pictures of COS7 cells transfected with mouse FGF-2. For detection the affinity-purified anti FGF-2 antibody 2 µg/ml was used in combination with the goat anti rabbit Cy3 1:500. The antibody incubation steps were performed in the presence (A) or absence (C) of 0.1 % saponin for permeabilization. B shows the phase contrast picture of A, D that of C. The scale bar in D is 50 µm.

3.12 Supplementary experiments and results

3.12.1 Peptide antibody raising, affinity purification and testing

The first 22 aminoacids of neurobin (intracellular part, MARGQPRRSEEQWTALQNR-TEC) coupled to keyhole limpet hemocyanin via Cys22 were used to immunize two rabbits at Primm (Italy). The resulting antisera R134 and R135 recognized the antigen well, but only when dot-blotted on a nitrocellulose membrane under native conditions (Figure 3.22a). Both R134 and R135 recognized neurobin in transfected HEK293T cells

only in immunofluorescence experiments but not in Western blotting. Taken together, this suggests a secondary structure motif epitope (secondary structure analysis programs predict a short N-terminal coil followed by an alpha helix). The sera were functional in immunofluorescence using HEK293T cells transfected with mycHis-tagged neurobin. However, using the sera for histochemistry experiments with P10 cerebellum and spinal cord sections, no signals were obtained that were not present with the preimmun sera taken as controls. Next, the peptide antigen was coupled to NHS-activated sepharose for affinity purification of the antibodies after ammonium sulfate precipitation and dialysis. Affinity-purified R134 and 135 showed much reduced background staining in immunofluorescence. However, the signals were still weaker than obtained with the anti tetraHis antibody (costainings) and affinity purification did not improve the situation for Western blotting and histochemistry.

With the result from our dot-blot experiments in mind, we thought that the antibodies might be functional in affinity purification of neurobin from extracts of transfected HEK293T cells. Therefore, we coupled the affinity purified R134 to NHS-activated sepharose. Indeed in subsequent batch purifications we were able to purify the noncatalytic part of wild-type neurobin from extracts of transfected HEK293T cells (Figure 3.22b). Using the same experimental conditions with P10 cerebellum extracts neurobin could not be affinity purified (Figure 3.22c). Taken together, the peptide antibodies worked under certain conditions. But since the affinity was low, the small amounts of neurobin expected in mouse tissues could not be detected or purified using this peptide antibody. An alternative or ancillary explanation could be that the cytosolic epitope might be shed off or destroyed by posttranslational modifications (e.g. sequence analysis by NetPhos2.0 predicted that Ser9 in this domain is embedded in a motif suitable for Ser/Thr phosphorylation. We do, however, not know, whether neurobin is indeed a kinase substrate *in vivo*) and thus renders the peptide antibody worthless for the analysis of the physiological situation.

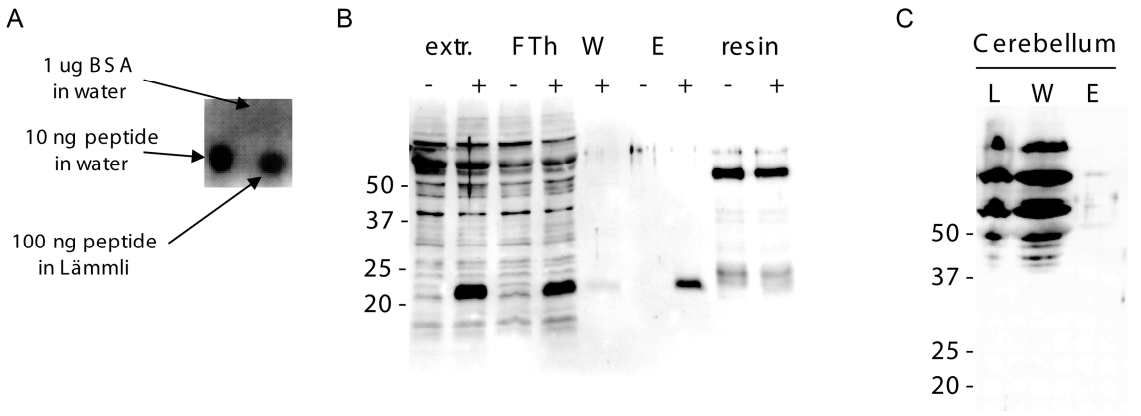

Figure 3.22: Trials to use the peptide antibody R134 directed against the cytosolic segment of neurobin. A, When dot-blotted onto a nitrocellulose membrane, the antigen was detected more than 10 times better when prior solubilized in water than when prior solubilized in Lämmli buffer. B, Western blotting (SEA domain antibody) monitoring the affinity-purification of the non-catalytic part of activated neurobin from extracts of transfected HEK293T cells via purified peptide antibodies coupled to NHS-activated sepharose. The purification was done in parallel for vector (-) and neurobin (+) transfected cells (extr.: loading, FTh: flow through,W: wash, E, elution; the resins were boiled after the purification – elution was complete, only IgG heavy and light chains detectable). C, The same purification using extract from P10 mouse cerebellum did not allow the detection of neurobin.

In the second approach we raised antibodies against a peptide of the protease domain of neurobin. We chose the peptide L258 to I271 (LLSKPQAPRAVKNI) as antigen, preceded by a cysteine for coupling to keyhole limpet hemocyanin. Peptide synthesis, coupling and immunization of two rabbits and two guinea pigs was performed at Pineda (Berlin). Third boost antisera of all animals and fifth boost antisera of the rabbits were tested in cytoimmunofluorescence and Western blotting using transfected HEK293T cells. Expression of myc-his tagged neurobin was confirmed with the tetraHis antibody in each experiment. In cytoimmunofluorescence at a dilution of 1:200, the rabbit peptide antiserum R1 produced very weak specific signals, but high background. No specific signals were detected in Western blotting, when testing the peptide antisera in dilution series ranging from 1:100 to 1:30’000.

Antiserum R1 was affinity-purified using the antigen coupled to NHS-activated sepharose. Affinity purification strongly reduced the background reactivity in immunofluorescence. In Western blotting, affinity-purified R1 was still not functional. In transfected cells neurobin immunoreactivity could be detected when fixed with PFA (and permeabilized with saponin) or methanol/aceton. In histochemistry, using PFA-fixed horizontal brain sections the affinity purified R1 at a concentration of 20 ug/ml resulted

in weak labeling of Purkinje cell bodies. In controls the R1 preimmune serum was used in a dilution of 1:100. At this concentration also the preimmune serum resulted in labeling of Purkinje cells. In methanol/aceton fixed brain sections the labeling caused by the affinity purified R1 disappeared completely while the staining caused by the preimmune serum remained detectable. The discrepancy between cyto- and histchemistry is difficult to explain. The fact that the fixation method did not influence reactivity of R1 in cytochemistry suggests that it was not the thechnique per se causing the disappearance of the specific signal in histochemistry after methanol/acetone fixation. Besides, comparing the immunofluorescence intensity of affinity purified R1 to that of the anti tetraHis antibody, it became apparent that this antibody was probably of lower affinity than the affinity purified R134.

3.12.2 Eukaryotic antigen production in HEK293T cells

Parallel to the peptide antibody approach we worked on the production of protein antigens. In our laboratory eukaryotically produced proteins have resulted in much better immune responses than prokaryotically produced antigens (possibly, because eukaryotic posttranslational modifications increased antigenicity or because the modification simply rendered the antigen mor similar to the target protein). The idea was to obtain the protein of interest in the supernatant of transfected cells. All generated constructs coded for an N-terminal secretion signal (from neuroserpin), then an Fc-tag and a subsequent PreScission cleavage motif. There was a MycHis-tag for detection at the C-terminus of each construct. Between the tags we icluded the whole extracelullar part of neurobin (FcSEAPDmycHis), only the SEA domain (FcSEAmycHis) and only the protease domain (FcPDmycHis), respectively. Initially it was planned to produce recombinant proteins without the C-terminal tag, once expression and purification were optimized (using protein A-Sepharose and elution by on column cleavage of the Fc-tag by PreScission would have resulted in tag-free recombinant protein). The possibility to obtain correctly folded and posttranslationally processed enzyme for activity assays made eukaryotic expression an attractive dual purpose approach. All three constructs were well expressed in HEK293T and COS-7 cells. Immunofluorescence with transfected COS-7 cells revealed marked differences in subcellular protein distribution. The FcSEAmycHis construct showed accumulation in a well defined Golgi-like area (Figure 3.23a). FcSEAPDmycHis and FcPDmycHis resulted in a scattered, network-like (ER-like) fluorescence (Figure 3.23b). Additionally, a perinuclear accumulation of fluorescence was observed in constructs

where the transmembrane domain of neurobin was present (Figure 3.23c). Only the construct without protease domain was secreted efficiently by transfected HEK293T and COS-7 cells. Therefore, FcSEAmycHis was purified from the supernatant (75 ml per 500 cm^2-plate) of transfected HEK293T cells. Purity was considered insufficient for immunization after protein A affinity chromatography. Therefore the C-terminal tag was maintained and used for a second chromatography step using immobilized metal affinity chromatography (HisSelect, an agarose bead resin with nickel chelate). This procedure allowed the production of pure antigen. Two rabbits were immunized in house with 30 ug mycHis-tagged SEA domain for both initial immunization and boosts.

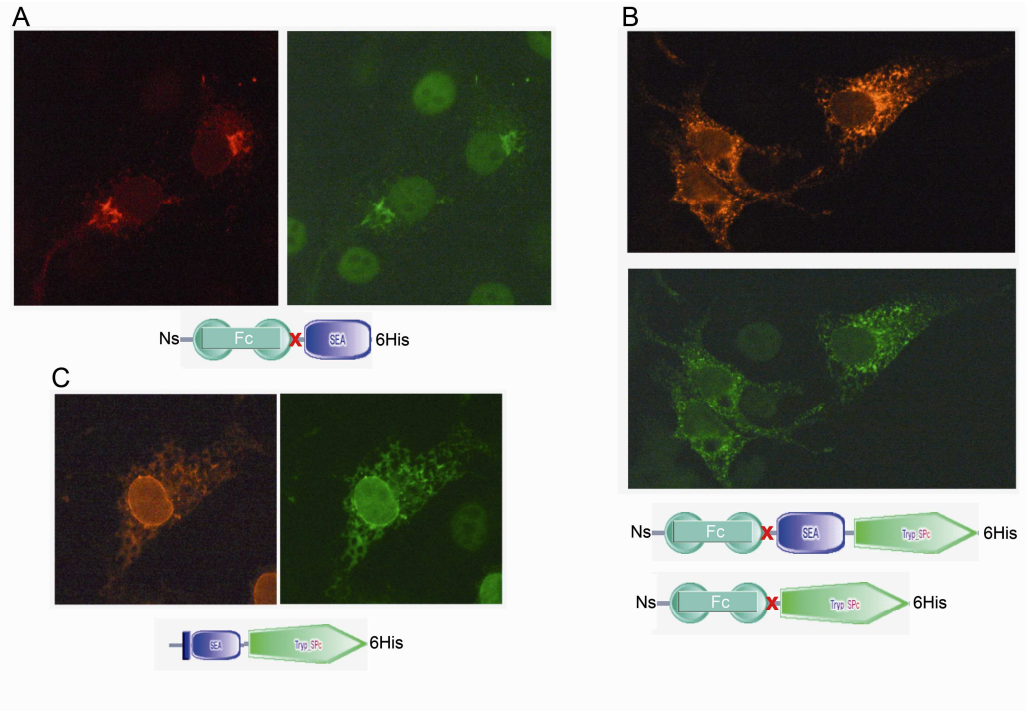

Figure 3.23: Imunofluorescence pictures of COS7 cells transfected with the eukaryotic expression constructs or wild-type neurobin. All constructs contained the C-terminal mycHis tag. Red fluorescence was obtained from the incubation with the anti SEA domain antibody after affinity-purification in combination with the donkey anti rabbit Cy3 antibody. The green fluorescence was obtained from the combination of the anti tetra His antibody with the goat anti mouse FITC antibody. Models of the constructs are shown below the pictures (Ns: neuroserpin secretion signal, Fc: Fc-tag). A, only the SEA domain construct is efficiently propagated in the secretory pathway, as seen from clear staining of the Golgi compartment. B, The constructs containing the tagged protease domain of neurobin remained in the ER network (example of the construct containing both, the SEA domain and the protease domain of neurobin is depicted). C, The tagged wild type neurobin containing the transmembrane segment appeared to be enriched in the ER close to the nucleus.

3.12.3 Testing and affinity purification of the SEA domain antibody using the prokaryotically expressed SEA domain

Both first and second boost sera of both rabbits (R143 and R145) recognized the antigen and could be used both for immunofluorescence and Western blotting (though high background was observed). For affinity purification the SEA domain (Ala55 to Lys199) was produced with N-terminal His-tag in *E.coli* strain BL21CodonPlus(DE3)-RIL using the pET-expression system (Figure 3.24a). After affinity purification on HisSelect (Figure 3.24b), 50 mg of soluble SEA domain were obtained from 1 liter of *E.coli* culture.

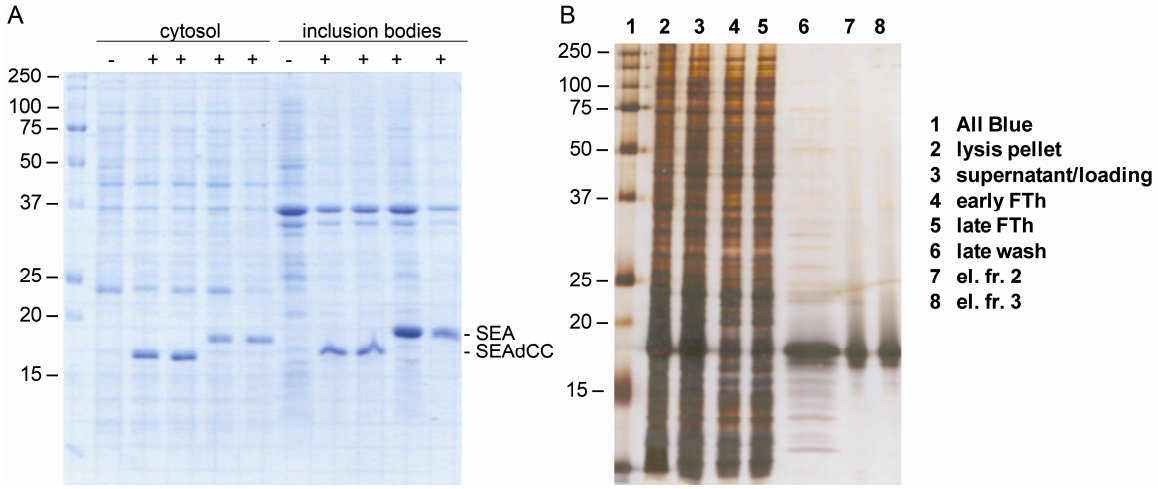

Figure 3.24: A, Coomassie gel analysis of *E.coli* clones overexpressing the SEA domain. A significant fraction of both, the short SEA domain (stopping in front of the two Cys in the zymogen region, SEAdCC) and the full length SEA domain (SEA) were expressed as soluble proteins upon induction with 1 mM IPTG (+). B, Silver stained polyacrylamid gel monitoring the purification of the soluble full length SEA domain. In lanes 7 and 8 were loaded with 1 µg protein from two different elution fractions.

The purified SEA domain was coupled to NHS-activated sepharose and used for affinity purification of the antibodies. This significantly improved the signal to background ratios in both Western blotting and immunofluorescence and rendered the anti SEA domain antibody an important tool (Figure 3.25 and preceding result sections).

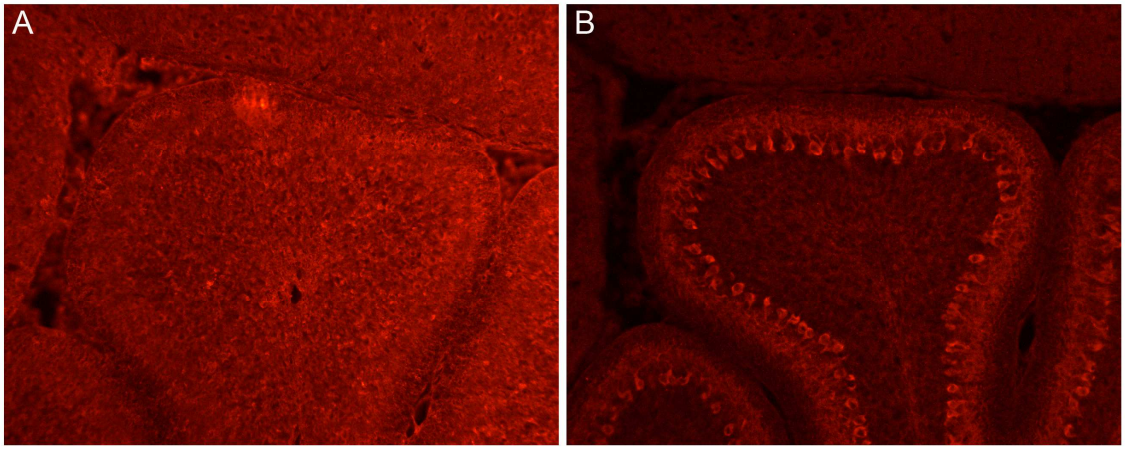

Figure 3.25: Affinity-purification resulted in a dramatic effect on the performance of SEA domain antibodies. Horizontal sections of a P10 mouse cerebellum were submitted to histochemistry using either the first boost serum of R143 in a dilution of 1:10 (A) or affinity purified IgGs of the second boost of R143 at a concentration of 3 µg/ml (B).

3.12.4 Antibodies against the protease domain from antigen refolded and purified from *E.coli* inclusion bodies

Since recombinant proteins containing the protease domain were not secreted by HEK 293T and COS-7 cells, we tried to find conditions allowing the soluble expression of the protease domain in *E.coli*. Since we never found suitable conditions (Figure 3.25a), we decided to use the protease domain refolded from inclusion bodies (Figure 3.25b).
The His-tagged protease domain was purified under denaturing conditions on HisSelect from washed inclusion bodies solubilized with guanidinium hydrochloride. Silverstaining revealed one very strong band of the expected size and additionally weak bands of smaller proteins when separating 3 ug of the eluted material by reducing SDS-PAGE. Like the strong band, the small bands were also detected in Western blotting using an antiHis antibody and were therefore considered to be N-terminal fragments of the protease domain.

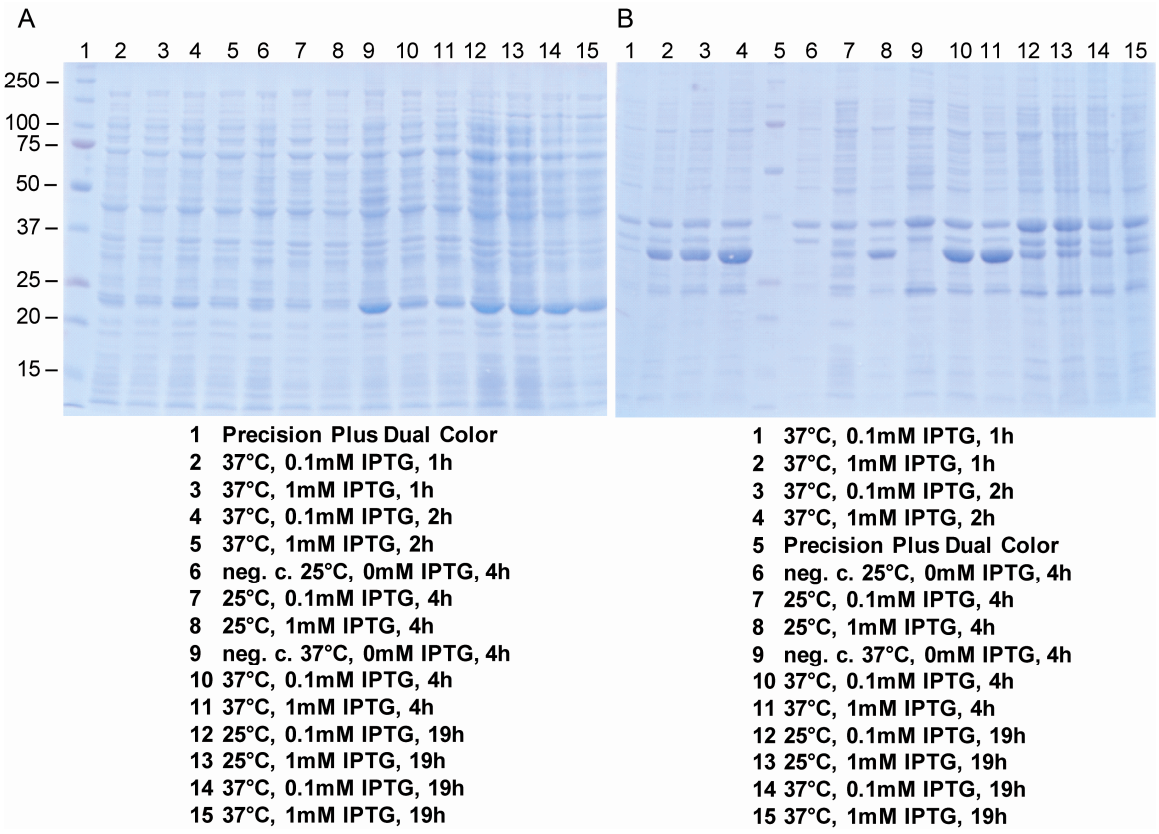

Figure 3.26: Coomassie stained gels showing an example of conditions tested for soluble protease domain (PD) expression. A, Extracts of *E.coli* cultures displayed the same band pattern independent whether IPTG was used for induction or not. B, In contrast, the inclusion body fractions of induced cultures showed a strong accumulation of a band running at the expected height. Labels of the molecular mass markers in kDa are indicated at the left of panel A.

Refolding trials eventually led to a soluble protein fraction. Non-reducing SDS-PAGE revealed a heterogeneous population of oligomers (in assays with chromogenic peptide substrates no activity was observed in these refolding samples after processing by enteropeptidase). The refolded material was purified on a HisSelect column using native conditions. As expected, the low molecular weight bands were co-purified (Figure 3.26a). MS-fingerprint analysis indeed proved them to be N-terminal fragments of the recombinat protease domain of neurobin. Thus, the material fulfilled our quality criteria and was used to immunize two rabbits.

The sera (R156 and R158) of the first and second boost were analysed. They performed weak in Western blotting with neurobin transfected HEK293T cell extracts, and were not functional in immunofluorescence experiments. From a Western blot analysis we learned that most immunoreactivity was caused by the N-terminal segment of the antigen which

is not part of neurobin (Figure 3.26b). Therefore, we did not inject further antigen into animals.

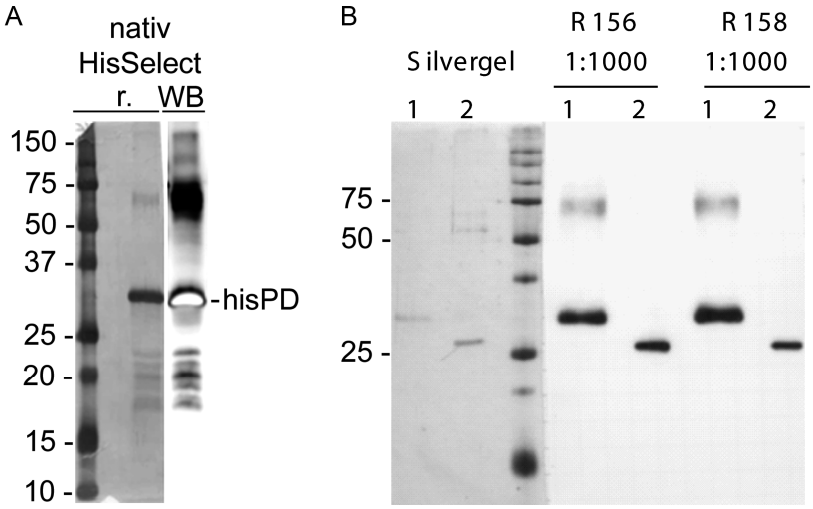

Figure 3.27: A, Reducing silvergel (r.) and Western blot (WB, with anti tetra His antibody) analysis of the refolded protease domain of neurobin (hisPD) after native HisSelect chromatographie. In both cases 1 µg protein was separated on 12.5 % polyacrylamide gels. The monomeric form of hisPD resulted in the strongest signals (in WB luminescence substrate was locally depleted). Since reduction was not quantitative, the dimer and in the case of WB also tri- and tetramer could be detected. Additional bands were detected below the monomer, both in silver staining and Western blotting. B, The second boost antibodies raised against the hisPD antigen were tested on 9 ng hisPD (1) and 18 ng PD after activation (as presented on the silver gel).From densiometric analysis we learned that the antigen with the His-tag, linker and enteropeptidase cleavage site present was recognized 3 and 10 times better respectively than the activated protease domain. Molecular mass markers in kDa are indicated at the left of panel A and B.

3.12.5 Potential of polishing the protease domain

To obtain an even more homogenous fraction of the correctly refolded neurobin protease domain (3.8) without the low molecular bands being present (e.g. for kinetic studies or crystallization attempts) a benzamidine column can be used (Figure 3.27). However in our trials binding was incomplete and the absence of the low molecular bands might in part be explained by the low amount of protein submitted to the silver staining analysis after such a polishing step.

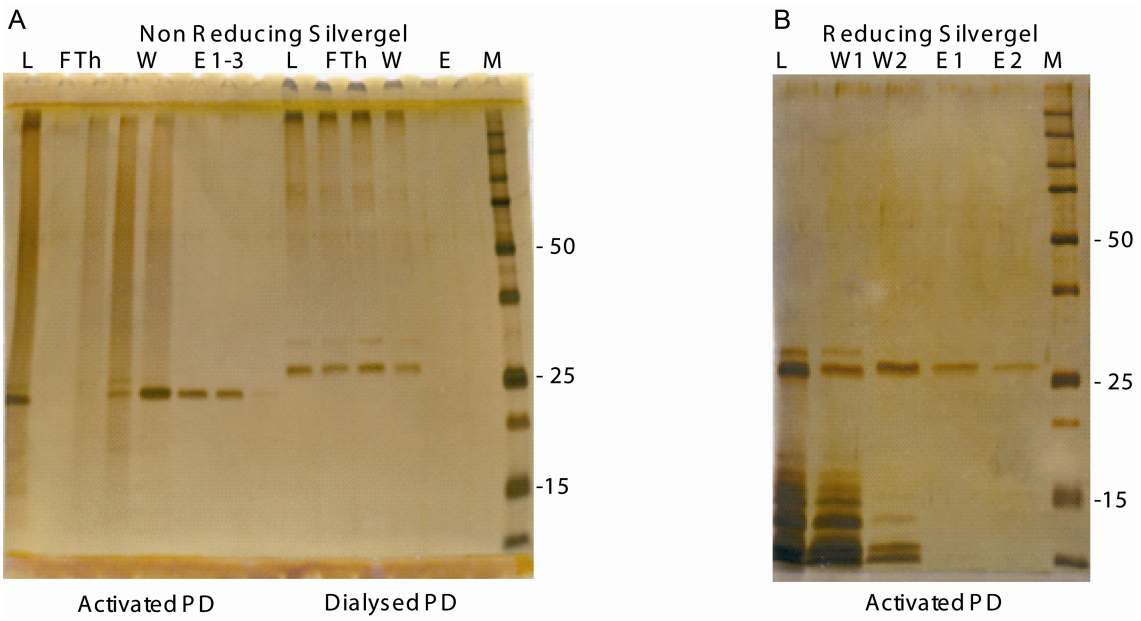

Figure 3.28: Silvergel analysis of the benzamidin-column purification of either the activated protease domain (Activated PD) or the protease domain prior to activation by enteropeptidase (Dialysed PD). A, The smear of ill-folded oligomers visible in the loading sample (L), was detected in the flowthrough (FTh) and wash fractions. As expected, only activated protease bound to the column and could be recovered in elution fractions (E1-3). B, Reducing conditions revealed that molecules without intradomain cleavage bind best to benzamidine. Labels of the molecular mass markers in kDa are indicated at the left of panel A.

3.12.6 Trials for periplasmic expression of the protease domain and the SEA domain in *E.coli*

As the formation of correct disulfide bridges might occur in the oxidizing environment of the bacterial periplasm, the DNA sequence of neurobin SEA or protease domain with C-terminal mycHis tag was ligated in frame to the N-terminal PelB periplasmic secretion signal in the pET20b+ vector. In all the tested expression conditions in *E.coli* strain BL21CodonPlus(DE3)-RIL, the recombinant proteins were only detected in the inclusion body fraction, but not in the soluble or periplasmic fraction, nor in the medium. Obviously the hydrophobic PelB sequence was unable to ensure secretion but led to aggregation of even the SEA domain which as such was highly soluble (see Figure 3.24).

3.12.7 Trials for expression in *pichia pastoris* strains

Yeast is a well established organism for the production of secreted proteins. The *Pichia pastoris* expression system offers both the benefits of *E. coli* (high-level expression, easy scale-up, and inexpensive growth) and the advantages of expression in a eukaryotic system (protein processing, folding, and posttranslational modifications). Besides, the glycosylation in *Pichia pastoris* is said to differ less from higher eukaryotes than the glycosylation in *Saccharomyces cerevisiae* (less hyperglycosylation, high mannose with only 8-14 mannose residues compared to 50 -150 in *Saccharomyces cerevisiae*, no alpha 1-3 glycan linkages). We therefore expected to obtain efficient protein secretion by producing recombinant proteins with N-terminal *Saccharomyces cerevisiae* alpha-factor (introduced by pPICZα vectors) in *Pichia pastoris*.

All generated constructs contained an N-terminal yeast signal peptide sequence. One of the constructs encoded the protease domain with N-terminal His-tag and enteropeptidase cleavage motif. Two other constructs (SEA from Ala55 to Lys199 and SEA plus protease domain from Ala55 to Leu431) were cloned with a C-terminal mycHis tag. Protein production from the three constructs was tried in the *Pichia pastoris* strain X-33, recommended when using the pPICZα vector, but also strains GS115 and KM71H following the instructions in the EasySelect *Pichia* Expression manual (http://www.invitrogen.com/content/sfs/manuals/easyselect_man.pdf). Growth conditions and methanol-induced gene expression under the AOX1 promotor were suitable for secretion as controlled with a GS115 mutant overexpressing human albumin under the AOX1 promotor as proven by the fact that in general, the albumin signal was observed in the supernatant by a simple Ponceau S staining already two days after induction start (Figure 3.29 a). The SEA and the protease domain constructs were expressed well in all strains as observed by performing Western blot analysis with extracts from induced yeast cultures (Figure 3.29 b). However, the supernatant of such cultures did not contain recombinant protein detectable by Western blotting at any time point of eight-day induction periods.

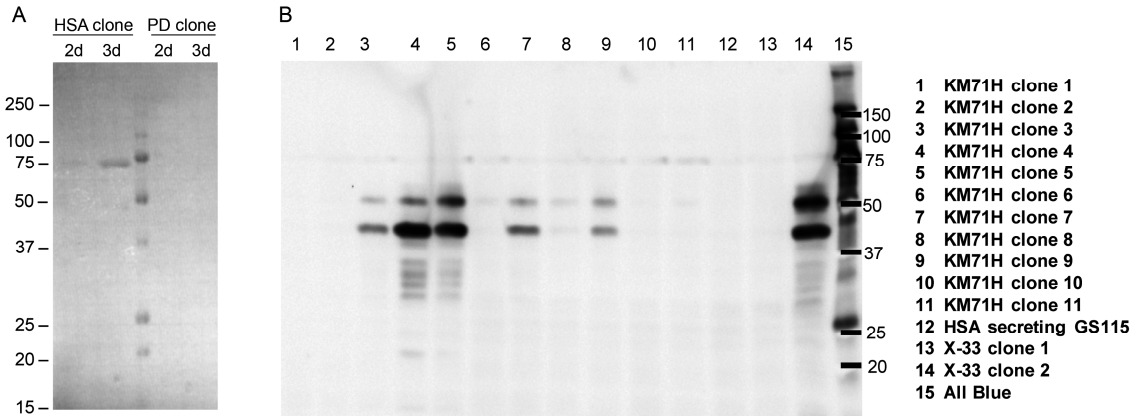

Figure 3.29: Example of the yeast expression trials. A, The human serum albumin signal was detectable in the medium by day 2 (d2) by Ponceau S staining when incubating an HSA secreting GS115 strain clone. The protease domain of neurobin (PD) could never be detected in the medium by Western blotting, testing 21 different clones. B, Extracts of several KM71H and X-33 clones showed clear expression of the PD (upper of the strong bands likely resulted from the protease domain with the signal sequence not cleaved off) after 3 days in culture. Detection was performed using the anti tetra His. Molecular mass markers in kDa are indicated at the left of panel A and the right of panel B.

4 Discussion

In summary, our work enabled the identification and biochemical characterization of a new TTSP, designated neurobin/TMPRSS11c. Neurobin has a short cytosolic N terminus, a single transmembrane domain, an SEA domain and the C-terminal protease domain. With this domain organization, neurobin mostly resembles the members of the DESC/HAT group of TTSPs. The protease has a restricted tissue distribution with prominent presence in Purkinje neurons. *In vitro*, neurobin is able to process FGF-2 after several basic residues, but it does not cleave extracellular matrix molecules such as laminin and fibronectin. Further analysis is needed to assess the *in vivo* relevance.

4.1 The insensitivity of neurobin towards calcium and sodium ions

Neurobin activity was not modulated by Ca^{2+} ions. As recently reviewed (Page et al., 2005), allosteric regulation of serine proteases is mediated via Ca^{2+} complexation by acidic amino acids in position 70 and 80 (chymotrypsin numbering). In neurobin, Phe and Leu, respectively, are present, consistent with the insensitivity of neurobin toward calcium concentration changes. Using a broad range of Na^+ concentrations for the peptide cleavage assays, we measured no significant differences in the catalytic activity of neurobin, suggesting that this enzyme is not allosterically regulated by Na^+ ions. With respect to allosteric regulation, site-directed mutagenesis with thrombin revealed that residue 225 (either Tyr or Pro in serine proteases) is implicated in Na^+-induced regulation of enzyme activity, because thrombin Tyr225Pro (chymotrypsin numbering) lost its ability to bind Na^+(Dang and Di Cera, 1996). In neurobin, Pro412, i.e. the residue compatible with Na^+ insensitivity, occupies the homologous position. Pro412 is embedded in the sequence Asn-Lys-**Pro**-Gly. The entire motif is conserved in all DESC/HAT-like enzymes, a further point suggesting a relationship among these enzymes.

4.2 The neurobin locus and neurobin preservation in other species

Using neurobin cDNA sequences our gene bank homology searches indicated that the neurobin gene lies on mouse chromosome 5. This region was recently described as a locus containing seven DESC and HAT-like TTSP genes in a cluster (Hobson et al., 2004). These authors also predicted the existence of neurobin (referred to as HAT-like 3). However, the protein sequence predicted from genome analysis was not fully identical to our cDNA-derived sequence (predicted length 418 amino acids, resulting from the absence of 13 amino acids forming the end of the SEA domain and the zymogen activation part). Sequence predicions revealed that these 13 amino acids are present in horse and short-tailed opossum, but absent in rat, dog, and cow. The relevance of this difference is, however, not known. Five of these DESC and HAT-like genes could be identified on human chromosome 4 (Hobson et al., 2004). Our gene bank homology analysis and own sequencing of human genomic DNA indicated that the predicted last exon in the genomic region, possibly encoding a human orthologue, contained an eight base-pair insertion shortly after the triplet encoding the catalytic S381. The insertion leads to a completely unrelated amino acid sequence after I393 and e.g. the loss of C406, mandatory for one of the three conserved disulfide bonds. The concerning sequence stretch is also forming part of the cavity of the catalytic triad and the S1 pocket (Figure 4.1). There is little chance that the resulting sequence would allow the assembly of a functional protease domain. Besides, the exons encoding a possible SEA domain of human neurobin can not be assigned. Taken together it is very likely that the human neurobin gene is completely psydogenized. More and more genomes were completed till date. The neurobin gen appears functional in rat, horse, dog, cattle, gray short-tailed opossum and possibly also in the platylus genome. Till date however, in the genomes of chimpanzees and macaques neurobin can not be assigned.

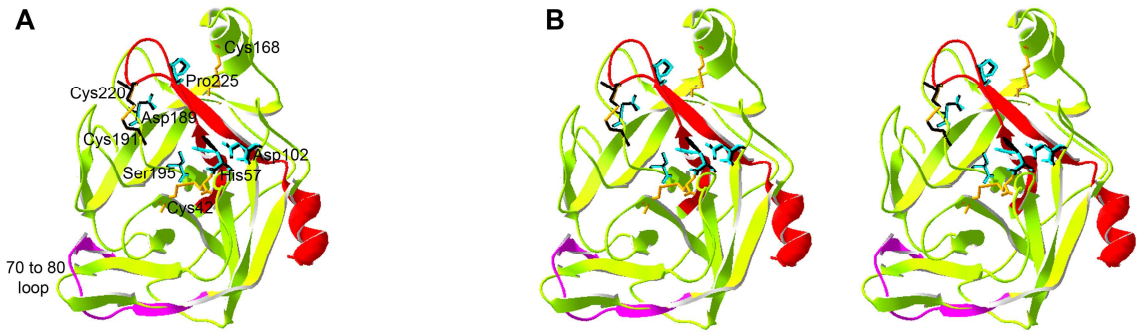

Figure 4.1: The ribbon model of the neurobin protease domain sequence is shown after alignment to the 3-D template (built by the overlay of the x-ray structures of four trypsin-like serine proteases from the PDB: 1ekb(B) - bovine enteropeptidase, 1eax(A) – human matriptase, 1z8g(A) – human hepsin and 2any(A) – human plasma kallikrein), chymotrypsin numbering with selected residues. Neurobin is colored in green until I393 and then in red until the C-terminus. The red part contains C220, P225 and contributes to the formation of the catalytic center and the S1 pocket. From the enteropeptidase structure the conserved disulfide bridges are shown in yellow and other selected residues in blue. Neurobin residues are depicted in black. The orientation of the 70 to 80 loop, associated with Ca^{2+} allostery, differs most comparing the enteropeptidase structure and the neurobin model (the ribbon model of enteropeptidase residues 70 to 84 is given in magenta). B, Stereo image, same orientation as in A. The D189 is clearly visible at the bottom of the S1 pocket.

4.3 Implications of neurobin-absence in man

A possible absence of neurobin in man does not exclude the absence of its function. The high sequence identity of the neurobin protease domain to the protease domain of the members of the highly related DESC/HAT group could have enabled one of these enzymes to take on proteolytic specificity and function in man similar to the one of neurobin in mouse. Such a concept is compatible with the finding that DESC2 (Netzel-Arnett et al., 2003) and DESC4 (Behrens et al., 2004) are expressed in human brain tissue. Human DESC1 can cleave fibronectin (Viloria et al., 2007), a protein not cleaved by neurobin. This points to not exactly neurobin-like specificity, despite the fact that DESC1 has highest homology to neurobin. Alternatively, a human protease with neurobin-like function might have remote homology only, as recently observed with the identification of the murine metalloprotease Mcol-1, a possible counterpart of human MMP-1 (Balbín et al., 2001). Finally, genomic analyses indicate that man and mouse share some 166 serine protease genes, whereas nine are human specific and 43 are mouse specific (Puente et al., 2003b). Hence, molecules present in one species only may be

instrumental in highly species-specific functions. Or, to stress another aspect of the same story: Neurobin might be one of the gene products leading to the manifestation of differences between mammals like mice and men.

4.4 Selfactivation of neurobin

Autoactivation has been described for other TTSPs (Afar et al., 2001; Guipponi et al., 2002; Szabo et al., 2005; Velasco et al., 2002). Catalytic activation of Neurobin can occur in an autocatalytic manner at the sequence-predicted site Gly-His-Lys199, as demonstrated by site-directed mutagenesis. However, alternative cleavage motifs were used whenever Lys199 was mutated to Ala. An activated neurobin molecule might excessively scan for cleavable motifs in a neurobin proenzyme molecule. This would particularly make sense assuming an activation mechanism in which intermolecular interactions only cease upon cleavage induced domain rearrangements. Supporting such a concept of scanning for alternative cleavage motifs is the recent finding, that thrombin can use alternative cleavage sites on a substrate when the primary cleavage position was mutated (Yu et al., 2007b).

Whether neurobin can also be activated by other proteases is unknown yet. Also, whether the observed further processing within the protease domain is of physiological relevance or due to e.g. unphysiologically high concentrations of the refolded protease domain after purification or the mycHis-tagged neurobin in the ER of HEK293T cells, could not be addressed with our available tools. An inactivating effect of such intradomain processing was suggested by reduced binding of fragmented protease domain to a benzamidine column.

Further analysis of autocatalytically activated wild-type neurobin under non-reducing conditions suggested that protease domain and the membrane-anchored N-terminal part were not covalently linked. This missing linkage might result from the absence of the predicted disulfide bridge, or alternatively, from a secondary not yet defined cleavage in front of the activation domain. Whether the protease domain remains at the plasma membrane or is released needs further investigations. In fact, shedding of TTSPs has been reported previously (Hansen et al., 2004; Kim et al., 2005).

4.5 Neurobin characteristics in the light of the x-ray structure of human DESC1

Several peculiarities struck us while characterizing neurobin. For example, neurobin constructs with a C-terminally tagged protease domain did not allow production of secreted proteins in any of the tested expression systems. Besides, subcellular distribution of such constructs differed from that of the untagged counterparts.

Another astonishing feature of neurobin was the potential lack of a disulfide bridge between the zymogen activation region and the protease domain although the suitable Cys residues are located in the expected sequence positions.

Tags are known to cause altered protein folding and/or sorting and can even act as aggregation chaperones (Jain et al., 2000). The lack of the disulfide linkage might simply be explained by postulating that Cys187 and Cys188 in the zymogen activation region react with one another. However, folding/secretion and the missing linkage phenomena might both be explicable by analogy considering knowledge gathered from the recent analysis of the x-ray structure of human DESC1 (Kyrieleis et al., 2007). In the crystal structure of DESC1 Kyrieleis et al. detected a salt bridge between the carboxylate group of the C-terminal Ile244 and the guanidyl group of Arg135 (all chymotrypsin numbering), which can stabilize a hydrophobic patch on the surface of the protease opposite to the catalytic left. In neurobin, the corresponding Arg235 is conserved and Ile244 is Leu. All other amino acids generating the hydrophobic patch are also conserved except Tyr208 in DESC1, which is Phe in neurobin, therefor even increasing the hydrophobicity of the area. Of note, hepsin was crystallized with its N-terminally preceeding scavenger receptor cysteine rich (SRCR) domain rigidly bound to a similar hydrophobic patch on the surface of its protease domain (Somoza et al., 2003). As Kyrieleis et al. analyzed, these hydrophobic patches and a hydrophobic canyon that can accommodate the zymogen activation region are conserved in all four subfamilies of the TTSPs. Therefore, Kyrieleis et al. postulate a general mode of interaction of TTSPs with their preceding non-catalytic domain(s) via these hydrophobic patches (Figure 4.2). Arg120 in the middle of the hydrophobic patch of DESC1 is postulated to form a salt bridge with the SEA domain. This Arg120 is also conserved in neurobin. Thus, also the protease domain of neurobin might be fixed and oriented by rigid binding to the SEA domain making a covalent linkage dispensable. Given the above assumptions are correct, it is obvious that both folding/stabilization of the protease domain and its interactions with the SEA domain

would be hampered by the presence of the mycHis tag. Influences on sorting and activation characteristics would thus find a direct explanation.

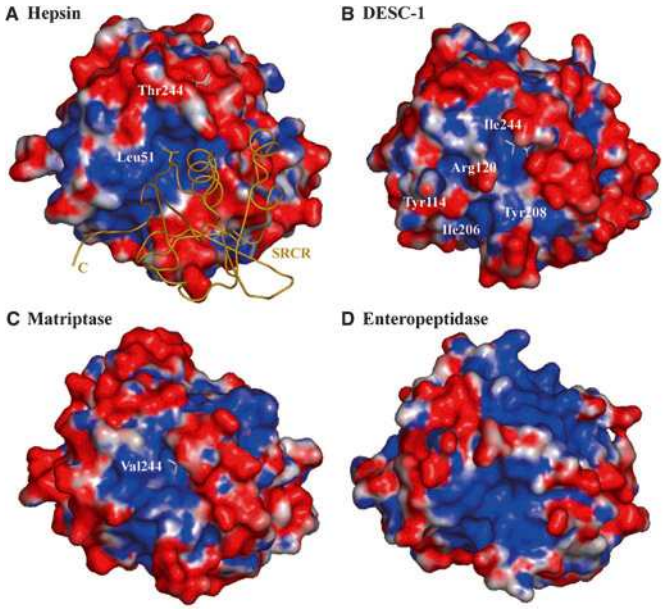

Figure 4.2: Solid-surface representations of human hepsin (A), human DESC1 (B), human matriptase (C) and human enteropeptidase (D). The enzymes are rotated around a vertical axis for 180° in comparison with the standard orientation where the catalytic cleft points towards the reader. Hepsin (A) is shown bound to the SRCR domain, which is drawn as golden Cα-trace. Hydrophobic residues are in blue, and polar residues are in red. The corresponding residues Ile244 (DESC1), Val244 (matriptase) and Thr244 (hepsin) are shown in ball-and-stick models. Taken from (Kyrieleis et al., 2007).

4.6 FGF-2 is cleaved by neurobin

Neurobin processed 17-kDa FGF-2 to defined products of 13, 8.5, 6.4 and 4.3 kDa and N-terminal sequence analysis confirmed neurobin preference for Lys or Arg in the P_1 position. The available data do not yet allow us, however, to define a sequence specificity of neurobin. Further experiments are needed to elucidate whether neurobin displays tightly defined amino acid selectivity in the P_2 - P_4 positions and specificity may also be controlled by an induced-fit mechanism or exosite interactions between substrate, the protease domain and/or the SEA domain of neurobin.

Proteolytic processing of FGF-2 was recently reported to occur by the hyaluronan-binding protease from human plasma (Etscheid et al., 2004). Similar to our finding,

proteolytic processing was inhibited by heparin. Degradation of FGF-2 was first reported to occur during incubation with plasmin (Saksela et al., 1988).

Interestingly, histochemical localization of FGF-2 in the cerebellum revealed strong expression in Purkinje cells with a distribution very similar to the distribution of neurobin (Matsuda et al., 1994; Reynolds et al., 2005), indicating that FGF-2 could indeed be an *in vivo* substrate of neurobin. Since FGF-2 plays a critical role in neuronal development (Abe and Saito, 2001; Ortega et al., 1998), cleavage of FGF-2 by neurobin may modulate FGF-2-dependent functions during cerebellar development.

4.7 Considering the cleavage specificity of neurobin

In our *in vitro* analysis only FGF-2 but not laminin, fibronectin or FGF-7 were processed by neurobin. Also in cell culture experiments neurobin displayed restricted proteolytic activity as discussed in the context of self-activation.

We also investigated a FGF-2 variant directed to the conventional ER/Golgi-dependent secretion pathway by an N-terminally fused calsyntenin secretion signal. Though appearing straight forward, the approach bears other difficulties. It is known for example, that introducing FGF-2 to this secretory pathway does not grant efficient secretion and that the formation of intra- and intermolecular disulfide bonds alter the folding of the molecule (Chen et al., 2007). Indeed, though well expressed, we had difficulties to detect the FGF-2 variant in the medium and we could never observe neurobin mediated cleavage of FGF-2 accuulated in the secretory pathway. It is fair to assume that neurobin is capable of self-activation already in the ER, since wild-type neurobin always appeared to be quantitatively processed when analyzing extracts of transfected cells. Therefore, the inability of neurobin to cleave the FGF-2 variant introduced to the secretory pathway could be taken as a further hint for selective cleavage under physiological conditions.

Similarly, in co-expression experiments with other proteins the proteolytic activity of neurobin was low or selective as observed for example in the case of the glutamate receptor delta 2 (GluRδ2) subunit. GluRδ2 was chosen for co-expression experiments because of its specific expression at parallel fiber-spine synapses in cerebellar Purkinje cells (Landsend et al., 1997). The mature form of the murine GluRδ2 protein consists of

984 amino acids of which 73 % are topologically exposed to the protease domain of neurobin. In three independent co-transfection experiments, co-expression with active neurobin but not with the S/A mutant leads to a moderately increased signal intensity of predominantly one band, running slightly higher than the 25 kDa marker band (Figure 4.3).

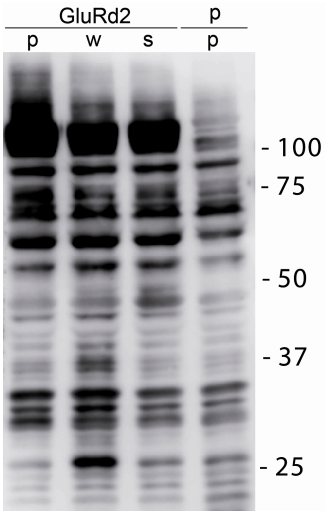

Figure 4.3: Western blot analysis of HEK293T cell extracts co-transfected with a cDNA construct of the glutamate receptor delta 2 (GluRd2) fused to a C-terminal ONEstrep tag and either pcDNA-vector (p), wild-type neurobin (w) or the S/A mutant thereof (s). Reproducibly, especially one bands detected running at about 27 kDa was stronger in the cotransfections of GluRd2 with wild-type neurobin. Molecular mass markers in kDa are indicated at the right.

It would be exiting to investigate whether conditions exist, under which this neurobin-dependent cleavage(s) of GluRδ2 can be enhanced. Particularly, since the GluRδ2 subunit (which is not known to occur in functional ionotropic glutamate receptors) was reported to exert its function on cerebellar LTD and motor learning via protein interactions of its C-terminal cytosolic domain (Uemura et al., 2007; Yawata et al., 2006). Exactly this segment, following on the cytosolic side of the last of three transmembrane helices, would be released from the rest of the GluRδ2 protein upon cleavage by neurobin in the last extracellular loop. Besides, limited proteolysis of the GluR subunit 3 by γ-secretase was recently proposed as mechanism to increase specializations among closely-related GluR subunits (Meyer et al., 2003). It was beyond the scope of this thesis to go into detail of the potential physiological relevance of GluRδ2 processing by neurobin. However, the initial observation is again good evidence, that neurobin displays strong cleavage site selectivity although the primary binding pockets of the catalytic cleft accept a considerable variety of different amino acids.

Interesting in this context was also the observation that the chromogenic substrate with only Arg preceding the pNA group was not cleaved by neurobin, while trypsin control-experiments suggested good substrate characteristics of the molecule.

4.8 Considerations concerning the cleavage of FGF-2 by neurobin

50 % of FGF-1 (acidic fibroblast growth factor, the closest relative of FGF-2 in the entire FGF-family) were reported to occur in an unfolded state at physiological temperature (Zakrzewska et al., 2004). If the same was true for FGF-2, one could argue that the observed cleavages by neurobin are rather unspecific since it is well known that unfolded proteins are more sensitive to proteolytic activity (Hubbard, 1998). An argument against this possibility of unspecific FGF-2 degradation is, however, that thrombin is able to process the high molecular weight (HMW) forms of FGF-2 *in vitro* and in endothelial cells, but not the short FGF-2 form we analyzed (Yu et al., 2007b) - and the protein substrate specificity of thrombin *in vitro* is not as high as might be assumed, as was learned e.g. from the multiple *in vitro* cleavages of the microtubule associated protein tau (Arai et al., 2005).
In the light of such findings it would also be interesting to examine neurobin activity towards the HMW forms of FGF-2 to learn more about the potential physiological relevance of our results. Particularly, it might be interesting to see, whether heparin binding of the HMW forms of FGF-2 has the same protective effect as was observed for the 17 kDa form. It can not be excluded, that under physiological conditions neurobin cleavage modulates the activity of only certain FGF-2 isoforms. In the spinal cord for example, the HMW forms interact with an assembly and splicing factor of the splicing machinery, called survival of motor neuron protein (SMN) because its absence leads to fatal degeneration of motor neurons (Claus et al., 2003). Neurobin, initially detected in spinal cord, might participate in the modulation of SMN-induced effects by possibly cleaving the HMW forms of FGF-2 under physiological conditions.

Possibly, the first cleavage of FGF-2 by neurobin occurs after Arg116. Since, from the *in vitro* digests neither by N-terminal sequencing from gels nor by MS measurement we got evidence for FGF-2 fragments spanning NTYR116-SRKY. This suggests that all other cleavages might occur after the postulated primary (or lead) cleavage, C-terminally of Arg116. FGF-2, lacking this C-terminal fragment might retain some of its signaling functions while not binding to proteoglycans any longer. Thus, neurobin would render an

alternative to the processing of proteoglycans by HtrA1 (Hou et al., 2007) to promote long range FGF-2 signaling. However, it is probably more likely that cleavages by neurobin – be it in a defined sequential or in a random order – might function as a local off switch for FGF-2 signaling, similar to e.g. neprilysin, a surface-bound metallo-protease, which slows down angiogenesis by FGF-2 degradation (Goodman et al., 2006).

We never observed FGF-2 cleavage by neurobin in our cell culture experiments. For the secretion of FGF-2, direct interactions with heparin sulfate proteoglycans are essential (Zehe et al., 2006) and we found FGF-2 attached to the surface of transfected COS7 cells – very likely via proteoglycans. Thus, neurobin might not encounter FGF-2 in an unbound state or bound in a way that is compatible with cleavage. And, since heparin suppresses FGF-2 cleavage by neurobin (see figure 3.18), cleavage might be prevented. Additionally, our finding might be due to the used cell lines and/or used cell culture conditions.

Interestingly, x-ray structures of FGF-2 bound to heparin or bound to heparin plus the FGF receptor, respectively, reveal that the cleavage positions determined by our N-terminal sequencing are rather surface exposed (Figure 4.4). It would be interesting to see whether heparin-binding still protects FGF-2 when bound to the receptor. Possibly, e.g. conformational changes upon receptor binding enable neurobin to cleave FGF-2 in a quasi two dimensional arrangement at the plasma membrane. In such a model, neurobin would exert its function to prevent self-stimulation of Purkinje cells secreting FGF-2 for e.g. signaling via FGF receptors 1 of type IIIb, which are specifically expressed on neighboring granule neurons in the cerebellum (Beer et al., 2000).

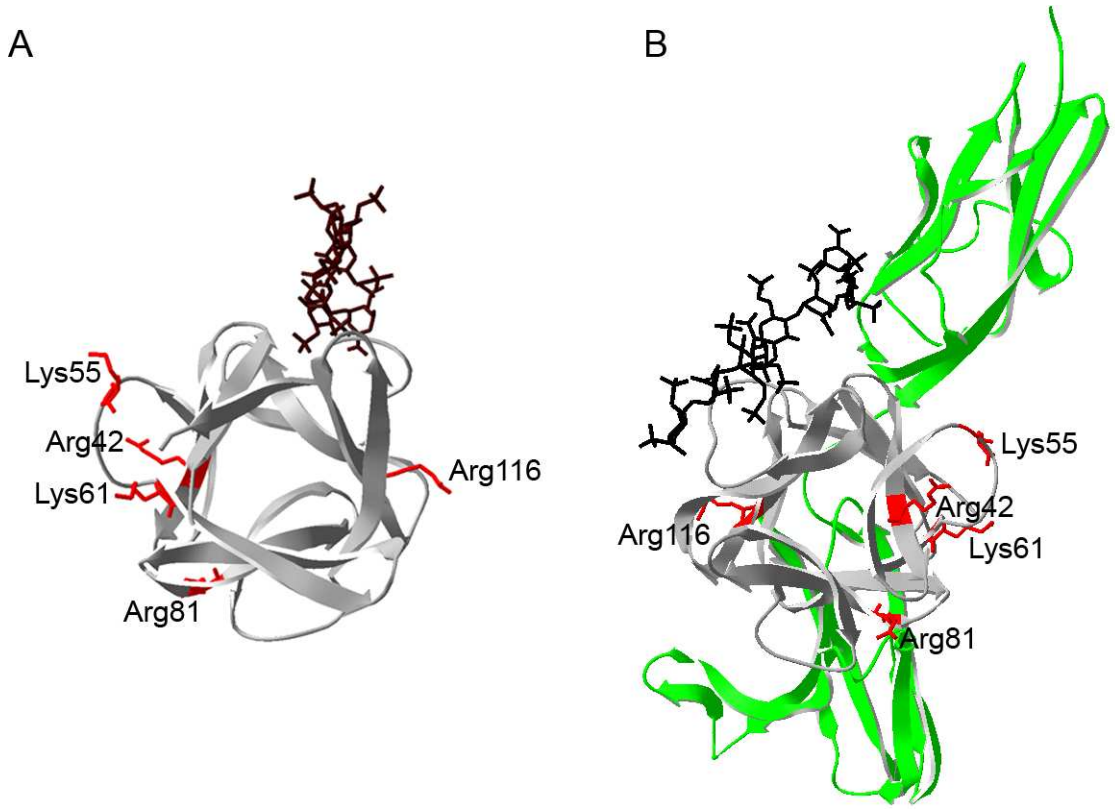

Figure 4.4: Ribbon models of FGF-2 x-ray structures in gray with the basic amino acids preceding the neurobin-cleaved bond highlighted in red. A, FGF-2 in complex with a heparin hexamer (brown) (PDB ID: 1BFC). B, FGF-2 (seen from the bottom side relative to A) in a ternary complex with FGF receptor 1 (green) and heparin (black) (PDB ID: 1FQ9). In both, A and B at least some of the cleavage motifs recognized by neurobin are exposed on the surface of the structures and should principally be accessible to the protease.

Given these difficulties and uncertainties in experiments using COS7 or HEK293T cell-lines, the analysis of FGF-2 cleavage by neurobin in cell-culture/*in vivo* should probably include neurobin-transfected rat Purkinje neuron cultures, either cotransfected with FGF-2 cDNA or incubated with exogenously applied recombinant FGF-2.

5 Materials and Methods

5.1 Chemicals and Additives

Acetic acid (Fluka, puriss.p.a)
Acetone (Fluka, puriss.p.a)
AEBSF, 4-(2-Aminoethyl)-benzenesulfonyl fluoride hydrochloride; Pefabloc SC (Roche)
Agarose (Eurogentech)
Ampicilline (Appligene)
Aprotinin (Roche Diagnostic)
APS, ammonium peroxy sulphate (Fluka, puriss.p.a)
Bacto agar (Difco)
Bacto tryptone (Difco)
Benzamidine (Fluka)
Blocking Reagent, casein digest (Amersham)
Bromphenol blue (Sigma)
BSA, bovine serum albumin (Serva, Promega)
Calcium chloride dihydrate (Fluka, puriss.p.a)
DMSO, dimethylsulphoxide (Sigma)
dNTPs, desoxyribonucleoside triphosphates (Promega)
E64, Cys-protease inhibitor (Sigma)
EDTA, ethylene diamino tetraacetic acid (Fluka, puriss.p.a)
Ethanol (Fluka, puriss.p.a)
Ethidium bromide (pharmacia)
FCS, fetal calf serum (Biochrom AG, Berlin)
Fluorescent Mounting Medium (DAKO)
Glacial acetic acid (Fluka, puriss.p.a)
Glutamine (Sigma)
Glycerol 87 % (Fluka, puriss.p.a)
Glycine (Fluka, purum)
HAT, media suplement 50x (Sigma)
HCl, hydrochloric acid (Fluka, puriss.p.a)
Hepes, N-(2-hydroxyethyl)piperazine-N’-2-ethane sulfonic acid (Serva)
Imidazole (Fluka)
Isopropanol (Fluka, puriss.p.a)

Leupeptin (Roche)
Magnesium chloride hexahydrate (Fluka, puriss.p.a)
β-Mercaptoethanol (Fluka, puriss.p.a)
MES (Sigma)
Methanol (Fluka, puriss.p.a)
MOPS (Sigma)
Pepstatin, Asp-protease inhibitor (Sigma)
PFA, paraformaldehyde (Fluka)
Phosphoramidon, metalloprotease inhibitor (Sigma)
PLL, poly-L-lysine (Sigma)
PMSF, phenylmethanesulfonylfluoride, Ser-protease inhibitor (Fluka)
Ponceau S (Sigma)
Potassium acetate (Fluka)
Potassium chloride (Fluka)
SDS, sodium dodecyl sulfate (Fluka, puriss.p.a)
Sodium chloride (Fluka, puriss.p.a)
Sodium hydroxide (Fluka, puriss.p.a)
StrepTactin (IBS)
Sulfosalicylic acid
TEMED, tetramethylethylendiamine (BioRad)
Trichloracetic acid (Fluka, puriss.p.a)
Trichlormetane (Fluka, puriss.p.a)
Tris base (AppliChem)
Triton X-100 (Fluka)
Tween 20 (Serva)
Yeast extract (Difco)

5.2 Buffers, Media and Solutions

Ampicilline stock:	100 mg/ml in UHP water, filtered (0.22 μm filter)
Blocking Buffer:	1 ml 20x PBS, 2 ml FCS (use exp./old aliquots), 0.02 g glycine, adjust volume to 20 ml by adding UHP water
Blocking solution:	5 % blocking reagent (Amersham) in TBS-T
DNA Loading Buffer (5x):	0.2 % (w/v) bromophenole blue, 0.2 % (w/v) xylene cyanol FF, 25 % glycerol

$DMEM^+$:	Dulbecco's modified Eagle's medium without sodium pyruvate (GibcoBRL), 10 % FCS, additional 2 mM L-glutamine, HAT
EDTA (0.5 M):	37.22 g disodium EDTA·$2H_2O$ in 160 ml water, ad NaOH (4.4 g) till solution gets clear, add water to volume of 200 ml
Fixative (4 % PFA)	60 ml water (50°C), 4 g PFA (add 0.5 M NaOH till PFA is dissolved), 5 ml 20x PBS, 4 g sucrose, add water to final 100 ml, check pH (should be 7.2 - 7.4).
5x(reducing) Lämmli buffer:	250 mM Tris-Cl (pH 6.8), 10 % (w/v) SDS, 0.005 % (w/v) bromophenole blue, 50 % (v/v) glycerol, (500 mM dithiothreitol)
LB Agar:	LB Medium, 15 g/l bacto agar, autoclave, (add 100 µg/ml Amp.)
LB Medium:	10 g/l bacto tryptone, 5 g/l yeast extract, 10 g/l NaCl, autoclave, (eventually add 50 µg/ml Amp.)
lower Tris (SDS-PAGE gel):	1.5 M Tris·Cl, pH 8.8, 0.04 % SDS
Lysis Buffer:	20 mM Tris, 150 mM NaCl, 1 mM EDTA, 1 % Triton X-100 (to 10 ml aliquots add one "Complete, EDTA-free; Protease Inhibitor Cocktail Tablet" from Roche)
PBS^-:	140 mM NaCl, 2.7 mM KCl, 8.1 mM Na_2HPO_4, 1.5 mM KH_2PO_4, pH 7.4
PBS^+:	PBS^- containing 0.9 mM $CaCl_2$ and 0.5 mM $MgCl_2$
Ponceau S:	2 % Ponceau S, 30 % trichloracetic acid, 30 % sulfosalicylic acid, in UHP water
SDS-PAGE running buffer:	25 mM Tris·Cl, pH 7.5, 190 mM glycine, 0.1 % SDS
"Semi-dry" Blotting buffer:	39 mM glycine, 48 mM Tris (add solid, no pH adjustment required), 3.75 ml 10 % SDS, 200 ml methanol add water to 1 L
Solution A (Transfection):	500 mM $CaCl_2$, sterile filtered (0.22 µm filter)
Solution B (Transfection):	140 mM NaCl, 50 mM Hepes, 1.5 mM Na_2HPO_4, pH 7.05 sterile filtered (0.22 µm filter)
Stripping Buffer	200 mM Glycine, HCl, pH 2.2, 1%Tween-20, 0.1 % SDS
TAE:	40 mM Tris·Cl, pH 8.0, 1 mM EDTA, 0.11 % glacial acetic acid
TBS:	20 mM Tris·Cl, pH 7.5, 137 mM NaCl

TBS-T:	0.1 % Tween in TBS
TE:	10 mM Tris·Cl, pH 7.5/8.0, 1 mM EDTA
TFBI (transformation b. I):	30 mM KAc, 50 mM $MnCl_2$, 100 mM KCl, 10 mM $CaCl_2$, 15 % glycerol (87 %, autoclaved), in sterile water
TFBII (transformation b. II):	10 mM Na-MOPS (pH 7.0), 75 mM $CaCl_2$ 10 mM KCl, 15 % glycerol (87 %, autoclaved), in sterile water
Tris (1M):	121.1 g Tris base in UHP water, let cool down, adjust pH to 7.4 (HCl), adjust volume to 1 L
upper Tris (SDS-PAGE gel):	0.5 M Tris·Cl, pH 6.8, 0.04 % SDS

5.3 Library construction

To generate a protease domain enriched cDNA library, degenerated primers were designed. Therefore a Hidden Markov Model based alignment of murine trypsin-like serine proteases (http://supfam.org/SUPERFAMILY/index.html, version 1.61) was used to determine the most frequent sequences around the catalytic His57 and Ser195. Primers +degH: 5'-CCGGAATTC TKB RTI NTI WCI GCI GCN CAY TG-3' and -degS: 5'-CCGGAATTC GG ICC ICC ISW RTC NCC-3' were generated that theoretically allow the amplification of more than eighty different protease sequences from the alignment. mRNA was isolated from spinal cord of three male and three female P 10 C57Bl/6 mice using RNeasy and Oligotex mRNA systems (both Qiagen). cDNA was synthesized from 2 µg mRNA using PowerScript™ reverse transcriptase (BD Biosciences) with oligo$(dT)_{20}$ primers (Invitrogen) and 20 U RNasin. In the subsequent PCR reaction with degenerated primers 100 ng cDNA template and the Expand High Fidelity PCR System (Roche) with 1.75 mM Mg^{2+} were used. PCR was as follows: 3 min. 94°C, 5 cycles 25 sec. 94°C, 40 sec. 45°C, 45 sec. 72°C, 30 cycles 15 sec. 94°C, 30 sec. 55°C, 45 sec. 72°C, finally 5 min. 72°C. PCR products in the range of 400 to 600 bp were extracted from agarose gels and cloned into EcoRI-cut pBSSK$^+$. DH5α *E.coli* strain (Invitrogen) was used for transformation. Transformants were plated on LB-agar plates with 100 µg/ml ampicilin. More than 85 % of the clones in the resulting library contained protease sequences.

5.4 Library screening

The protease domain-enriched cDNA library was screened in an iterative two-step manner. First, 20 clones were randomly selected and submitted to DNA sequencing by a

CEQ 2000XL DNA Analysis System (Backman Coulter). Secondly, sequences occurring frequently in this selection were used to generate digoxigenin(DIG)-labeled DNA probes to deselect identical clones by colony hybridization following "The DIG System User's Guide for Filter Hybridization" (Boehringer/Roche). The necessary components were from Roche. Totally six probes were generated by PCR using a dNTP mix in which 9 % of the dTTP was replaced by DIG-labeled dUTP. For the PCR the degenerated primers were used on plasmids containing the sequence encoding His57 to Ser 195 of the protease domains of tissue-type plasminogen activator, neurotrypsin, hepsin, neurosin, neuropsin, and additionally, a plasmid containing a non protease sequence (all plasmids were sequenced clones from the library). The probes could be used in combination and allowed the deselection of more than 90 % of the clones in the library. From the remaining library, clones were again selected randomly and analyzed by DNA sequencing.

5.5 Full length cloning

The BD SMART™ RACE cDNA amplification Kit was used. In the first strand cDNA synthesis for 5' RACE the primer -atS: 5'-CCGGAATTCAACACGTCCCTTCAGGA-3' was used. In addition to the supplied primers four gene specific primers were used in PCR amplifications (primers -GSP1: 5'-GACAGCTCGTGGTGCTTGTGGTTTA-3' and -GSP2: 5'-CCACCTTCCCTTTGGCTTTGCTTACT-3' for 5' RACE; primers +GSP3: 5'-GCTGTTGTGCGTCTGTCTTCGCCAG-3' and +GSP4: 5'-CCCACCCAACTCAG-ATGTAGT-3' for 3' RACE). The sequence information from 5' and 3' RACE was used to generate full length neurobin using primers +5'N: 5'-GGAGGATG-ACTGTGCCACCCAGCA-3' and -3'N: 5'-ATTTGCGGCCGCAGATATGCAAC-CACTGAGCTTGA-3' in a hot-start PCR reaction as follows: 1 min. 94°C, 42 cycles 15 sec. 94°C, 30 sec. 68°C, 1.5 min (+ 2 sec./cycle) 72°C, 7 min. 72°C. To insert the catalytically inactivating S381A mutation the Transformer Site-Directed Mutagenesis Kit (BD Biosciences) was used. (Primer S>A: 5'-CCAATGGTCCACCAG**C**ATCACCCTGGCAGGC-3').

5.6 Eukaryotic expression constructs

Full-length neurobin cDNA was cloned into pcDNA3.1 vector (Invitrogen) with either the endogenous stop codon to generate untagged neurobin (primers +5'N and –NstopHindIII: 5'-CCCAAGCTTCTAGAGACCAGTTTTGGATGTGATCCA-3') or in frame with the C-terminal myc-His tag from pcDNA3.1myc-His(-)A (primers +5'N and –NHindIII: 5'-CCCAAGCTTGAGACCAGTTTTGGATGTGATCCA-3'). The construct bearing the S381A mutation and the myc-His tag was termed m1 and used as template in

megaprimer based site-directed mutagenesis for the generation of mutants m2 to m5, and the mutants K156A, K158A, K171A and K156AK158AK171A, respectively.

5.7 RT-PCR analysis

Liver, lung, spleen, kidney, heart cortex, cerebellum, and spinal cord were dissected from C57Bl/6 mice. The shock-frozen tissues were homogenized by either a rotor-stator or by shaking with stainless steel beads. Total RNA was prepared from 50 mg tissue. Of each RNA preparation, 1µg was used for cDNA synthesis using the ThermoScript™ RT-PCR System (Invitrogen) with oligo$(dT)_{20}$ primers. 10% of the cDNA synthesis reaction was used for PCR with the Expand High Fidelity PCR System (Roche). The PCR cycles were as follows: for GAPDH 22 cycles 15 sec. 94°C, 30 sec. 58°C, 30 sec. 72°C, finally 5' 72°C. GAPDH-PCR (primers: +TGCCATCAACGACCCCTTC, -GGATGATGTTCTG-GGCTGC) was restricted to 22 cycles to assess the exponential phase of product formation. No product was formed in the PCR even after 42 cycles, when the reverse transcriptase was omitted. For neurobin (primers +atH: 5'-CCGGAATTCTGTTTCAT-ACGGGCTGCA-3', -atS: 5'-CCGGAATTCAACACGT-CCCTTCAGGA-3') 22 cycles 15 sec. 94°C, 1 min. 60°C, 30 sec. 72°C, 20 cycles 15 sec. 94°C, 30 sec 60°C, 1 min. 72°C, finally 7 min 72°C. The neurobin PCR product was cut with EcoRI, cloned into $pBSSK^+$, and verified by sequencing.

5.8 Verification of the 8 bp insertion in human neurobin using human genomic DNA

During a blood donation, 8.5 ml of blood were collected in an extra BD Vacutainer with 1.5 ml acid citrate dextrose. 0.2 ml of the leukocyte-enriched buffy coat preparation were collected (after 20 min at 4000 RCF) and submitted to genomic DNA preparation using a QIAamp DNA mini kit. The DNA was used as template in a standard PCR with primers +hNRBafterSer: 5' –Ggtacagattctaaaggcat - 3' and –hNRBafterStop: 5' – Tgagctttaat-ctacagaga - 3' at 52°C annealing temperature. The resulting PCR product (running as expected for the calculated 175 bps) was purified using a QIAquick PCR purification kit and directly submitted to sequencing with primer +hNRBafterSer.

5.9 Production, refolding and activation of recombinant neurobin

PCR using primers +NepPD: 5'-CCCGAGCTCGACGATGACGATAAAGTAGCAG-GAGGCCAGGATGCT-3' and –NHindIII resulted in a product encoding Val200-Leu431 preceded by the enteropeptidase cleavage motive. Cloning into pET-28a(+) (Novagen) in frame with the N-terminal His-tag (via introduced SacI and HindIII sites) resulted in the protease domain expression construct (hisPD). After overexpression in the *E.coli* strain BL21 CodonPlus(DE3)-RIL (Novagen) hisPD was purified from washed and solubilized inclusion bodies using HisSelect nickel affinity resin (Sigma). Purified hisPD (600 µg/ml) in 8 M urea, 0.1 M Tris-HCl pH 7.5, 4 mM DTT was slowly diluted into 10 volumes of refolding buffer (0.1 M Tris-HCl pH 9, 0.5 M Arg, 150 mM NaCl, 3 mM GSH, 0.7 mM GSSG, 1.3 mM $CaCl_2$) at 4°C using a peristaltic pump. The solution was stirred for at least 8 h and then dialyzed 3 times against 100 volumes of 20 mM Tris-HCl pH 7.5, 150 mM NaCl, 1 mM $CaCl_2$, 0.1 % Tween-20. The refolded HisPD was activated either directly or first concentrated using a Vivaspin 20 concentrator (MWCO 50 kDa, Vivascience AG). For activation 2 mg of HisPD were incubated overnight at room temperature with 1 U EKMax™ (bovine enteropeptidase, Invitrogen). For the cleavage assay with different chromogenic peptides, directly activated neurobin was used. For the subsequent experiments, neurobin (theor. pI 8.4), activated after concentration and additionally purified by cation-exchange chromatography, to remove enteropeptidase (theor. pI 5.2), was used. For cation-exchange chromatography a MonoS PC1.6/5 (0.1 ml CV) on an Ettan chromatography system (Amersham Pharmacia Biotech, 0.1ml/min during all steps) was used. After loading and washing for 20 CV in buffer A (20 mM Tris pH 7.0, 15 mM NaCl, 0.1 % Tween-20, pH 7.0), a linear gradient to 100 % buffer B (20 mM Tris pH 7.0, 1 M NaCl, 0.1 % Tween-20, pH 7.0) was applied within 20 CV. Purified neurobin was stored in 50% glycerol at –20°C for several months without detectable loss of activity. The yield was 200 µg active protease domain from 1 L *E. coli* culture.

For size exclusion chromatography a Superdex200 (23.6 ml CV) was used on an Ettan chromatography system (0.5 ml/min) with 200 µl purified PD in a buffer containing 50 mM Phosphate, pH 6.5, 50 mM NaCl and 0.1 % Tween.

For trial purifications of via a benzamidine column, 0.5ml of Benzamidin Sepharose 4FF resin were used in gravity flow chromatography. 120 µg purified neurobin PD in 0.5 ml equilibration buffer (500 mM NaCl, 20 mM Tris pH 7.5, 0.1 % Tween) were used. Washing was done with the equilibration buffer (10 -15 CV) and elution with 2 CV 50 mM glycine, pH 2.9, 0.1 % Tween (direct neutralization with 0.2 volumes 1M Tris, pH 7.5).

5.10 Antibodies

5.10.1 The neurobin-SEA domain antibodies R142 and R143

Generation and expression of the antigen

First the eukaryotic expression construct FcNRBSEAdomMycHis was generated. Therefore primers +NRBntermFCtag: CCCAGCGCTgCCGCCTGTGGAAAAGACTCT and -NRBendeSEAmycHis: cccAAgcttgtgacctctatgaataattgtgcg were used in a standard PCR with full length neurobin template and 58°C annealing temperature. Via Eco47/HindIII, the resulting PCR product was ligated into a pcDNA3.1A(-)-based preconstruct (by G. Galliciotti) encoding the neuroserpin secretion signal and an Fc-tag followed by the sequence LeuGluValLeuPheGlnGlyPro which is specifically cleaved by PreScission protease (GE Healthcare) between the Gln and Gly residues (Cordingley et al., 1990). The resulting FcNRBSEAdomMycHis encodes the SEA domain containing only a C-terminal MycHis-tag upon PreScission-cleavage of its N-terminal Fc-tag (Similarly, five other constructs were generated encoding, after the Fc-tag, the whole extracellular part of neurobin - with and without C-terminal MycHis-tag and with and without the catalytic Ser195 mutated to Ala, and with only the protease domain, C-terminally tagged with MycHis. All these latter constructs suffered from ill secretion and/or insufficient detectability (see results section).

For the calcium phosphate transfection of HEK293T cells, growing in four 500 cm^2-plates (>90 % confluent), 2 mg FcNRBSEAdomMycHis were used in combination of 20 ml of each transfection buffer A and B. 5 hours post transfection the plates were washed 3 times with 100 ml PBS and 100 ml serum free DMEM were added. Three days post transfection, the medium was collected, centrifuged for 20 min at 200 RCF, shock-frozen in liquid nitrogen and stored at – 20°C. Of a small aliquot, efficient secretion of the Fc-tagged SEAmycHis protein was checked by Western Blotting using a tetra His antibody.

Purification of the antigen and rabbit immunization

After thawing, 30 mg of sodium azide were added to 300 ml of the medium tested for Fc-tagged SEAmycHis protein expression. The samples were filtered using folded paper filters (Schleicher and Schuell) and loaded onto 1.2 ml of Protein A Sepharose 4FF resin (econo-system, 0.25 ml/min, overnight). Then washing at 0.5 ml/min with 50 ml wash buffer (500 mM NaCl, 50 mM Tris pH7.5, 0.1% Tween 20) followed by 30 ml Cleavage Buffer (50 mM Tris pH 7.0, 300 mM NaCl, 1 mM DTT, 0.1 % Tween) was applied. Then

the resin was incubated in 2 ml Cleavage buffer containing 70 µl PreScission for 16 h at 4° C with 3x resin resuspension. The released SEAmycHis protein was eluted in 6 ml Cleavage buffer and loaded onto 0.3 ml His Select (Sigma) resin at 0.07 ml/min (econo system, Bio-Rad Laboratories, UK). 12 ml washing buffer (50 mM Tris pH 7.5, 300 mM NaCl, 20 mM imidazol, 0.1 % Tween) at 0.2 ml/min preceded the elution (50 mM Tris pH 7.5, 300 mM NaCl, 250 mM imidazol, 0.1 % Tween) at 0.1 ml/min. All purification steps were carried out at 4°C.

Two rabbits (strain Hsdllf:NZW) were immunized each with 30 µg of eukaryotically expressed and purified SEAmycHis protein. Two 30 µg boost injections followed two and five months later.

Antibody purification using prokaryotically expressed SEA domain

First For this, a standard PCR with primers +NRBseaNheI: CCCgctagcGCCGC-CTGTGGAAAAGACT and –NRBendeSEAstop: ccAAgcttCTActtgtgacctctatgaata on a full length neurobin template was performed with 52°C annealing temperature. Cloning into pET-28a(+) (Novagen) in frame with the N-terminal His-tag (via introduced NheI and HindIII sites) resulted in the full-length SEA domain expression construct with N-terminal His-tag (HisfullSEA). The construct was used to transform *E.coli* strain BL21CodonPlus(DE3)-RIL. A 1 L culture of such a clone expressing HisfullSEA was grown at 37°C with 180rpm till OD_{600} reached 1. Then, 0.8 mM IPTG were added for induction. After 3h (37°C, 180rpm) cells were pelleted (20min. 10‘000 RCF). The pellet was resuspended in 100 ml 50 mM Tris, pH 7.5, 500 mM NaCl, DNaseI and stored at -20°C. For purification via HisSelect resin, the bacteria suspension was thawed and lysed by passing twice through the Emulsiflex. The supernatant containing the fraction of cytosolic HisfullSEA was cleared (20 min 10‘000xg) and loaded overnight onto 1.9 ml HisSelect resin (4°C). 70 ml wash buffer (50mM phosphate buffer, pH 8, 0.5 M NaCl, 0.1% Tween-20, 10mM imidazol) were used at 0.4 ml/min and elution (50mM phosphate buffer, pH 8, 0.5 M NaCl, 0.1% Tween-20, 250mM imidazol) was performed at 0.2ml/min. Total 50 mg of purified HisfullSEA were obtained out of 1L E.coli culture. 12 mg of HisfullSEA were directly coupled to 0.5 ml NHS-activated Sepharose 4FF (Amersham Biosciences) resin. This HisfullSEA column in an econo-system was used to affinity-purify IgG fractions obtained from 10 ml rabbit sera aliquots using Protein A Sepharose 4FF chromatography (Amersham Biosciences). As in all cases mentioned below, affinity purification was done by overnight loading of a sterile filtered IgG-containing fraction diluted in sterile-filtered PBS (final volume 100 ml). After extensive washing in PBS containing 0.1 % Tween-20, elution was achieved with 50 mM Glycin

pH 2.8-2.9 containing 0.1 % Tween-20. 0.8 ml elution fractions were collected in eppendorf tubes containing 0.2 ml 1M Tris, pH 7.5 and gently shaken for rapid complete neutralization. All steps were carried out at 4°C.

The affinity-purified antibody preparations from both rabbits R142 and R143 gave virtually identical results both in western blotting and indirect immunofluorescence.

5.10.2 The neurobin-PD antibodies R156 and R158

Two rabbits (strain Hsdllf:NZW) were immunized each with 50 µg of prokaryotically expressed, purified and refolded HisPD protein (see above and results section). Two 30 µg boost injections followed two and four months later. However, the resulting antibodies mainly reacted with the His-tag-containing N-terminal fragment (not part of neurobin, see results section).

5.10.3 Peptide antibodies

N-Term of neurobin as antigen

A peptide containing the first 22 aa of neurobin (MARGQPRRSEEQWTALQNRTEC) was synthesized couplet to keyhole limpet haemocyanin (KLH) and used to immunize and boost two rabbits (R134 + R135) at Primm Biotech in Italy. 4 mg of the peptide were coupled to 0.4 ml NHS-activated Sepharose 4Fast Flow (Amersham Biosciences) and used to affinity-purify IgGs from an IgG fraction of 10 ml serum submitted to ammonium sulfate (AS) precipitation (43 % final AS-concentration w/v, by dropwise addition of 20 ml 65 % AS, overnight, 4°C, dialysis in Spectral Por 3 membrane 3x3 L PBS, 20 h, 4°C) or directly from 10 ml serum aliquots.

Protease domain loop of neurobin as antigen

Similar to the approach at Primm we tried to raise peptide antibodies against a loop of the neurobin protease domain by immunizing two rabbits (R1+R2) and two guinea pigs (GP1+GP2) at Pineda Antibody Services in Berlin. For the choice of the peptide (neurobin residues 258-271 + Cys for coupling to KLH) we relayed on a report by Parker (Parker et al., 1986) and on our own considerations. First, we checked for surface exposure to maximize the chance of epitope accessibility in histochemistry. For this purpose the neurobin protease domain was aligned to the superposition of several x-ray determined serine protease domains, as shown in Figure 4.1. Secondly, to reduce the risk of crossreactivity, peptide sequences with maximal differences were selected from

sequence alignments of neurobin with the HAT/DESC family members of different species. The peptides were subsequently checked for minimal nearly exact matches by blasting against the translated sequence databases. Finally, to increase the chance of good antigenicity the peptide displaying at least some differences to the corresponding rat neurobin peptide was chosen since the rabbit and guinea pig genomes are not available yet. Additionally the peptide had been checked for charged and bulky hydrophobic amino acids which in general are thought to increase antigenicity.
The fifth boost of rabbit serum R1 looked most promising in IF. Therefore 10 ml of fifth boost serum were affinity-purified on a column prepared by coupling 10 mg peptide neurobin258-271+Cys to 0.5 ml NHS activated Sepharose 4FF. With 9.3 mg purified IgGs (8.8% of the average amount of IgGs in 10 ml serum) the yield was very high and of good purity as determined by silver staining.

5.11 Peptide cleavage assays

Chromogenic peptide substrates were from Sigma, Fluka, Chromogenix and Jerini, respectively. Trypsin was from hog pancreas (Fluka). Absorptions at 405 nm were measured from 100 µl reaction volumes in 96 well plates using a 1420 Multilable Counter VICTOR^3 (PerkinElmer). The initial assay buffer was 20 mM Tris-HCl, pH 7.5, 150 mM NaCl, 1 mM $CaCl_2$, 0.1 % Tween-20. Calcium was omitted subsequent assays, unless otherwise stated. For testing of different peptides, reaction volumes contained 4.5 µl activation buffer with refolded neurobin (HisPD) activated with enteropeptidase (EKMax), or 150 nM trypsin. In control reactions no enzyme, HisPD, or EKMax were used, respectively. In the later assays 250 µM GHRpNA were incubated with 30 nM activated MonoS-purified neurobin protease domain. All reactions were monitored by 5 minute-interval absorbance measurements. Trypsin control reactions rapidly reached completion, whereas reactions containing activated neurobin did not reach completion within the 2 hrs measurement period.

5.12 Protein cleavage

Proteins at a concentration of 100 ng/µl in either PBS (FGF-7, 140 amino acid form from AMGEN, gift from Dr. Sabine Werner), TBS (bovine fibronectin from Sigma) TBS-T (laminin from Invitrogen), or 10 mM Tris-HCl, pH 7.6 (human FGF-2 from Invitrogen) were added to the enzyme in 50 mM Tris-HCl, pH 7.5 with 150 mM NaCl. The resulting

concentrations were 50 ng/µl protein substrate and 0.5 ng/µl enzyme. After 4 h at 37°C the reaction was stopped by the addition of loading buffer.

5.13 FGF-2 cleavage analysis

For Edman degradation, FGF-2 incubated with neurobin was separated on a 4–12% NuPAGE gel (Invitrogen) using MES-buffer and transferred onto a PVDF membrane. Bands were cut out and sequenced on a Procise 492 cLC Sequencer (Applied Biosystems, CA, USA) at the Functional Genomics Center Zurich. Additionally, FGF-2 incubated with neurobin was directly submitted to matrix assisted laser desorption time of flight mass spectrometry (MALDI-TOF-MS) analysis. The analysis was performed on a Ultraflex II (Bruker, Germany) at the Functional Genomics Center Zurich.

5.14 Cloning of eukaryotic expression constructs of FGF-2 and GluRδ2

The cDNA of FGF-2 was retrieved from P10 mouse spinal cord cDNA using primers +F1: 5'- cccGctagcATGGCTGCCAGCGGCATCA – 3' and -F2: 5'- cccGcggccgcGCT-CTTAGCAGACATTGGAAG – 3' in a PCR with 45 cycles and 57°C annealing temperature. Cloning into pcDNA3.1 ONEstrep (special preconstruct from D. Lüscher) via the introduced NheI and NotI sites, allows FGF-2 expression with three repeated strep-tag motifs at the C-terminus.

The construct was used as template in a standard PCR with primers +F3: 5'-cccGTTAACgctgccagcggcatcacct – 3' and -F4: 5' – cccGcggccgctcaGCTCTTAGCA-GACATTGGA – 3'. Cloning of the PCR product into pEAK8CstSecr (preconstruct from S. Hettwer) via the introduced HpaI and NotI sites allowed expression of an untagged FGF-2 variant directed to the conventional secretory pathway via the N-terminal secretion signal of human calsyntenin-1.

PCR with the primer pair +F1 and –F4 and cloning into pcDNA3.1 ONEstrep via the NheI and NotI sites, allows expression of normal low molecular weight FGF-2.

The cDNA of GluRδ2 in vector pBKSApa37-14 (gift from Masayoshi Mishina) was used in a PCR with primers +G1: 5' – cccGctagcATGGAAGTTTTCCCCTTGCT – 3' and -G2: 5' – cccGcggccgcTATGGACGTGCCTCGGTC – 3'. Cloning into pcDNA3.1 ONEstrep via the introduced NheI and NotI sites, allows GluRδ2 expression with three repeated strep-tag motifs at the C-terminus.

5.15 Cell culture and transfection

HEK293T cells (human embryonic kidney cell line) were grown in 3 cm plates with 2 ml Dulbecco's modified Eagle's medium without sodium pyruvate (Invitrogen), 10% FCS and 2 mM L-glutamine at 37 °C in 10 % CO_2. For calcium-phosphate transfection, 2 µg DNA were used. In cotransfection experiments up to 5 µg of each plasmid were used. COS 7 cells were transfected with Lipofectamine^{TM}2000 (Invitrogen) like suggested in the manual. The growth-media were exchanged 5 hrs after transfection. Cells were further processed 24 or 48 h post transfection.

5.16 SDS-PAGE, Western Blotting and Silver Staining

12.5 or 15 % polyacrylamide gels were used. With purified protein, concentration was determined by UV absorption measurement at 280 nm using the calculated extinction coefficient. Protein concentration in extracts was determined with the BCA system (Pierce). Whole cell extracts were prepared by lysing the cells in lysis buffer. For deglycosylation extracts (30 µg protein) were treated with 2.5 mU endoglycosidaseH (Roche) or 0.5 U N-glycosidaseF (Roche) and 50 mM Na-acetat pH 5 for 1h at 37°C. Before loading, samples were boiled for 5 minutes in reducing Lämmli buffer. 25 µg protein extract were loaded per lane. Proteins were transferred to nitrocellulose (Schleicher and Schuell) or PVDF membranes (Millipore). Transfer quality was controlled with Ponceau S staining. The membranes were blocked in TBS-T containing 10 % Western Blocking Reagent (Roche diagnostics GmbH, Mannheim) over night at 4 °C. The membranes were incubated for 2 h at RT with TBS-T containing 1 µg/ml of affinity-purified polyclonal anti SEA domain antibody or 0.1 µg/ml anti Tetra His monoclonal antibody (Qiagen). Membranes were washed 3 times for 5 min in TBS-T. Membranes were incubated for 45 minutes in TBS-T containing either 25 ng/ml peroxidase-coupled goat anti rabbit IgG (Chemicon) or 0.2 µg/ml peroxidase-coupled goat anti mouse IgG (KPL). Membranes were washed again 3 times for 10 min. in TBS-T. After incubation in CHEMIGLOW^{TM} substrate (Alpha Innotech Corp), chemiluminescence was detected by a CCD Camera (Alpha Innotech Corp). For silver staining, SDS-PAGE gels were fixed with 30% EtOH and 10% acetic acid for 30 min (room temperature) to ON (4°C). Reducing and crosslinking was achieved with 30% EtOH, 6.8 g NaOAc, 0.2 g Na2S2O3, 0.25 ml glutaraldehyde (50%) in 100 ml final volume for 10 min. This was followed by washing of the gels 4 times 3 min with H2O, silver incubation with 0.2 g AgNO3 and 20 ml formaldehyde in 100 ml final volume for 15 min; washing for 1 min with H2O and development with 5 g Na2CO3 and 20 ml

formaldehyde in 200 ml final volume. Development was stopped with 3% acetic acid for 5-10 minutes. The gels were rinse with H2O and dried by heating in a low pressure atmosphere.

5.17 Immunofluorescence

COS-7 cells grown on glass cover slips were fixed one day post transfection in 4 % paraformaldehyde (PFA) in PBS for 10 min. Then the cells were incubated for 1 h in blocking buffer (PBS, 10 % FCS, 3 % BSA, 0.5 % glycine) and incubated overnight at 4 °C in blocking buffer containing 3 µg/ml affinity purified anti SEA IgG or 2 µg/ml Tetra His monoclonal antibody (Qiagen). Cells were rinsed and washed 3 times for 10 min in TBS-T and then incubated for 45 minutes at room temperature in blocking buffer containing 1.3 µg/ml Cy3-labeled donkey anti rabbit IgG (Jackson) or 2.5 µg/ml FITC-labeled donkey anti mouse IgG (Jackson). Washing was performed as before. In case of the analysis of permeabilized cells 0.1 % saponin was included in all antibody incubation steps. The cover slips were mounted upside down onto glass slides using DarkoCytomation Mounting Medium (DarkoCytomation) and stored at 4 °C. Analysis was performed on a Leica Leitz DM RXE microscope with PL Fluotar objectives. Pictures were taken with a Leica DFC350FX camera.

5.18 Histochemistry

Anesthetized P10 mice were perfused with PBS containing 4% PFA and the isolated organs incubated in an increasing sucrose gradient. Cryosections of tissue tek (Sakura) embedded brain (20 µm) sections on glass slides were processed with a similar protocol as cells in immunofluorescence (omission of the Tetra His and corresponding secondary antibody, inclusion of 0.1 % saponin during antibody incubation). Analysis was performed on a Olympus IX81F-2 microscope. Pictures were taken with an F-ViewII camera.

6 References

Abe, K., and Saito, H. (2001). Effects of basic fibroblast growth factor on central nervous system functions. Pharmacol Res *43*, 307-312.

Afar, D.E.H., Vivanco, I., Hubert, R.S., Kuo, J., Chen, E., Saffran, D.C., Raitano, A.B., and Jakobovits, A. (2001). Catalytic cleavage of the androgen-regulated TMPRSS2 protease results in its secretion by prostate and prostate cancer epithelia. Cancer Res *61*, 1686-1692.

Arai, T., Guo, J.P., and McGeer, P.L. (2005). Proteolysis of non-phosphorylated and phosphorylated tau by thrombin. J Biol Chem *280*, 5145-5153.

Arakawa, T., Hsu, Y.R., Schiffer, S.G., Tsai, L.B., Curless, C., and Fox, G.M. (1989). Characterization of a cysteine-free analog of recombinant human basic fibroblast growth factor. Biochem. Biophys. Res. Commun. *161*, 335-341.

Arnaud, E., Touriol, C., Boutonnet, C., Gensac, M.C., Vagner, S., Prats, H., and Prats, A.C. (1999). A new 34-kilodalton isoform of human fibroblast growth factor 2 is cap dependently synthesized by using a non-AUG start codon and behaves as a survival factor. MolCell Biol *19*, 505-514.

Balbín, M., Fueyo, A., Knäuper, V., López, J.M., Álvarez, J., Sánchez, L.M., Quesada, V., Bordallo, J., Murphy, G., and López-Otín, C. (2001). Identification and enzymatic characterization of two diverging murine counterparts of human interstitial collagenase (MMP-1) expressed at sites of embryo implantation. J Biol Chem *276*, 10253-10262.

Bandtlow, C.E., and Zimmermann, D.R. (2000). Proteoglycans in the developing brain: new conceptual insights for old proteins. Pysiol Rev *80*, 1267-1290.

Beer, H.D., Vindevoghel, L., Gait, M.J., Revest, J.M., Duan, D.R., Mason, I., Dickson, C., and Werner, S. (2000). Fibroblast growth factor (FGF) receptor 1-IIIb is a naturally occurring functional receptor for FGFs that is preferentially expressed in the skin and the brain. J Biol Chem *275*, 16091-16097.

Behrens, M., Bufe, B., Schmale, H., and Meyerhof, W. (2004). Molecular cloning and characterisation of DESC4, a new transmembrane serine protease. Cell Mol Life Sci *61*, 2866-2877.

Bezakova, G., and Ruegg, M.A. (2003). New insights into the roles of agrin. Nat Rev Mol Cell Biol *4*, 295-308.

Bode, W., and Huber, R. (2000). Structural basis of the endoproteinase-protein inhibitor interaction. Biochimica et biophysica acta *1477*, 241-252.

Bode, W., May, R.I., Baumann, U., Huber, R., Stone, S.R., and J., H. (1989). The refined 1.9 A crystal structure of human alpha-thrombin: interaction with D-Phe-Pro-Arg chloromethylketone and significance of the Tyr-Pro-Pro-Trp insertion segment. EMBO J *11*, 3467-3475.

Bowen, M.A., Aruffo, A.A., and Bajorath, J. (2000). Cell surface receptors and their ligands: in vitro analysis of CD6-CD166 interactions. Proteins *40*, 420-428.

Carter, W.J., Cama, E., and Huntington, J.A. (2005). Crystal structure of thrombin bound to heparin. J Biol Chem *280*, 2745-2749.

Chan, J.C.Y., Knudson, O., Wu, F., Morser, J., Dole, W.P., and Wu, Q. (2005). Hypertension in mice lacking the proatrial natriuretic peptide convertase corin. Proc Natl Acad Sci USA *102*, 785-790.

Chang, Y., Zajicek, J., and Castellino, F.J. (1997). Role of tryptophan-63 of the kringle 2 domain of tissue-type plasminogen activator in its thermal stability, folding, and ligand binding properties. Biochemistry *36*, 7652-7663.

Chen, P., Tsuge, H., Almassy, R.J., Gribskov, C.L., Katoh, S., Vanderpool, D.L., Margosiak, S.A., Pinko, C., Matthews, D.A., and Kan, C.C. (1996). Structure of the human cytomegalovirus protease catalytic domain reveals a novel serine protease fold and catalytic triad. Cell *86*, 835-843.

Chen, S.T., Gysin, R., Kapur, S., Baylink, D.J., and Lau, K.H. (2007). Modifications of the fibroblast growth factor-2 gene led to a marked enhancement in secretion and stability of the recombinant fibroblast growth factor-2 protein. J Cell Biochem *100*, 1493-1508.

Claus, P., Doring, F., Gringel, S., Muller-Ostermeyer, F., Fuhlrott, J., Kraft, T., and Grothe, C. (2003). Differential intranuclear localization of fibroblast growth factor-2 isoforms and specific interaction with the survival of motoneuron protein. J Biol Chem *278*, 479-485.

Cleves, A.E. (1997). Protein transports: the nonclassical ins and outs. Curr Biol *7*, R318-320.

Cordingley, M.G., Callahan, P.L., Sardana, V.V., Garsky, V.M., and Colonno, R.J. (1990). Substrate requirements of human rhinovirus 3C protease for peptide cleavage in vitro. J Biol Chem *265*, 9062-9065.

Coughlin, S.R. (2000). Thrombin signalling and protease-activated receptors. Nature *407*, 258-264.

Czapinska, H., and Otlewski, J. (1999). Structural and energetic determinants of the S1-site specificity in serine proteases. European journal of biochemistry / FEBS *260*, 571-595.

Dang, Q.D., and Di Cera, E. (1996). Residue 225 determines the Na+-induced allosteric regulation of catalytic activity in serine proteases. Proc Natl Acad Sci USA *93*, 10653-10656.

Di Cera, E. (2007). Thrombin as procoagulant and anticoagulant. J Thromb Haemost *5 Suppl 1*, 196-202.

Dodson, G., and Wlodawer, A. (1998). Catalytic triads and their relatives. Trends Biochem Sci *23*, 347-352.

Enshell-Seijffers, D., Lindon, C., and Morgan, B.A. (2008). The serine protease Corin is a novel modifier of the agouti pathway. Development (Cambridge, England) *135*, 217-225.

Esmon, C.T. (2003). The protein C pathway. Chest *124*, 26S-32S.

Etscheid, M., Beer, N., Kress, J.A., Seitz, R., and Dodt, J. (2004). Inhibition of bFGF/EGF-dependent endothelial cell proliferation by the hyaluronan-binding protease from human plasma. Eur J Cell Biol *82*, 597-604.

Flaumenhaft, R., and Rifkin, D.B. (1991). Extracellular matrix regulation of growth factor and protease activity. Current opinion in cell biology *3*, 817-823.

Florkiewicz, R.Z., Majack, R.A., Buechler, R.D., and Florkiewicz, E. (1995). Quantitative export of FGF-2 occurs through an alternative, energy-dependent, non-ER/Golgi pathway. Journal of cellular physiology *162*, 388-399.

Gingrich, M.B., Junge, C.E., Lyuboslavsky, P., and Traynelis, S.F. (2000). potentiation of NMDA receptor function by the serine protease thrombin. J Neurosci *20*, 4582-4595.

Gleizes, P.E., Noaillac-Depeyre, J., Amalric, F., and Gas, N. (1995). Basic fibroblast growth factor (FGF-2) internalization through the heparan sulfate proteoglycans-mediated pathway: an ultrastructural approach. European journal of cell biology *66*, 47-59.

Goodman, O.B., Jr., Febbraio, M., Simantov, R., Zheng, R., Shen, R., Silverstein, R.L., and Nanus, D.M. (2006). Neprilysin inhibits angiogenesis via proteolysis of fibroblast growth factor-2. J Biol Chem *281*, 33597-33605.

Griffin, J.H. (1995). Blood coagulation. The thrombin paradox. Nature *378*, 337-338.

Gruber, A., Marzec, U.M., Bush, L., Di Cera, E., Fernandez, J.A., Berny, M.A., Tucker, E.I., McCarty, O.J., Griffin, J.H., and Hanson, S.R. (2007). Relative antithrombotic and antihemostatic effects of protein C activator versus low-molecular-weight heparin in primates. Blood *109*, 3733-3740.

Guex, N., and Peitsch, M.C. (1997). SWISS-MODEL and the Swiss-PdbViewer: an environment for comparative protein modeling. Electrophoresis *18*, 2714-2723.

Guipponi, M., Tan, J., Cannon, P.Z.F., Donley, L., Crewther, P., Clarke, M., Wu, Q., Shepherd, R.K., and Scott, H.S. (2007). Mice deficient for the type II transmembrane serine protease, TMPRSS1/hepsin, exhibit profound hearing loss. Am J Pathol *171*, 608-616.

Guipponi, M., Vuagniaux, G., Wattenhofer, M., Shibuya, K., Vazquez, M., Dougherty, L., Scamuffa, N., Guida, E., Okui, M., Rossier, C., *et al.* (2002). The transmembrane serine protease (TMPRSS3) mutated in deafness DFNB8/10 activates the epithelial sodium channel (ENaC) in vitro. Hum Mol Gen *11*, 2829-2836.

Hamano, Y., Zeisberg, M., Sugimoto, H., Lively, J.C., Maeshima, Y., Yang, C., Hynes, R.O., Werb, Z., Sudhakar, A., and Kalluri, R. (2003). Physiological levels of tumstatin, a fragment of collagen IV alpha3 chain, are generated by MMP-9 proteolysis and suppress angiogenesis via alphaV beta3 integrin. Cancer cell *3*, 589-601.

Hansen, I.A., Fassnacht, M., Hahner, S., Hammer, F., Schammann, M., Meyer, S.R., Bicknell, A.B., and Allolio, B. (2004). The adrenal secretory serine protease AsP is a short secretory isoform of the transmembrane airway trypsin-like protease. Endocrinol *145*, 1898-1905.

Hedstrom, L. (2002). Serine protease mechanism and specificity. Chem Rev *102*, 4501-4523.

Hedstrom, L., Perona, J.J., and Rutter, W.J. (1994). Converting trypsin to chymotrypsin: residue 172 is a substrate specificity determinant. Biochemistry *33*, 8757-8763.

Hobson, J.P., Netzel-Arnett, S., Szabo, R., Réhault, S.M., Church, F.C., Strickland, D.K., Lawrence, D.A., Antalis, T.M., and Bugge, T.H. (2004). Mouse DESC1 is located within a cluster of seven DESC1-like genes and encodes a type II transmembrane serine pprotease that forms serpin inhibitory complexes. J Biol Chem *279*, 46981-46994.

Hooper, J.D., Campagnolo, L., Goodarzi, G., Truong, T.N., Stuhlmann, H., and Quigley, J.P. (2003). Mouse matriptase-2: identification, characterization and comparative mRNA expression analysis with mouse hepsin in adult and embryonic tissues. Biochem J *373*, 689-702.

Hooper, J.D., Clements, J.A., Quigley, J.P., and Antalis, T.M. (2001). Type II transmembrane serine proteases. J Biol Chem *276*, 857-860.

Hooper, J.D., Scarman, A.L., Clarke, B.E., Normyle, J.F., and Antalis, T.M. (2000). Localization of the mosaic transmembrane serine protease corin to heart myocytes. Eur J Biochem *267*, 6931-6937.

Hou, S., Maccarana, M., Min, T.H., Strate, I., and Pera, E.M. (2007). The secreted serine protease xHtrA1 stimulates long-range FGF signaling in the early Xenopus embryo. Developmental cell *13*, 226-241.

Hubbard, S.J. (1998). The structural aspects of limited proteolysis of native proteins. Biochimica et biophysica acta *1382*, 191-206.

Huntington, J.A., Read, R.J., and Carrell, R.W. (2000). Structure of a serpin-protease complex shows inhibition by deformation. Nature *407*, 923-926.

Jain, R.K., Joyce, P.B., and Gorr, S.U. (2000). Aggregation chaperones enhance aggregation and storage of secretory proteins in endocrine cells. J Biol Chem *275*, 27032-27036.

Jing, H., Macon, K.J., Moore, D., DeLucas, L.J., Volanakis, J.E., and Narayana, S.V. (1999). Structural basis of profactor D activation: from a highly flexible zymogen to a novel self-inhibited serine protease, complement factor D. The EMBO journal *18*, 804-814.

Kandel, E.R. (2001). The molecular biology of memory storage: a dialog between genes and synapses. Bioscience reports *21*, 565-611.

Khan, A.R., and James, M.N. (1998). Molecular mechanisms for the conversion of zymogens to active proteolytic enzymes. Protein Sci *7*, 815-836.

Kim, C., Cho, Y., Kang, C.-H., Kim, M.G., Lee, H., Cho, E.-G., and Park, D. (2005). Filamin is essential for shedding of the transmembrane serine protease, epithin. EMBO J.

Kirchhofer, D., Peek, M., Lipari, M.T., Billeci, K., Fan, B., and Moran, P. (2005). Hepsin activates pro-hepatocyte growth factor and is inhibited by hepatocyte growth factor activator inhibitor-1B (HAI-1B) and HAI-2. FEBS Lett *579*, 1945-1950.

Kjellen, L., and Lindahl, U. (1991). Proteoglycans: structures and interactions. Annu Rev Biochem *60*, 443-475.

Klein, S., Carroll, J.A., Chen, Y., Henry, M.F., Henry, P.A., Ortonowski, I.E., Pintucci, G., Beavis, R.C., Burgess, W.H., and Rifkin, D.B. (2000). Biochemical analysis of the arginine methylation of high molecular weight fibroblast growth factor-2. J Biol Chem *275*, 3150-3157.

Klezovitch, O., Chevillet, J., Mirosevich, J., Roberts, R.L., Matusik, R.J., and Vasioukhin, V. (2004). Hepsin promotes prostate cancer progression and metastasis. Cancer cell *6*, 185-195.

Kyrieleis, O.J., Huber, R., Ong, E., Oehler, R., Hunter, M., Madison, E.L., and Jacob, U. (2007). Crystal structure of the catalytic domain of DESC1, a new member of the type II transmembrane serine proteinase family. The FEBS journal *274*, 2148-2160.

Landsend, A.S., Amiry-Moghaddam, M., Matsubara, A., Bergersen, L., Usami, S., Wenthold, R.J., and Ottersen, O.P. (1997). Differential localization of delta glutamate receptors in the rat cerebellum: coexpression with AMPA receptors in parallel fiber-spine synapses and absence from climbing fiber-spine synapses. J Neurosci *17*, 834-842.

Lang, J.C., and Schuller, D.E. (2001). Differential expression of a novel serine protease homologue in squamous cell carcinoma of the head and neck. Br J Cancer *84*, 237-243.

Lee, M.C., Miller, E.A., Goldberg, J., Orci, L., and Schekman, R. (2004). Bi-directional protein transport between the ER and Golgi. Annual review of cell and developmental biology *20*, 87-123.

List, K., Bugge, T.H., and Szabo, R. (2006). Matriptase: potent proteolysis on the cell surface. Molecular medicine (Cambridge, Mass *12*, 1-7.

List, K., Haudenschild, C.C., Szabo, R., Chen, W., Wahl, S.M., Swaim, W., Engelholm, L.H., Behrendt, N., and Bugge, T.H. (2002). Matriptase/MT-SP1 is required for postnatal survival epidermal barrier function hair follicle development, and thymic homeostasis. Oncogene *21*, 3765-3779.

List, K., Szabo, R., Molinolo, A., Sriuranpong, V., Redeye, V., Murdock, T., Burke, B., Nielsen, B.S., Gutkind, J.S., and Bugge, T.H. (2005). Deregulated matriptase causes ras-independent multistage carcinogenesis and promotes ras-mediated malignant transformation. Gen Dev *19*, 1934-1950.

Lopez-Otin, C., and Matrisian, L.M. (2007). Emerging roles of proteases in tumour suppression. Nature reviews *7*, 800-808.

Lu, D., Futterer, K., Korolev, S., Zheng, X., Tan, K., Waksman, G., and Sadler, J.E. (1999). Crystal structure of enteropeptidase light chain complexed with an analog of the trypsinogen activation peptide. J Mol Biol *292*, 361-373.

Lu, D., Yuan, X., Zheng, X., and Sadler, J.E. (1997). Bovine proenteropeptidase is activated by trypsin, and the specificity of enteropeptidase depends on the heavy chain. J Biol Chem *272*, 31293-31300.

Macao, B., Johansson, D.G., Hansson, G.C., and Hard, T. (2006). Autoproteolysis coupled to protein folding in the SEA domain of the membrane-bound MUC1 mucin. Nature structural & molecular biology *13*, 71-76.

Magklara, A., Mellati, A.A., Wasney, G.A., Little, S.P., Sotiropoulou, G., Becker, G.W., and Diamandis, E.P. (2003). Characterization of the enzymatic activity of human kallikrein 6: Autoactivation, substrate specificity, and regulation by inhibitors. Biochem. Biophys. Res. Commun. *307*, 948-955.

Mann, K.G. (2003). Thrombin formation. Chest *124*, 4S-10S.

Mason, I.J. (1994). The ins and outs of fibroblast growth factors. Cell *78*, 547-552.

Matsuda, S., Ii, Y., Desaki, J., Yoshimura, H., Okumura, N., and Sakanaka, M. (1994). Development of Purkinje cell bodies and processes with basic fibroblast growth factor-like immunoreactivity in the rat cerebellum. Neuroscience *59*, 651-662.

Matsumoto-Miyai, K., Ninomiya, A., Hironobu, Y., Tamura, H., Nakamura, Y., and Shiosaka, S. (2003). NMDA-dependent proteolysis of presynaptic adhesion molecule L1 in the hippocampus by neuropsin. J Neurosci *23*, 7727-7736.

Matthews, D.A., Alden, R.A., Birktoft, J.J., Freer, S.T., and Kraut, J. (1975). X-ray crystallographic study of boronic acid adducts with subtilisin BPN' (Novo). A model for the catalytic transition state. J Biol Chem *250*, 7120-7126.

Meyer, E.L., Strutz, N., Gahring, L.C., and Rogers, S.W. (2003). Glutamate receptor subunit 3 is modified by site-specific limited proteolysis including cleavage by gamma-secretase. J Biol Chem *278*, 23786-23796.

Molinari, F., Meskanaite, V., Munnich, A., Sonderegger, P., and Colleaux, L. (2003). Extracellular proteases and their inhibitors in genetic diseases of the central nervous system. Human molecular genetics *12 Spec No 2*, R195-200.

Molinari, F., Rio, M., Meskenaite, V., Encha-Razavi, F., Augé, J., Bacq, D., Briault, S., Vekemans, M., Munnich, A., Attié-Bitach, T., *et al.* (2002). Truncating neurotrypsin mutation in autosomal recessive nonsyndromic mental retardation. Science (New York, NY *298*, 1779-1781.

Moran, P., Li, W., Vij, R., Eigenbrot, C., and Kirchhofer, D. (2006). Pro-urokinase-type plasminogen activator is a substrate for hepsin. J Biol Chem *281*, 30439-30446.

Moscatelli, D., Joseph-Silverstein, J., Manejias, R., and Rifkin, D., B. (1987). Mr 25,000 heparin-binding protein from guinea pig brain is a high molecular weight form of basic fibroblast growth factor. Proc Natl Acad Sci USA *84*, 5778-5782.

Nemoda, Z., and Sahin-Toth, M. (2005). The tetra-aspartate motif in the activation peptide of human cationic trypsinogen is essential for autoactivation control but not for enteropeptidase recognition. J Biol Chem *280*, 29645-29652.

Netzel-Arnett, S., Hooper, J.D., Szabo, R., Madison, E.L., Quigley, J.P., Bugge, T.H., and Antalis, T.M. (2003). Membrane anchored serine proteases: a rapidly expanding group of cell surface proteolytic enzymes with potential roles in cancer. Cancer Met Rev *22*, 237-258.

Nickel, W. (2005). Unconventional secretory routes: direct protein export across the plasma membrane of mammalian cells. Traffic (Copenhagen, Denmark) *6*, 607-614.

Oberst, M.D., Williams, C.A., Dickson, R.B., Johnson, M.D., and Lin, C.Y. (2003). The activation of matriptase requires its noncatalytic domains, serine protease domain, and its cognate inhibitor. J Biol Chem *278*, 26773-26779.

Okada-Ban, M., Thiery, J.P., and Jouanneau, J. (2000). Fibroblast growth factor-2. The international journal of biochemistry & cell biology *32*, 263-267.

Ortega, S., Ittmann, M., Tsang, S.H., Ehrlich, M., and Basilico, C. (1998). Neuronal defects and delayed wound healing in mice lacking fibroblast growth factor 2. Proc Natl Acad Sci USA *95*, 5672-5677.

Page, M.J., Macgillivray, R.T.A., and Di Cera, E. (2005). Determinants of specificity in coagulation proteases. J Thromb Haemost *3*, 2401-2408.

Pang, P.T., Teng, H.K., Zaitsev, E., Woo, N.T., Sakata, K., Zhen, S., Teng, K.K., Yung, W.H., Hempstead, B.L., and Lu, B. (2004). Cleavage of proBDNF by tPA/plasmin is essential for long-term hippocampal plasticity. Science (New York, NY *306*, 487-491.

Parker, J.M., Guo, D., and Hodges, R.S. (1986). New hydrophilicity scale derived from high-performance liquid chromatography peptide retention data: correlation of predicted surface residues with antigenicity and X-ray-derived accessible sites. Biochemistry *25*, 5425-5432.

Patthy, L. (2003). Modular assembly of genes and the evolution of new functions. Genetica *118*, 217-231.

Pineda, A.O., Carrell, C.J., Bush, L.A., Prasad, S., Caccia, S., Chen, Z.W., Mathews, F.S., and Di Cera, E. (2004). Molecular dissection of Na+ binding to thrombin. J Biol Chem *279*, 31842-31853.

Puente, X.S., Sanchez, L.M., Overall, C.M., and Lopez-Otin, C. (2003a). Human and mouse proteases: a comparative genomic approach. Nat Rev Genet *4*, 544-558.

Puente, X.S., Sánchez, L.M., Overall, C.M., and López-Otín, C. (2003b). Human and mouse proteases: a comparative genomic approach. Nat Rev Genet *4*, 544-558.

Qian, Z., Gilbert, M.E., Colicos, M.A., Kandel, E.R., and Kuhl, D. (1993). Tissue-plasminogen activator is induced as an immediate-early gene during seizure, kindling and long-term potentiation. Nature *361*, 453-457.

Rawlings, N.D., and Barrett, A.J. (1999). MEROPS: the peptidase database. Nucleic Acids Res *27*, 325-331.

Rawlings, N.D., Morton, F.R., and Barrett, A.J. (2006). MEROPS: the peptidase database. Nucleic Acids Res *34*, D270-272.

Rawlings, N.D., Morton, F.R., Kok, C.Y., Kong, J., and Barrett, A.J. (2007). MEROPS: the peptidase database. Nucleic Acids Res.

Reif, R., Sales, S., Hettwer, S., Dreier, B., Gisler, C., Wolfel, J., Luscher, D., Zurlinden, A., Stephan, A., Ahmed, S., *et al.* (2007). Specific cleavage of agrin by neurotrypsin, a synaptic protease linked to mental retardation. Faseb J *21*, 3468-3478.

Renatus, M., Engh, R.A., Stubbs, M.T., Huber, R., Fischer, S., Kohnert, U., and Bode, W. (1997). Lysine 156 promotes the anomalous proenzyme activity of tPA: X-ray crystal structure of single-chain human tPA. The EMBO journal *16*, 4797-4805.

Reynolds, J., Logan, A., Berry, M., Dent, R.G., Gonzales, A.M., and Toescu, E.C. (2005). Age-dependent changes in fibroblast growth factor 2 (FGF-2) expression in mouse cerebellar neurons. J Cell Mol Med *9*, 398-406.

Saksela, O., Moscatelli, D., Sommer, A., and Rifkin, D.B. (1988). Endothelial cell-derived heparan sulfate binds basic fibroblast growth factor and protects it form proteolytic degradation. J Cell Biol *107*, 743-751.

Schechter, I., and Berger, A. (1967). On the size of the active site in proteases. I. Papain. Biochem. Biophys. Res. Commun. *27*, 157-162.

Scott, H.S., Kudoh, J., Wattenhofer, M., Shibuya, K., Berry, A., Chrast, R., Guipponi, M., Wang, J., Kawasaki, K., Asakawa, S., *et al.* (2001). Insertion of b-satellite repeats identifies a transmembrane protease causing both congenital and childhood onset autosomal recessive deafness. Nat Gen *27*, 59-63.

Sedghizadeh, P.P., Mallery, S.R., Thompson, S.J., Kresty, L., Beck, F.M., Parkinson, E.K., Biancamano, J., and Lang, J.C. (2006). Expression of the serine protease DESC1 correlates directly with normal keratinocyte differentiation and inversely with head and neck squamous cell carcinoma progression. Head & neck *28*, 432-440.

Seeds, N.W., Basham, M.E., and Ferguson, J.E. (2003). Absence of tissue plasminogen activator gene or activity impairs mouse cerebellar motor learning. J Neurosci *23*, 7368-7375.

Sher, Y.P., Chou, C.C., Chou, R.H., Wu, H.M., Wayne Chang, W.S., Chen, C.H., Yang, P.C., Wu, C.W., Yu, C.L., and Peck, K. (2006). Human kallikrein 8 protease confers a favorable clinical outcome in non-small cell lung cancer by suppressing tumor cell invasiveness. Cancer research *66*, 11763-11770.

Somoza, J.R., Ho, J.D., Luong, C., Ghate, M., Sprengeler, P.A., Mortara, K., Shrader, W.D., Sperandio, D., Chan, H., McGrath, M.E., *et al.* (2003). The structure of the extracellular region of human hepsin reveals a serine protease domain and a novel scavenger receptor cysteine-rich (SRCR) domain. Structure *11*, 1123-1131.

Song, H.-W., Choi, S.-I., and Seong, B.L. (2002). Engineered Recombinant Enteropeptidase Catalytic Subunit: Effect of N-Terminal Modification. Arch Biochem Biophys *400*, 1-6.

Stahl, L.E., Wright, R.L., Castle, J.D., and Castle, A.M. (1996). The unique proline-rich domain of parotid proline-rich proteins functions in secretory sorting. J Cell Sci *109 (Pt 6)*, 1637-1645.

Striggow, F., Riek-Burchardt, M., Kiesel, A., Schmidt, W., Henrich-Noack, P., Breder, J., Krug, M., Reymann, K.G., and Reiser, G. (2001). Four different types of protease-activated receptors are widely expressed in the brain and are up-regulated in hippocampus by severe ischemia. The European journal of neuroscience *14*, 595-608.

Szabo, E., Venekei, I., Bocskei, Z., Naray-Szabo, G., and Graf, L. (2003a). Three dimensional structures of S189D chymotrypsin and D189S trypsin mutants: the effect of polarity at site 189 on a protease-specific stabilization of the substrate-binding site. J Mol Biol *331*, 1121-1130.

Szabo, R., Netzel-Arnett, S., Hobson, J.P., Antalis, T.M., and Bugge, T.H. (2005). Matriptase-3 is a novel phylogenetically preserved membrane-anchored serine protease with broad serpin reactivity. Biochem J *390*, 231-242.

Szabo, R., Wu, Q., Dickson, R.B., Netzel-Arnett, S., Antalis, T.M., and Bugge, T.H. (2003b). Type II transmembrane serine proteases. Thromb Haemost *90*, 185-193.

Szmola, R., and Sahin-Toth, M. (2007). Chymotrypsin C (caldecrin) promotes degradation of human cationic trypsin: identity with Rinderknecht's enzyme Y. Proc Nat Acad Sci *104*, 11227-11232.

Uemura, T., Kakizawa, S., Yamasaki, M., Sakimura, K., Watanabe, M., Iino, M., and Mishina, M. (2007). Regulation of long-term depression and climbing fiber territory by glutamate receptor delta2 at parallel fiber synapses through its C-terminal domain in cerebellar Purkinje cells. J Neurosci *27*, 12096-12108.

Velasco, G., Cal, S., Quesada, V., Sánchez, L.M., and López-Otín, C. (2002). Matriptase-2, a membrane-bound mosaic serine protease predominantly expressed in human liver and showing degrading activity against extracellular matrix proteins. J Biol Chem *277*, 37637-37646.

Viloria, C.G., Peinado, J.R., Astudillo, A., Suarez-Garcia, O., Gonzzales, M.V., Suarez, C., and Cal, S. (2007). Human DESC1 serine protease confers tumorigenic properties to MDCK cells and it is upregulated in tumours of different origin. Br J Cancer *97*, 201-209.

Voet D. and Voet J., Biochemistry 2nd Edition (1995) John Wiley&Sons, Inc.

Walsh, M.K., and Lichtman, J.W. (2003). In vivo time-lapse imaging of synaptic takeover associated with naturally occurring synapse elimination. Neuron *37*, 67-73.

Wesche, J., Malecki, J., Wiedlocha, A., Skjerpen, C.S., Claus, P., and Olsnes, S. (2006). FGF-1 and FGF-2 require the cytosolic chaperone Hsp90 for translocation into the cytosol and the cell nucleus. J Biol Chem *281*, 11405-11412.

Wilson, S., Greer, B., Hooper, J.D., Zijlstra, A., Walker, B., Quigley, J., and Hawthorne, S. (2005). The membrane-anchored serine protease, TMPRSS2, activates PAR-2 in prostate cancer cells. Biochem J *388*, 967-972.

Wolfer, D.P., Lang, R., Cinelli, P., Madani, R., and Sonderegger, P. (2001). Multiple roles of neurotrypsin in tissue morphogeness and nervous system development suggested by the mRNA expression pattern. Mol Cell Neurosci *18*, 407-433.

Wu, Q. (2003). Type II transmembrane serine proteases. Curr Topics Dev Biol *54*, 167-206.

Xue, S., Madison, E.L., and Miles, L.A. (2001). The Kringle V-protease domain is a fibrinogen binding region within Apo(a). Thrombosis and haemostasis *86*, 1229-1237.

Yamaguchi, N., Okui, A., Yamada, T., Nakazato, H., and Mitsui, S. (2002). Spinesin/TMPRSS5, a novel transmembrane serine protease, cloned form human spinal cord. J Biol Chem *277*, 6806-6812.

Yamaoka, K., Masuda, K., Ogawa, H., Takagi, K., Umemoto, N., and Yasuoka, S. (1998). Cloning and characterization of the cDNA for human airway trypsin-like protease. J Biol Chem *273*, 11895-11901.

Yan, W., Wu, F., Morser, J., and Wu, Q. (2000). Corin, a transmembrane cardiac serine protease, acts as a pro-atrial natriuretic peptide-converting enzyme. Proc Natl Acad Sci USA *97*, 8525-8529.

Yawata, S., Tsuchida, H., Kengaku, M., and Hirano, T. (2006). Membrane-proximal region of glutamate receptor delta2 subunit is critical for long-term depression and interaction with protein interacting with C kinase 1 in a cerebellar Purkinje neuron. J Neurosci *26*, 3626-3633.

Yu, P.J., Ferrari, G., Galloway, A.C., Mignatti, P., and Pintucci, G. (2007a). Basic fibroblast growth factor (FGF-2): the high molecular weight forms come of age. J Cell Biochem *100*, 1100-1108.

Yu, P.J., Ferrari, G., Pirelli, L., Galloway, A.C., Mignatti, P., and Pintucci, G. (2007b). Thrombin cleaves the high molecular weight forms of basic fibroblast growth factor (FGF-2): a novel mechanism for the control of FGF-2 and thrombin activity. Oncogene.

Yuan, X., Zheng, X., Lu, D., Rubin, D.C., Pung, C.Y., and Sadler, J.E. (1998). Structure of murine enterokinase (enteropeptidase) and expression in small intestine during development. Am J Physiol *274*, G342-G349.

Zakrzewska, M., Krowarsch, D., Wiedlocha, A., and Otlewski, J. (2004). Design of fully active FGF-1 variants with increased stability. Protein Eng Des Sel *17*, 603-611.

Zamolodchikova, T.S., Sokolova, E.A., Lu, D., and Sadler, J.E. (2000). Activation of recombinant proenteropeptidase by duodenase. FEBS Lett *466*, 295-299.

Zehe, C., Engling, A., Wegehingel, S., Schafer, T., and Nickel, W. (2006). Cell-surface heparan sulfate proteoglycans are essential components of the unconventional export machinery of FGF-2. Proc Nat Acad Sci *103*, 15479-15484.

Curriculum vitae

STALLMACH
Robert
born the 17th of February 1979
in Mainz (Germany)

2003 – Present	Doctoral Research Department of Biochemistry, University of Zurich Lab: Dr. Peter Sonderegger, Subgroup: Dr. Sergio Gloor
2001-2002	Diploma Research Department of Biochemistry, University of Zurich Lab: Dr. Peter Sonderegger Title: The Role of the Non-catalytic Domains of Murine Neurotrypsin in Protein Sorting
2003	Diploma in Biochemistry with Subsidiary Subject Bioinformatics University of Zurich Academic Grade Achieved: Dipl. Biochem. - equivalent to M.Sc. Areas of Study: Biochemistry, Bioinformatics, Molecular Biology, Biophysics, Molecular Medicine, Gene Technology, Immunology, Genetics, Proteomics
2000	2nd Preliminary Diploma, University of Zurich Areas of Study: Inorganic Chemistry, Organic Chemistry, Physical Chemistry, Biochemistry
1999	1st Preliminary Diploma, University of Zurich Areas of Study: Chemistry, Physics, Mathematics, Informatics
1998	Matura (Type B: Latin and English) - general qualification for university entrance Kantonsschule Hohe Promenade Zürich

Acknowledgements

First, I want to thank Sergio Gloor for giving me the opportunity to work on this highly interesting project as well as for his great supervision, scientific enthusiasm, hands-on help with the mice and permanent guidance throughout my time at the Department of Biochemistry of the UZH.

I am very grateful to Peter Sonderegger for giving me the chance to work in his laboratory and for providing me the opportunity to practically be a full member of his research group. I profited greatly in this scientific atmosphere of congregated, outstanding protease-expertise as well as of the general immense experience in biochemical and biological methods.

I want to thank Ned Mantei for joining my thesis steering committee of the ZNZ International Ph.D. Program in Neuroscience.

I am grateful to Beat Kunz for his permanent dedication to keep the lab running on a high standard and for his expert assistance in antibody production. I'm also indebted to him and Daniel Blaser for the supply with mice.

Thanks go to Masayoshi Mishina for providing the cDNA of GluRδ2.

For providing modified expression vectors, thanks go to Daniel Lüscher (ONEstrep-tag in pcDNA3.1), Giovanna Galliciotti (Fc-tag in pcDNA3.1) and Stefan Hettwer (Calsyntenin-1-secretion signal in pEAK8).

A special 'thank you' goes to my brothers in pipettes: Daniel Lüscher and Raymond Reif.

Furthermore, a big 'thank you' goes to all past and present members of the Sonderegger lab for providing the pleasant atmosphere and for their helpful advice and comments.

I specially want to thank Manuela Stimpfl for bringing back magic into my life.

Last but not least, I want to thank friends and family and especially, I want to express deepest gratitude to my parents, Ingrid and Thomas Stallmach for paving the way for my education and for the loving support they always provided.